COMPARISON OF SAFETY LEVELS OF REINFORCED MASONRY AND CONCRETE WALLS USING RELIABILITY ANALYSIS

by

Oswald Casaverde Lopez

A thesis submitted in partial fulfillment of the requirements for the degree of

Master of Science

in

STRUCTURAL ENGINEERING

Department of Civil and Environmental Engineering

University of Alberta

ABSTRACT

The strength reduction factors in the Canadian masonry design standard were last calibrated in the 1980s. The factors were last updated (2004) based on reliability studies performed on reinforced-concrete structures, but no masonry-specific reliability analyses were conducted to support this change. Uncertainty remains as to whether the current masonry standard leads to unsafe or overly conservative designs.

Modern masonry construction is comprised, in its majority, of walls (shear walls and out-of-plane walls). This study investigates the reliability levels for non-slender reinforced masonry walls under combined axial load and out-of-plane bending, and compares the results with reliability analyses performed in walls made of reinforced concrete. Comparing walls made of two materials under similar loads will allow an objective analysis of the reliability levels in the current masonry standard.

The results show reliability indices for masonry and concrete walls are influenced by the amount of reinforcement in the walls and the compressive strength of the materials. Overall, for the same compressive strength and reinforcement ratio, masonry and concrete walls had similar reliability indices, although masonry showed higher sensitivity to changes in these parameters. The reliability of singly reinforced walls of either material was not significantly sensitive to changes in the compressive strength and reinforcement ratio. In contrast, doubly reinforced walls exhibited sensitivity to these parameters. Doubly reinforced masonry walls were more sensitive to changes in compressive strength and reinforcement ratios than doubly reinforced concrete walls. Doubly reinforced walls of either material generally had higher reliability values than singly reinforced walls.

Overall, the study shows that it is reasonable to assume similar reliability values for masonry and concrete walls with comparable compressive strengths and reinforcement ratios. However, enhanced supervision control is required for masonry construction because their reliability is very sensitive to workmanship factors. Reducing variability through enhanced supervision control of masonry would lead to increase in safety and, consequently, an increase in the strength reduction factor. This, in turn, results in a higher design capacity of structural masonry.

DEDICATION

This thesis is dedicated to my parents, whose unconditional love and support have made it for me be possible to complete this journey.

ACKNOWLEDGEMENTS

I would like to give thanks to God, who knows what you need to progress in this self discovering adventure.

I would like to express my deepest gratitude to my supervisor, Dr. Lobo, for giving me the opportunity to be part of his research team, without which I would not even have been able to initiate this learning experience. Thanks for being a role model and for showing me kindness and thoroughness in your guidance.

I would also like to thank my committee members, Dr. Leila Hashemian, Dr. Shay Abtahi, Dr. Vivek Bindiganavile for serving as my committee members.

In a special way, I would also like to thanks to all my professors at University of Alberta: Prof. Ying Hei Chui, Prof. Douglas Tomlinson, Prof. Ali Imanpour, Prof. Yong Li, Prof. Mustafa Gul, Prof. F. Albert Liu, and Prof. Clayton Pettit. Thank you for sharing your knowledge and mentoring, and for making complicated things simple. Being in your class was a constant motivation and fabulous experience.

Many thanks to all the members of the wolfpack. Thank you for your valuable support throughout this process. A special thanks to: Odin Guzman who taught me and introduce me in the reliability world, and Rafael Gonzalez for being a generous and good friend.

I would also like to give sincere thanks to Dr. Allan Okodi. One of the most humble and smart persons that I have ever met. Thank you for your patient and feedback. Without your help this research it could not be completed.

Finally, thanks to the Peruvian government, which through its national scholarship and education grant program (PRONABEC), provided me with the funding to pursue my dream.

TABLE OF CONTENTS

Abstract ii

Dedication iv

Acknowledgements v

Table of Contents vi

List of Tables ix

List of Figures x

1 INTRODUCTION 1

1.1 Background 1

1.2 Problem Statement 2

1.3 Objectives of the study 2

1.4 Scope 2

1.5 Thesis Organization 3

2 LITERATURE REVIEW 4

2.1 Introduction 4

2.2 Structural Reliability Analysis 4

2.2.1 Limit State Function 5

2.2.2 Reliability Analysis Problem 5

2.2.3 Second Moment Reliability Index 6

2.2.4 First Order Reliability Method (FORM) 10

2.2.5 Monte Carlo Simulation 12

2.2.6 Summary of the methods for structural reliability analysis 13

2.3 Relevant studies about Reliability Analyses 14

2.3.1 Development of a Canadian Limit States Masonry Standard 14

2.3.2 Reliability studies on Structural Elements subjected to flexure and axial load 17
3 BEHAVIOURAL MODEL AND SENSITIVITY ANALYSIS 24
3.1 Introduction 24
3.2 Stress-strain behaviour for Load-Bearing Walls 24
3.2.1 Stress-strain relationship - Masonry 24
3.2.2 Stress-strain relationship - Concrete 25
3.2.3 Stress-strain relationship – Steel Rebar 26
3.3 Behavioural Model for Non-slender Walls 27
3.3.1 The nominal and factored resistances 28
3.3.1.1 Behavioural Model – Singly Reinforced (SR) Masonry Walls 30
3.3.1.2 Behavioural Model – Doubly Reinforced (DR) Masonry Walls 31
3.3.1.3 Behavioural Model – Singly Reinforced (SR) Concrete Walls 32
3.3.1.4 Behavioural Model – Doubly Reinforced (DR) Concrete Walls 33
3.3.1.5 Parameters for masonry and concrete walls - Summary 35
3.3.2 Loads side of the reliability equation – Optimal design 35
3.4 Sensitivity Analysis 36
3.4.1 Reinforcement Ratio Variation 36
3.4.2 Compressive Strength Variation 38
3.4.3 Thickness Variation 39
3.4.4 Summary of the sensitivity analysis 41
4 STRUCTURAL RELIABILITY ANALYSIS OF MASONRY AND CONCRETE WALLS, RESULTS AND DISCUSSION 42
4.1 Introduction 42
4.2 The Structural Reliability Approach 42

4.3 Limit state function for Eccentrically Applied Gravity Loads 43
4.4 Analysis procedure 49
4.5 Analysis of non-slender walls - Summary 50
4.6 Statistical Information for Loading 51
4.7 Statistical Information for Resistance Parameters 52
4.7.1 Masonry compressive strength 53
4.7.2 Concrete compressive strength 54
4.7.3 Wall thickness 55
4.7.4 Reinforcement location 55
4.7.5 Yield strength 55
4.7.6 Rate of loading 55
4.7.7 Workmanship factor 56
4.8 Properties of Analyzed Walls 56
4.9 Results and Discussion 57
4.9.1 Parametric Analysis 57
4.9.2 Comparison between Singly and Doubly Reinforced Walls 66
4.9.3 Comparison between Masonry and Concrete Walls 71
5 CONCLUSIONS AND RECOMMENDATIONS 78
5.1 Recommendations for future work 80
REFERENCES 82
APPENDICES 85

LIST OF TABLES

Table 2.1: Main characteristics of methods for structural reliability analysis 13
Table 2.2: Target Reliability Indices (β_T) from CSA S408 (2011) for 30-year (50-year). 15
Table 2.3: Target Reliability Indices (β_T) from JCSS (2001a) for 1-year (50-year) reference period and ultimate limit states. 15
Table 3.1: Parameters for the nominal interaction diagram, and for the factored interaction diagram computation according to Canadian Standards Association (CSA). 35
Table 3.2: Summary of the sensitivity analysis. 41
Table 4.1: Reliability index comparison. 50
Table 4.2: Statistical Information for loads (Bartlett et al., 2003). 52
Table 4.3: Statistical Information for loads. 53
Table 4.4: Properties of masonry analyzed walls. 57
Table 4.5: Properties of concrete analyzed walls. 57
Table 4.6: Results of Monte Carlo simulation – SR concrete wall - $e/t = 1.5$. 63
Table 4.7: Results of Monte Carlo simulation – DR concrete wall - $e/t = 1.5$. 63
Table 4.8: Results of Monte Carlo simulation – SR masonry wall - $e/t = 1.5$. 64
Table 4.9: Results of Monte Carlo simulation – DR masonry wall - $e/t = 1.5$. 64

LIST OF FIGURES

Figure 2.1: Geometrical illustration of the Cornell reliability index (Madsen et al., 1986). 6
Figure 2.2: Geometrical illustration of the Hasofer and Lind index (Madsen et al., 1986)..... 9
Figure 2.3: Reliability index defined as the shortest distance in the space of reduced variables (Nowak, 2000). 10
Figure 2.4: Rackwitz-Fiessler procedure (Nowak, 2000)..... 11
Figure 2.5: Schematic of the Monte Carlo Method (Nowak, 2000). 13
Figure 2.6: Three possible Limit-State Functions on the P-M interaction diagram. 19
Figure 3.1: Stress-strain relationship for masonry..... 25
Figure 3.2: Stress-strain relationship for concrete 26
Figure 3.3: Stress-strain relationship for reinforcement steel..... 27
Figure 3.4: P-M interaction diagram..... 28
Figure 3.5: P-M interaction diagram..... 29
Figure 3.6: Strain profile, stress profile, and resultant forces for SR masonry walls. 30
Figure 3.7: Strain profile, stress profile, and resultant forces for DR masonry walls. 31
Figure 3.8: Strain profile, stress profile, and resultant forces for SR concrete walls. 33
Figure 3.9: Strain profile, stress profile, and resultant forces for DR concrete walls..... 34
Figure 3.10: Optimal design on the P-M interaction Diagram. 36
Figure 3.11: Effect of the change in the reinforcement ratio: (a) Singly reinforced masonry wall; (b) Doubly reinforced masonry wall; (c) Singly reinforced-concrete wall; (d) Doubly reinforced-concrete wall. 37
Figure 3.12: Effect of the change in the compressive strength: (a) Singly reinforced masonry wall; (b) Doubly reinforced masonry wall; (c) Singly reinforced-concrete wall; (d) Doubly reinforced-concrete wall. 39
Figure 3.13: Effect of the change in the thickness: (a) Singly reinforced masonry wall; (b) Doubly reinforced masonry wall; (c) Singly reinforced-concrete wall; (d) Doubly reinforced-concrete wall. 40
Figure 4.1: (a) Nominal and factored P-M interaction diagrams; (b) Optimal design on the P-M interaction diagram. 43

Figure 4.2: Three possible Limit-State Functions on the P-M interaction diagram. 44
Figure 4.3: Wall under axial load and equal eccentricities. 45
Figure 4.4: P-M interaction diagram with nominal and factored resistance, and nominal load curves. 46
Figure 4.5: Effect of the change in the reinforcement ratio: (a) Singly reinforced (SR) masonry wall; (b) Doubly reinforced (DR) masonry wall; (c) Singly reinforced (SR) concrete wall; (d) Doubly reinforced (DR) concrete wall. 58
Figure 4.6: Effect of the change in the coefficient of variation (COV): Doubly reinforced (DR) masonry wall. 59
Figure 4.7: Effect of the change in the reinforcement ratio: (a) Singly reinforced masonry wall; (b) Doubly reinforced masonry wall. 60
Figure 4.8: Effect of the change in the compressive strength on reliability index: (a) SR masonry wall; (b) DR masonry wall; (c) SR concrete wall; (d) DR concrete wall. 62
Figure 4.9: Effect of the change in the coefficient of variation (COV) with an increment of the compressive strength: (a) Singly reinforced-concrete wall; (b) Doubly reinforced-concrete wall; (c) Singly reinforced masonry wall; (d) Doubly reinforced masonry wall. 65
Figure 4.10: Comparison between SR masonry and DR masonry walls for the same $fm' = 25\ MPa$ and for different reinforcement ratios. 66
Figure 4.11: Comparison between SR masonry and DR masonry walls for the same $\rho = 0.0035$ and for different compressive strength. 67
Figure 4.12: Comparison between SR concrete and DR concrete walls for the same $fm' = 30\ MPa$ and for different reinforcement ratios. 69
Figure 4.13: Comparison between SR concrete and DR concrete walls for the same $\rho = 0.0035$ and for different compressive strength. 70
Figure 4.14: Contribution to the moment capacity: (a) Doubly reinforced wall; (b) Singly reinforced wall. 71
Figure 4.15: Reliability levels comparison for the same $fm' = fc' = 25\ MPa$ and $\rho = 0.0015$: Singly reinforced (SR) masonry wall. 72

Figure 4.16: Reliability levels comparison for the same $fm' = fc' = 25\ MPa$ and $\rho = 0.0015$: SR masonry and concrete walls. 72
Figure 4.17: Reliability levels comparison for the same $fm' = fc' = 25\ MPa$ and $\rho = 0.0015$: SR masonry, concrete walls and Doubly reinforced (DR) masonry wall. 73
Figure 4.18: Reliability levels comparison for the same $fm' = fc' = 25\ MPa$ and $\rho = 0.0015$: SR and DR masonry and concrete walls. 73
Figure 4.19: Reliability levels comparison between masonry and concrete walls, $fm' = fc' = 25\ MPa$ and $\rho = 0.0015$. 74
Figure 4.20: Reliability levels comparison between masonry and concrete walls, $fm' = fc' = 25\ MPa$ and $\rho = 0.0025$. 75
Figure 4.21: Reliability levels comparison between masonry and concrete walls, $fm' = fc' = 25\ MPa$ and $\rho = 0.0035$. 75
Figure 4.22: Comparison between masonry and concrete walls, minimum standard requirements. 77

1 INTRODUCTION

1.1 Background

The Canadian standard for the design of masonry (CSA S304) has been in the limit states format since 1994. It was developed from reliability studies performed on masonry elements during 1970s and 1980s (Turkstra and Daly, 1978; Turkstra and Ojinaga, 1980; Turskstra et al., 1983; Turskstra, 1989). The studies were based on working stress design approach, and utilised the limited experimental data and statistical information available at the time.

In 2004, the material resistance factor for masonry (ϕ_m) in the standard was revised from 0.55 to 0.60 and the value was retained in the last revision of the standard, CSA S304-14. This change was justified by simple calculations (Laird et al., 2005), rather than being backed by masonry-specific reliability analyses. There remains uncertainty as to whether the masonry standard leads to unsafe or overly conservative designs.

More recent studies have been made to assess the reliability levels of the design expressions in the current standard (CSA-S304-14) using recent statistical information of loads and resistances. These studies proposed a more comprehensive limit state function (Moosavi, 2017), and tackled parameters such as slenderness, and second order and lateral load effects (Guzman, 2022). However, there is a lack of studies that compare the reliability levels of reinforced masonry walls with that of walls made of similar material, such as reinforced-concrete.

Because of the similarities between reinforced masonry (RM) and reinforced-concrete (RC), many of the equations and principles used in their designs are similar. However, it is not known if the structural elements made from either material offer the same safety or reliability levels as the statistical parameters of masonry and concrete materials have fundamental differences. Clearly, there is a need to know how the reliability levels of masonry walls compare with that of walls made with reinforced-concrete.

In this research, the reliability levels of non-slender reinforced masonry and concrete walls were assessed and compared for walls under combined axial load and out-of-plane bending. The assessment used the limit state function proposed by Moosavi (2017) and the fixed eccentricity approach for gravity loads. The First Order Reliability Method (FORM) was used to determine the

reliability index, making use of the most recent statistical information of loads and resistance. Walls having single and double reinforcement bars within the cross-section were analysed, reinforcement ratios and compressive strengths of masonry and concrete were varied, and their effects on the reliability indices were assessed.

1.2 Problem Statement

To the authors' knowledge, there are no reliability-based studies that compare the safety levels of non-slender reinforced-masonry and reinforced-concrete walls subjected to gravity loads (dead load plus live load). There is a need of reliability studies that consider the most recent statistical information of loads and resistance to compare the safety levels of the current masonry standard (CSA S304-14) and concrete standard (CSA A.23.3-19) for loadbearing walls under out-of-plane effects.

1.3 Objectives of the study

The main objective of this study is to compare the reliability levels of non-slender masonry and concrete walls subjected to axial load and out-of-plane moments. To achieve this, the following specific objectives were defined:

i. Conduct a literature review on the techniques available to perform reliability analyses of non-slender masonry and concrete walls, and previous research efforts related to reliability analysis of masonry and concrete elements.
ii. Determine the behavioural model for non-slender masonry and concrete walls and perform a sensitivity analysis to assess the effect of the material and geometrical parameters on the behaviour of non-slender walls under axial load and out-of-plane bending.
iii. Perform a parametric reliability analysis comparison between masonry and concrete walls taken into consideration different reinforcement schemes (singly and doubly reinforced walls), different reinforcement ratios and compressive strengths.

1.4 Scope

This research focused on singly and doubly reinforced non-slender masonry and concrete walls designed as per the Canadian masonry and concrete design standard (CSA S304-14, CSA A23.3-19). Only fully grouted masonry walls and concrete walls, under axial compression and out of

plane bending, with pinned-pinned boundary conditions were studied. Out-of-plane shear is assumed not to govern the failure mode of the wall, which is assumed to be flexural.

1.5 Thesis Organization

This thesis is divided into five chapters, and their content is described as follows:

Chapter 1: Presents an introduction to the problem investigated, and the objectives and scope of this thesis are discussed.

Chapter 2: Contains a review of the literature available, including concepts and definitions of structural reliability analysis, a summary about previous research relevant to reliability analysis of masonry and concrete structures.

Chapter 3: Contains the behavioural model used to build the interaction diagram between axial compression and out-of-plane bending moment, as well as the effect of the variation in the most important parameters (reinforcement ratio, compressive strength, thickness) on P-M interaction diagram. A sensitivity analysis is carried out to determine the effect of the material and geometrical parameters on the interaction diagram.

Chapter 4: Presents the limit state function for eccentric gravity loads in non-slender elements. The first order reliability method is used to assess the reliability levels. The most recent statistical information for loading and resistance parameters is summarized. Properties of analyzed walls are discussed. Reliability levels of walls made of masonry and concrete are compared.

Chapter 5: Outlines the conclusions drawn from this study and a series of recommendations for future studies on this topic.

2 LITERATURE REVIEW

2.1 Introduction

This chapter contains a review of the literature available, including concepts and definitions of structural reliability analysis. Firstly, the relevance of structural reliability analysis is presented, as well as definitions and descriptions of limit state, reliability analysis problem, and methods for structural reliability analysis. Secondly, a summary of the most relevant studies about reliability analysis of masonry and concrete structural elements subjected to an axial load and out of plane bending moment is presented.

2.2 Structural Reliability Analysis

The limit-state deign (LSD) philosophy was introduced in the Canadian masonry standard in 1994 (CSA S304-94) and in the Canadian concrete standard in 1984 (CSA A23.3-84). The LSD states that the design of a structural member is satisfactory if the factored load effects are smaller than or equal to the factored design resistance (Equation 2.1):

$$\phi R_n \geq \gamma S_n \tag{2.1}$$

Where ϕ is the material strength reduction factor that accounts for variability of material properties and dimensions of structural elements, R_n is the nominal resistance or the true resistance of a structural element, and γ is the so-called load factor, used to account for the variability of loading and the probability of having loads from different sources simultaneously. The parameter γ depends on the type of load. Finally, the load effect, S_n, corresponds to a specific nominal load or a load combination acting on the member.

In structural design, there are many sources of uncertainty either in the loads or in the resistance. Reliability analysis is an important tool for rational decision-making in the face of uncertainty, it deals with random variables instead of deterministic values, and the rational treatment of uncertainties. Because of these uncertainties, structures are expected to be designed with a reasonable safety level or finite probability of failure.

Standards have evolved so that design criteria take into account some of the sources of uncertainty. Acceptable safety levels are achieved by specifying design values for minimum design loads,

maximum allow deflection as well as load/resistance factors in design guidelines. Such standard requirements are calibrated through reliability analyses (Moosavi, 2017).

2.2.1 Limit State Function

The first step to perform a reliability analysis is to establish a limit state that is a criterion for deciding whether the performance of the engineered product is satisfactory. It is the boundary that separates the safe (desired performance) and failure (undesired performance) domains (Nowak, 2000). To perform a reliability analysis for a given limit state, the limit state needs to be defined mathematically as a limit state function (failure function). This function specifies the failure surface, typically obtained through a strength of materials or mechanical analysis for the structure. The limit state function ($g(\boldsymbol{X})$) for strength is normally defined as shown in Equation (2.2),

$$g(\boldsymbol{X}) = R(\boldsymbol{X}) - S(\boldsymbol{X}) \tag{2.2}$$

where R and S are the random variables that represent the resistance and the load effect, respectively, and $\boldsymbol{X}$ represents the vector containing all random variables such as those related to geometrical, material, load and workmanship parameters.

2.2.2 Reliability Analysis Problem

The reliability problem can be expressed as the calculation of the probability of failure, p_f, defined as $p_f = P[g(X) < 0]$. Melchers and Beck (2018) generalized the reliability problem with n-dimensional vector X of random variables involved, and it can be expressed as follows:

$$p_f = P[R(\boldsymbol{X}) \leq S(\boldsymbol{X})] = P[g(\boldsymbol{X}) \leq 0] = \int \dots \int_{G(X) \leq 0} f_{\boldsymbol{X}}(\boldsymbol{X}) d\boldsymbol{X} \tag{2.3}$$

Here $f_X(X)$ is the joint probability density function (PDF) for the n-dimensional vector X of basic variables. Even for the case of $g = R - S$, which considers only two random variables, these integrals are difficult to evaluate, in general (Nowak, 2000). Therefore, the probability of failure is calculated indirectly using other procedures (Second Moment Reliability Index, First Order Reliability Method, the Monte Carlo Method, etc.). In the following section some of these methods are briefly discussed for completeness.

2.2.3 Second Moment Reliability Index

As noted earlier, the probability of failure in Equation 2.3 is difficult to evaluate, so the concept of a reliability index is used to quantify structural reliability. The idea behind second moment reliability theory is that each variable is expressed solely in terms of its first two statistical moments, for example, by its mean and standard deviation. Some definitions of reliability indices proposed by different authors are presented as follows:

The Cornell Reliability Index

Cornell (1969) defined a reliability index (or safety index) β_C as:

$$\beta_C = \frac{E[g]}{D[g]} \tag{2.4}$$

Where the symbols $E[g]$, and $D[g]$ are the expected values and standard deviation of the limit state function (g) respectively. This definition is illustrated geometrically in Figure 2.1. For one dimensional case the failure surface is simply the point $g = 0$. The concept behind this definition is that the distance from expected value to the limit state surface provides a good measure of reliability. The distance is measured in units of the standard deviation $D[g]$.

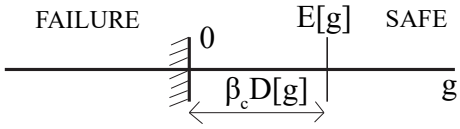

Figure 2.1: Geometrical illustration of the Cornell reliability index (Madsen et al., 1986).

The original formulation by Cornell was written as the difference between a resistance R and the corresponding load effect S:

$$g = R - S \tag{2.5}$$

And if R and S are uncorrelated, the reliability index becomes.

$$\beta_C = \frac{E[R] - E[S]}{\sqrt{Var[R] + Var[S]}} = \frac{\mu_R - \mu_S}{\sqrt{{\sigma_R}^2 + {\sigma_S}^2}} \tag{2.6}$$

Where the symbols μ_R, μ_S, σ_R, σ_S are the means and standard deviations of the resistance and loads. If the random variables are normally distributed and uncorrelated, the reliability index is related to the probability of failure by

$$P_f = \Phi(-\beta) \tag{2.7}$$

If the random variables are normally distributed and uncorrelated, then this formula is exact in the sense that β and P_f are related by Equation (2.7). Otherwise, this equation provides only an approximate means of relating β to a probability of failure.

If the failure surface is a hyperplane (linear limit state function):

$$g(X_1, X_2, \dots, X_n) = a_0 + a_1X_1 + a_2X_2 + \cdots + a_nX_n = a_0 + \sum_{i=1}^{n} a_iX_i \tag{2.8}$$

Where the a_i terms (i=0, 1, 2, …, n) are constants and the X_i terms are uncorrelated random variables. The reliability index is determined as:

$$\beta = \frac{a_0 + \sum_{i=1}^{n} a_i\mu_{X_i}}{\sqrt{\sum_{i=1}^{n}(a_i\sigma_{X_i})^2}} \tag{2.9}$$

As seen in Equation (2.9), the reliability index, β, is calculated only using the means and standard deviations of the random variables. Therefore, this β is called a second-moment measure of structural safety, only the first two moments (mean and variance) are required to determine β.

First Order Second Moment Reliability Index

In the case of a nonlinear function, its mean value and standard deviation cannot be calculated solely from the second moment representation of the random variables. One way to approach this is to linearize the limit state function. One possible procedure is to use the linear term in a Taylor series expansion around a point. The result is

$$g(X_1, X_2, \dots, X_n) \approx g(x_1^*, x_2^*, \dots, x_n^*) + \sum_{i=1}^{n}(X_i - x_i^*)\frac{\partial g}{\partial Xi}\Big|_{\{x_i^*\}} \tag{2.10}$$

Where $(x_1^*, x_2^*, \dots, x_n^*)$ is the point about which the expansion is performed. One choice for this linearization point could be the mean values of the random variables. Since Equation (2.10) is a linear function, it can be written to look exactly like Equation (2.8), and after some algebraic manipulations, the following expression for β results:

$$\beta = \frac{g(\mu_{X_1}, \mu_{X_2}, \dots, \mu_{X_n})}{\sqrt{\sum_{i=1}^{n}(a_i \sigma_{X_i})^2}} \quad where \quad a_i = \left.\frac{\partial g}{\partial Xi}\right|_{\{\mu_{X_i}\}} \tag{2.11}$$

The reliability index above is called First-Order Second Moment Mean Value Reliability Index. First order because first-order terms in the Taylor series expansion are used. Second moment because only means and variances are needed. Mean value because the Taylor series is about the mean values.

One severe drawback of First-Order Second-Moment Mean Value Index is the invariance problem. This refers to the fact that the value of the reliability index depends on the specific form of the limit state function. Since the limit state function represents the failure surface ($g(X) = 0$), it is possible to determine a new limit state function, which is equivalent to the first one, by dividing the first one by positive quantity that could represent a positive random variable. By doing this, the boundary or the regions in which the limit state function is positive or negative does not change. Therefore, the same fundamental limit state forms the basis for both limit state functions, so the probability of failure (as reflected by the reliability index) should be the same, which is not true due to the invariance problem. Hasofer-Lind (1974) solved this problem in their modified reliability index (as outlined in the section below).

Hasofer-Lind Reliability index

Hasofer and Lind (1974) proposed a modified reliability index that did not exhibit the invariance problem. The correction is to evaluate the limit state function at a point known as the "design point" instead of the mean values. This point is a point in the failure surface $g = 0$.

Hasofer and Lind (1974) expanded the Cornell reliability index definition (in which the reliability index can be interpreted as a measure of the distance to the failure surface) for the case of more basic variables.

Hasofer and Lind (1974) proposed a nonhomogeneous linear mapping of the set of basic variables into a set of normalized and uncorrelated variables Z_i. The mean value point in x-space is mapped into the origin of z-space, and the failure surface L_X in x-space is mapped onto corresponding failure surface L_Z in z-space as shown in Figure 2.2. The geometrical distance from the origin in z-space to any point on L_Z is simply the number of standard deviations from the mean value point in x-space to the corresponding point on L_X. The smallest distance from the origin to a point on the failure surface was proposed by Hasofer and Lind (1974) as definition of a reliability index.

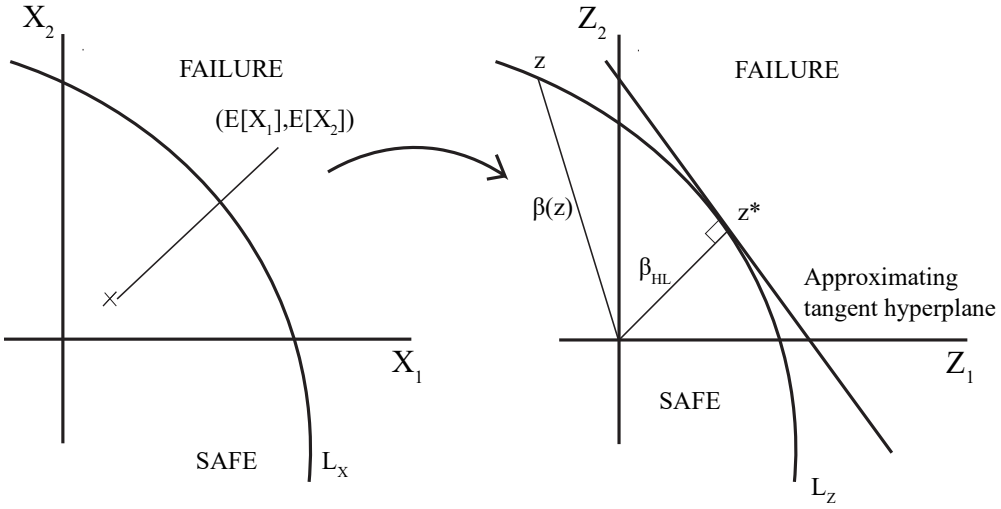

Figure 2.2: Geometrical illustration of the Hasofer and Lind index (Madsen et al., 1986).

For the simple case of two random variables *R* and *S*, these can be expressed in its standard form or reduced variables (nondimensional form of the variables) as follows:

$$Z_R = \frac{R - \mu_R}{\sigma_R} \tag{2.12}$$

$$Z_S = \frac{Q - \mu_S}{\sigma_S} \tag{2.13}$$

The limit state function $g(R, Q) = R - S$ can be expressed in terms of the reduced variables, by expressing the resistance R and the load Q in terms of the reduced variables:

$$g(Z_R, Z_Q) = \mu_R + Z_R\sigma_R - \mu_Q - Z_Q\sigma_Q = (\mu_R - \mu_Q) + Z_R\sigma_R - Z_Q\sigma_Q \tag{2.14}$$

For any specific value of $g(Z_R, Z_Q)$, Equation (2.14) represents a straight line, in the space of reduced variables Z_R and Z_Q. The line of interest to us in reliability analysis is the line corresponding to $g(Z_R, Z_Q) = 0$.

The general definition of reliability index was introduced by Hasofer and Lind (1974) as the shortest distance from the origin of reduced variables to the line $G(Z_R, Z_Q) = 0$, and it is illustrated in Figure 2.3:

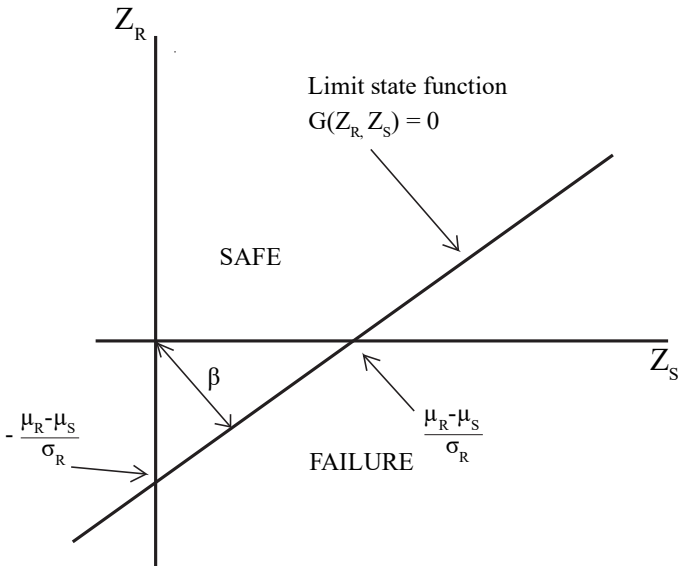

Figure 2.3: Reliability index defined as the shortest distance in the space of reduced variables (Nowak, 2000).

2.2.4 First Order Reliability Method (FORM)

In general, the basic random variables are not normally distributed. The fact that probability contents in various sets are well approximated in a standardized normal space leads to the idea of finding a one-to-one transformation. One of the most important improvements made to the Second Moment Reliability Index is that the actual probability distribution function can be approximated with normal probability distributions, and still good estimates of failure probability is obtainable. Also, the failure surface can be approximated by a linear surface. A reliability method based on this procedure is called First order reliability method (FORM). One drawback of this method arises when the failure surface exhibits very sharp curves (highly non-linear function). In such cases, FORM can provide practical approximations (Melchers, 1999).

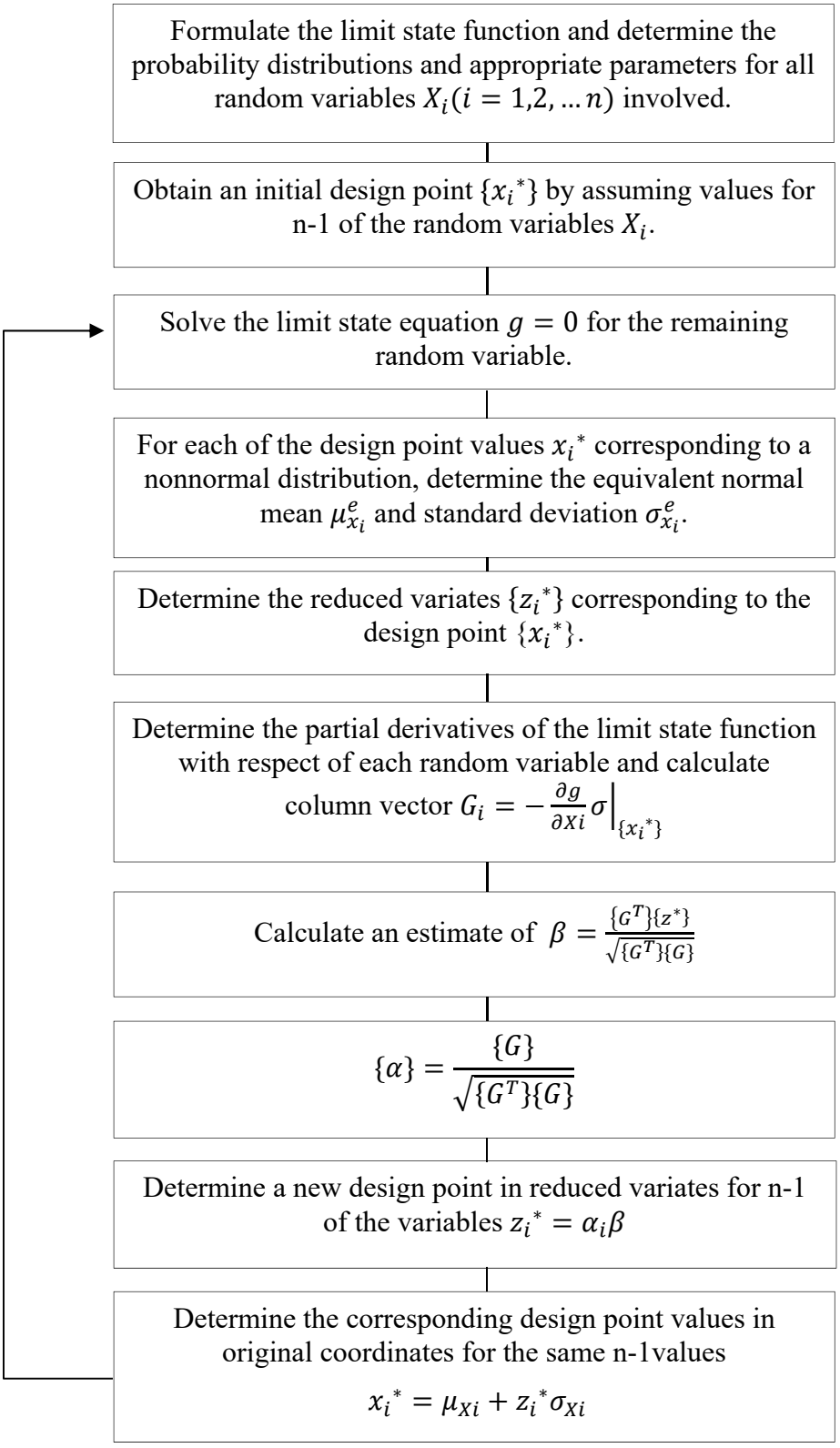

Figure 2.4: Rackwitz-Fiessler procedure (Nowak, 2000)

In this study, FORM is used to calculate reliability indexes (β). This procedure considers the mean, Coefficient of variation (COV), and distribution type for each of the random variables. The algorithm for FORM procedure proposed by Rackwitz – Fiessler in 1978 is used in this research, following this procedure a computer code was developed in Wolfram Mathematica programming language (see Appendix A) and its validation was made by comparing results with those obtained with Rt software (Rt is a reliability software developed by researcher at University of British Columbia in Vancouver - Canada), see section 4.4. Details for the Rackwitz – Fiessler procedure can be found in Nowak (2000). The steps for the algorithm are described in Figure 2.4 above.

2.2.5 Monte Carlo Simulation

Simulation techniques are one possible way to solve reliability problems. The basic idea behind simulation is, as the name implies, to numerically represent some phenomenon and then observe the number of times some event of interest occurs (Nowak, 2000). The basic concept behind simulation is relatively straightforward, but the procedure can become computationally expensive and time consuming.

Monte Carlo simulation uses a previous information data from testing that has certain mean and standard deviation and which can be fit with a certain probability distribution function in order to generate some results numerically without actually doing any physical testing. The basic idea of Monte Carlo Method is illustrated in Figure 2.5, where having information of test results, we can generate a sample of n test results using a special technique, this special technique is referring to Monte Carlo Method.

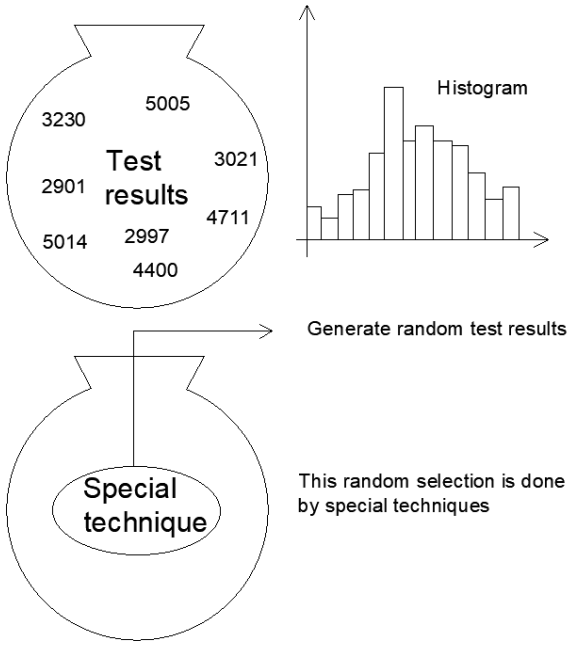

Figure 2.5: Schematic of the Monte Carlo Method (Nowak, 2000).

The Monte Carlo method is often applied in three situations:

1. It is used to solve complex problems for which closed-form solutions are either not possible or extremely difficult.
2. It is used to solve complex problems that can be solved (at least approximately) in closed form if many simplifying assumptions are made.
3. It is used to check the results of other solution techniques.

2.2.6 Summary of the methods for structural reliability analysis

Table 2.1 summarizes the main characteristics of the methods discussed above.

Table 2.1: Main characteristics of methods for structural reliability analysis

Method	Characteristics
Second Moment Reliability index	Each variable is represented only by its mean and standard deviation
First Order Reliability Method (FORM)	In addition to the mean and standard deviation, the distribution type is considered. The problem arises when the failure surface exhibits very sharp curves
Monte Carlo Simulation	It can become computationally expensive and time consuming

2.3 Relevant studies about Reliability Analyses

This section presents the most relevant studies on reliability analyses of masonry and concrete elements, with emphasis on those that refer to elements subjected to axial load and out-of-plane moment. The literature survey that follows is divided into two parts. The first part focuses on the reliability studies on masonry structures that are relevant to the development of a Canadian limit states masonry standard. In the second part, studies related to reliability studies on structural elements subjected to flexure and axial load are discussed.

2.3.1 Development of a Canadian Limit States Masonry Standard

As mentioned before, reliability analysis is often used in the development of design standards based on limit states. The scientific method of experiment and prediction began in Italy during the Renaissance with tests on the strength of trusses and beams, and test results were interpreted rationally in terms of stress (Madsen et al., 1986). Therefore, early design standards were formulated based on the concept of allowable stress. The Canadian masonry standard S304 was not an exception and was originally written in a working (allowable) stress design format. Then, a series of first order reliability analyses performed by Turkstra (1978, 1980, 1982, 1983, 1984, 1989) helped to transform the Canadian masonry standard from working stresses to a limit states approach, with the objective of providing more uniform and economical designs. The load and resistance factors design philosophy was implemented in the 1994 edition of the Canadian masonry standard S304.

Turkstra and Daly (1978) reviewed and compared the two moment criteria proposed by Hasofer and Lind (H-L), Paloheimo and Hannus (P-H), Ditlevsen and Skov (D-S), and the European Joint Committee on Structural Safety (J-C). One of the examples that was analyzed was a brick loadbearing masonry wall subjected to axial load and bending moment. Two nonlinear limit state function were analyzed based on a stress analysis, in which the stress due to the axial load and the out-of-plane bending moment applied to the wall was compared to the ultimate strength of the masonry material. The first limit state function was formulated for the case when the eccentricity was within one-sixth of the wall thickness, and the second was formulated when this limit was exceeded. The results indicated a significant sensitivity of the safety index to the criterion used in

analysis. The reliability index considering was found to be in the 4.25-2.70 range for the highest and lowest criterion, respectively.

In standard calibration, the calculated reliability index (β) are compared to target reliability indices, β_T, proposed by regional and national code committees. The target reliability index (β_T) depends on different variables such as the type of failure, the expected cost of failure, the cost of increasing the safety level, and the existing safety level. Table 2.2 shows recommended target reliabilities in the guidelines for the development of limit states design in Canada (CSA S408-11), and Table 2.3 shows the recommended values by the Joint Committee on Structural Safety (JCSS 2001a).

Table 2.2: Target Reliability Indices (β_T) from CSA S408 (2011) for 30-year (50-year).

Safety Class	Type of Failure	
	Gradual	Sudden
Not Serious	2.5 (2.3)	3.0 (2.8)
Serious (normal building)	3.5 (3.4)	4.0 (3.9)
Very Serious*	4.0 (3.9)	4.5 (4.4)

*It is assumed that for very serious consequences there is better quality control

Table 2.3: Target Reliability Indices (β_T) from JCSS (2001a) for 1-year (50-year) reference period and ultimate limit states.

Relative cost for enhancing the structural reliability	Failure consequences		
	Minor[a]	Average[b]	Major[c]
Large	3.1 (1.7)	3.3 (2.0)	3.7 (2.6)
Medium	3.7 (2.6)	4.2 (3.2) [d]	4.4 (3.5)
Small	4.2 (3.2)	4.4 (3.5)	4.7 (3.8)

[a]e.g. agricultural buildings
[b]e.g. office buildings, residential buildings or industrial buildings
[c]e.g. bridges, stadiums or high-rise buildings
[d] recommendation for regular cases

Due to the necessity and requirement of the building standard authorities in Canada to develop limit states design standards for all materials, Turkstra and Ojinaga (1980) conducted studies toward the development of a masonry standard based on limit states. Existing masonry wall design procedures were discussed and a reliability safety index for walls loaded by vertical forces causing minor axis bending was determined. Some of the challenges in the development of the masonry standard were the specification of basic material strengths, the treatment of the very significant uncertainties due to workmanship factor and the structural analysis available at the time.

Tursktra et al. (1983) outlined the evolution of the limit states design procedures for masonry based on rational mechanics and a comprehensive safety index analysis. This study highlighted the workmanship factor as an important factor in masonry reliability because available test data shown that masonry strength depended on the construction practice, mason qualifications, and inspection. Three levels of workmanship factor were defined, namely, rigorous work inspection, moderate work inspection, and uninspected construction. Based on an analysis of available experimental data for masonry walls under axial compression and out-of-plane bending, Tursktra suggested to use 0.7 for masonry material resistance factor for rigorously inspected workmanship and 0.4 for normally inspected workmanship; however, these factors were determined with a value of 0.5 as strength reduction factor for reinforcement steel.

In the early draft of the 1994 edition of the Canadian masonry design standard S304 (CSA 1994), the limit states design method was included as an alternative to the traditional allowable stress design method (ASD). Turkstra suggested a single class of inspection and a value of 0.40 for the masonry material resistance factor (ϕ_m) for both non-slender and slender elements. This value was not adopted because it was decided that slenderness effects would be taken into account separately using a resistance factor applied to the effective flexural stiffness of walls and columns. Based on an analysis by R.G. Drysdale (1992), published later as an appendix to the study by Laird et al. (2005), the masonry strength reduction factor was taken as 0.55.

In the 1992 analysis by Drysdale, the reliability equation suggested by Lind (1971) was used. However, the Lind (1971) procedure was suggested to have several limitations (CSA S408-11), such as a lower accuracy than first order reliability methods that could overestimate material

resistance factors. Another disadvantage of the Lind equation is that load is separated from resistance, so different load combinations cannot be investigated.

Laird et al. (2005) presented changes in the 2004 edition of Canadian masonry standard S304 from the previous 1994 edition. The most important changes were: the masonry material resistance factor changed from 0.55 to 0.60, and the resistance factor for member stiffness increased from 0.65 to 0.75, and the limit state design became mandatory. These changes were motivated by the increase in the resistance factor for concrete in the 2004 edition of the Canadian standard A23.3 from the previous 1994 edition (from 0.60 to 0.65). The changes in the masonry standard, however, were not accompanied by masonry-specific studies.

2.3.2 Reliability studies on Structural Elements subjected to flexure and axial load

Reliability analyses of elements subjected to an axial load and bending moment can be broadly classified based on whether or not second order effects are considered. Section 10 of CSA S304-14 addresses the requirements for design of reinforced masonry walls and columns. According to CSA S304, slenderness effects can be neglected when the ratio of effective height-to-thickness (slenderness ratio), $^{kh}/_{t}$, is less than $(10 - 3.5(^{e_1}/_{e_2}))$, where k is the effective length factor and e_1 and e_2 are the smaller and larger virtual eccentricity of axial load acting on top and bottom of the wall. Slenderness effects are considered if $^{kh}/_{t} < 30$. If $^{kh}/_{t} > 30$ second-order effects are also considered and additional provisions apply such as: pinned conditions must be assumed at each end of the wall, walls shall be constructed with masonry units of 140 mm or more in thickness, the factored axial load cannot exceed 10% of the maximum axial load resistance, ductile response must be guaranteed.

For non-slender elements, where the additional moment due to second order effects is negligible, the limit states are usually formulated comparing the resistance or capacity of the element, which is given by the axial load – bending moment interaction diagram, and the factored load effect, namely, the factored moment and axial load. The factored load effect is plotted as a point within the P-M interaction diagram and then related to the strength of the element based on the location of the point with respect to the interaction diagram (inside: safe, outside: not safe).

For slender elements, second order effects are accounted for in the determination of the total factored moment (M_{ft}), which is defined as the sum of the factored primary moment (M_{fp}) and a secondary moment arising from the combined effect of the axial load and out-of-plane deflections. the element can be designed using either the $P\delta$ method or the Moment Magnifier (MM) Method. The $P\delta$ method takes the designer to an iterative procedure until convergence is achieved; if the convergence is not achieved, then the wall is not stable. A simpler procedure is presented in the Moment Magnifier method, where the total moment is determined by multiplied the factored primary moment by a factor that takes into account the moments at each end of the wall, the critical axial load, the flexural stiffness of the wall, the factored axial load, etc.

Tichy and Vorlicek (1962) proposed a new concept of safety for eccentrically loaded non slender reinforced-concrete columns based on the probabilities of occurrence of some minimum strength and allows to introduce statistical methods. For simple cases such as pure bending and pure compression, when one variable is analyzed, the concept of safety factor is straightforward. The problem is more complex for combined loading of axial load and moment because two different values of safety factors are associated, one for the axial load and another for the moment. It was pointed out that the safety levels depend on how the limit state function is defined. For a given load combination effect (P_f and M_f), expressed by a point *S* on the P-M interaction diagram, three possible distances can be drawn to the interaction curve (Figure 2.6). These can be seen as the reserve of strength that a column possesses. By taking the moment constant ("fixed moment" approach – line *SA*), the axial load is assumed to be the only parameter that varies, and the vertical distance between the load and the resistance is seen as reserve of strength or safety factor of the element. By taking the axial load constant (the "fixed axial load" approach – line *SC*), the moment is allowed to vary, and the horizontal distance is seen as reserve of strength or safety factor of the element. Finally, if both variables , the axial load and the bending moment, are assumed to increase in the same proportion, the eccentricity is kept constant (the "fixed eccentricity" approach – line *SB*), and the distance in the direction of the given eccentricity is taken as a reserve of strength or safety factor of the element.

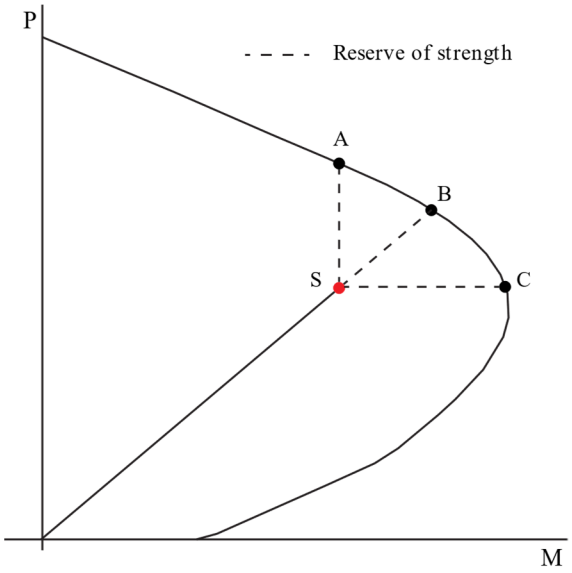

Figure 2.6: Three possible Limit-State Functions on the P-M interaction diagram.

Ellingwood (1977) examined the resistance of a non-slender reinforced-concrete (RC) column using Monte-Carlo techniques, and determined the sensitivity of the uncertainty in resistance to changes in the section geometry, strength properties, quality control, and load eccentricity. Ellingwood agreed with Tichy that resistance of a reinforced-concrete column or its margin of safety may be defined in several ways, finding that the fixed eccentricity approach was often applicable in columns under axial load and bending moment. The quality control was addressed by considering different coefficient of variation in the concrete compressive strength variable, f_c', pointing out three levels of quality control: coefficients of variation of 0.10, 0.15, and 0.25 were taken to represent good, average, and poor quality control, respectively. The workmanship factor was considered in the bar placement parameter, d and d', where d is the effective depth to the tensile reinforcement and d' is the effective depth for the compressive reinforcement. Three levels of coefficients of variation were given: 0.04, 0.07, and 0.09 for good, average, and poor types of workmanship, respectively. This study concluded that good concrete quality control is essential for gravity loads applied at low eccentricities, and it is unimportant at large eccentricities. For the latter case bar placement is a key parameter.

Grant et al. (1978) studied the effect of the variation of the strength of concrete and steel, the cross-section dimensions, and the location of steel reinforcement on the variability of the ultimate strength of rectangular reinforced-concrete tied short columns (non-slender element). The Monte

Carlo Technique was used in this study, and the fixed eccentricity limit state was used. This study indicated that the variability in the concrete compressive strength and steel strength seem to be the major contributing factor to strength variability in the compression failure region and tension failure region, respectively.

Israel et al. (1987) performed a reliability study of RC beams and short columns (non-slender element), analyzing flexure, compression plus bending, and shear limit states. First order second moment (FOSM) reliability method and the fixed limit state were used to calculate safety indices. Partial safety factors for concrete and steel were proposed: 0.60 and 0.90 for concrete and steel, respectively. Partial safety factors applied separately at each material resistance; conversely, overall safety factors (similar to those used in ACI 318) are based on the failure mode expected in the element and affect the overall resistance of the element.

Ruiz (1993) conducted a reliability study of short columns (non-slender element) subjected to axial load and bending, and compared reliability levels of the ACI 318-89 standard and the Mexican standard NTC-87. The Monte Carlo simulation technique and the fixed eccentricity limit state were used to calculate reliability indices. The results revealed that the Mexican standard had higher reliability indices than the American code. Also, for greater values of reinforcement ratio, the reliability indices grow. Moreover, it was observed that the higher the load ratio (dead-to-live load ratio), the greater the magnitude of the reliability index, that was due to the decreasing influence of the coefficient of variation (COV) of the live load.

Ruiz and Aguilar (1994) presented an extension of previous study (Ruiz, 1993), in the latter research, values of reliability indices have been calculated for short (non-slender element) and slender columns, complying with ACI 318-89 and Mexico City concrete design regulations. The Monte Carlo simulation technique was used, and the reliability index was calculated using the Rosenblueth-Esteva formulation. It was found that reliability indices corresponding to slender columns are higher than those for short columns. Also, the Mexican standard was found to have higher reliability values than the American standard due to the maximum loads adopted by each standard, the definition of concrete compressive strength used in the design, and the reductions factors established in each standard.

Stewart and Lawrence (2002) proposed a method to calculate the structural reliability of unreinforced masonry walls subjected to out-of-plane bending moment, second order effects were not considered. The Monte Carlo simulation was used and a limit state that considered first-cracking, the possible redistributions of stresses, possible additional cracking and continuing until collapse occurs was adopted. It was found that structural reliability was very sensitive to the effect of the workmanship factor. Also, it was observed that reliability indices obtained for masonry walls (for vertical bending β=4.92) are similar, although somewhat higher than, for other structural material such as concrete and steel (β=3.5-4.0). However, it was pointed out that such comparison is likely to be misleading since the calculation of the reliability indices depends of the failure criteria (limit state function).

Stewart and Lawrence (2007) developed a probabilistic model to calculate the structural of typical unreinforced brick masonry walls in compression designed according to Australian standard AS3700-2001. This study compared design strengths with actual test data to estimate a model error in probabilistic terms, for slender and non-slender unreinforced masonry walls in compression. It was found that existing safety levels of masonry were much higher than expected, so it was recommended that design capacity for Australian masonry walls loaded concentrically in compression can be increased by up to 66%.

Bartlett (2007) presented the rationale for increasing the material resistance factor for concrete in compression in the 2004 edition of the Canadian concrete standard association (CSA A23.3, 2004), from 0.60 to 0.65 for cast-in-place concrete. The concrete material resistance factor in compression was calibrated using first-order, second-moment formulations (Madsen al., 1986). The reliability index considering the new resistance factor of 0.65 was found to be in the 3.9-4.0 range.

Zhai and Stewart (2008) performed structural reliability analyses of reinforced-concrete masonry walls designed according to Chinese Standard GB 50003. The walls were loaded concentrically and eccentrically. The limit state considered the effect of the probability distribution model error, materials strengths, live-to-dead ratio, reinforcement ratio, discretization of the walls thickness, and eccentricity. It was found that structural reliability is very sensitive to the probability

distribution of model error and slightly influenced by masonry compressive strength and live-to-dead load ratio.

Moosavi et al. (2014) performed a reliability analysis on concrete masonry under axial compression using First Order Reliability Method (FORM) to evaluate the safety levels of the 2004 and 1994 editions of the Canadian masonry design standard S304.1. This study revealed that material resistance factors of 0.60 and 0.55 used in the 2004 and 1994 editions of the Canadian masonry design standard, respectively, did not achieve the target reliability value recommended by the Canadian standard S408.11 (Guidelines for the development of limit states design).

Moosavi (2017) studied the reliability levels of non-slender masonry walls subjected to axial load and out-of-plane bending moment according to the Canadian masonry standard S304-14. The First Order Reliability Method (FORM) and the fixed eccentricity approach were used to determine the reliability indices. Different combinations were analyzed such as dead plus live load, dead plus snow load, and dead plus wind load. The dead plus snow load combination provides the lowest reliability values.

Steward and Masia (2019) conducted a reliability study for single skin infill masonry walls subjected to a lateral load (wind) and where there is no vertical pre-compression. To evaluate the limit state based on resistance, the Monte Carlo simulation was used. To determine the resistance or the capacity of the wall two predictive models were used: (i) Finite Element Analysis (FEA) model, and (ii) AS3700 design model (Australian masonry structure code). The structural reliability analyses considered the random variability of model errors, flexural bond strength, and wind load. After comparing annual reliability indices to the target reliability recommended by AS5104-2017 (General Principles on Reliability for structures standard), it was found that there is some evidence to support increasing the reduction factor for flexure from 0.60 to 0.65, that is, and 8% increase in design capacity. Also, Steward and Masia stated the importance in estimating the model error, which is the actual (experimental) capacity divided by the predicted capacity, because reliability values are sensitive to this.

Gonzalez et al. (2021) presented a parametric analysis of single-storey slender masonry walls. A finite element 2D model was developed using the open-source FE software framework OpenSEES.

The results showed that increasing reinforcement ratio and rebar depth is the most efficient way to increase the stiffness of the walls. Also, changing the reinforcement arrangement from singly reinforced to doubly reinforced masonry walls increase the capacity of the wall section.

Guzman (2022) presented a reliability analysis for slender reinforced-concrete masonry walls under axial compression and out-of-plane uniform load. It took into account second-order effects and realistic loads. The Monte Carlo simulation technique and the fixed axial load approach were used to calculate reliability indexes. The results showed that the reliability indices (β) increase as the slenderness factor increase, while for walls with low slenderness the reliability indices remain similar and constant over different eccentricities.

Metwally et al. (2022) investigated the probabilistic behaviour of slender reinforced masonry walls under out-of-plane loading. Due to inherent uncertainties associated with masonry structures, experimentally or analytically predicted behaviour results in large scatter. A finite-element model was developed considering uncertainties in material and geometric properties. The masonry walls were modeled using displacement-based fiber beam-column elements in OpenSees. The results indicated that model uncertainty contributes to the variance in lateral load capacity more than all the other uncertainties in material and geometric properties, so in future reliability-based standard development special attention should be given in model accuracy and quantifying model error. This is consistent with results obtained by Steward and Masia (2019).

3 BEHAVIOURAL MODEL AND SENSITIVITY ANALYSIS

3.1 Introduction

As discussed in chapter 2, to solve a probability-based structural reliability analysis problem, it is necessary to have a behavioural model that predicts strength of the structure based on its mechanical and geometrical properties.

The strength of a wall cross-section subjected to a combination of axial force (P) and bending moment (M) is represented by its P-M interaction diagram. The P-M interaction diagram of a wall defines the combinations of axial force and bending moments for which the wall is safe. It is usually nonlinear arising from the nonlinear constitutive stress-strain relation of masonry and concrete materials in compression, tensile cracking and yielding of the steel reinforcement. In addition, nonlinearity can arise from second order bending effects in geometrically slender walls.

This chapter presents the behavioural model used to define the interaction diagram between axial compression and out-of-plane bending moment, as well as the sensitivity analyses carried out to determine the effect of the variation in the most important parameters (reinforcement ratio, compressive strength, thickness) on P-M interaction diagram.

3.2 Stress-strain behaviour for Load-Bearing Walls

3.2.1 Stress-strain relationship - Masonry

In this research, the constitutive law for the material is constructed using a model proposed by Priestley and Elder (1983), in which the maximum stress occurs at a strain equal to 0.0015. This model has been shown to have a good agreement with experimental data for unconfined and confined masonry (Moosavi, 2017). Moosavi (2017) revised the strain value to 0.002 based on more recent data (Drysdale and Hamid, 2005), and the model with the revised strain was adopted in this study. Equations (3.1) and (3.2) are used to calculate the relationship between the stress (σ) and the strain (ε) on masonry walls.

$$\sigma = \begin{cases} f'_m \left[\frac{2\varepsilon}{0.002} - \left(\frac{\varepsilon}{0.002}\right)^2\right], & \varepsilon < 0.002 \\ f'_m[1 - Z(\varepsilon - 0.002)], & 0.002 < \varepsilon < \varepsilon_{0.2u} \\ 0.2f'_m, & \varepsilon_{0.2u} < \varepsilon \end{cases} \quad (3.1)$$

Where:

$$Z = \frac{0.5}{\left(\frac{3 + 0.29f'_m}{145f'_m - 1000}\right) - 0.002} \tag{3.2}$$

Where f'_m is the maximum masonry compressive strength, $\varepsilon_{0.2u}$ is the strain where the constant stress initiates, and Z is a parameter that controls the slope of the linear falling branch ($0.002 < \varepsilon < \varepsilon_{0.2u}$). Figure 3.1 shows the plot of the stress-strain relationship given by Equation 3.1.

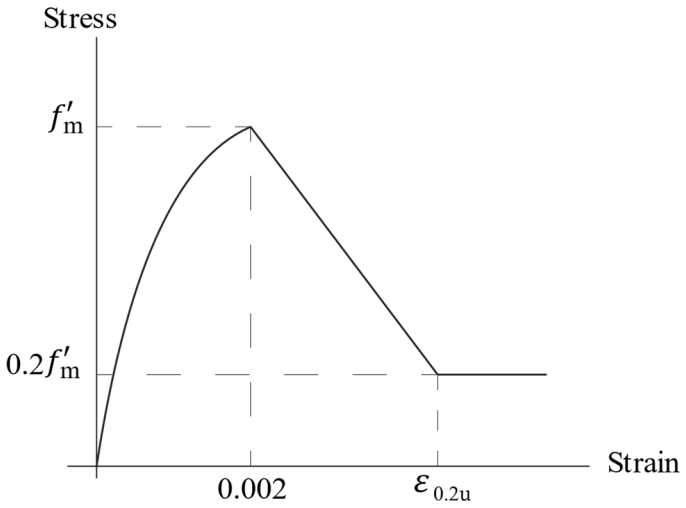

Figure 3.1: Stress-strain relationship for masonry

3.2.2 Stress-strain relationship - Concrete

In this investigation, the curve used for concrete stress-strain relationship is the one proposed by Thorenfeldt et al. (1987). The Thorenfeldt curve not only works well for most normal strength concrete but also for high-strength concrete, and it is one of the most common stress-strain relationship curves found in the literature. The concrete stress (fc) is calculated using Equations (3.3) – (3.6):

$$fc(\varepsilon_c) = f'_c \frac{n(\frac{\varepsilon_c}{\varepsilon_0})}{(n-1) + (\frac{\varepsilon_c}{\varepsilon_0})^{nk}} \tag{3.3}$$

Where:

$$n = 0.8 + \frac{f_c'}{17.2} \tag{3.4}$$

$$\varepsilon_0 = \frac{f_c'}{E_c}\left(\frac{n}{n-1}\right) \tag{3.5}$$

$$k = \begin{cases} 1, & \varepsilon_c \leq \varepsilon_0 \\ max\left(\begin{matrix} 0.67 + \frac{f_c'}{62} \\ 1 \end{matrix}\right), & \varepsilon_c > \varepsilon_0 \end{cases} \tag{3.6}$$

Where f_c' is the maximum concrete compression stress, ε_c is the concrete strain, ε_0 is the concrete strain at peak stress, E_c is the concrete modulus of elasticity, n and k are shape modifier parameters.

Figure 3.2 shows a plot of the stress-strain relationship given by Equation 3.3.

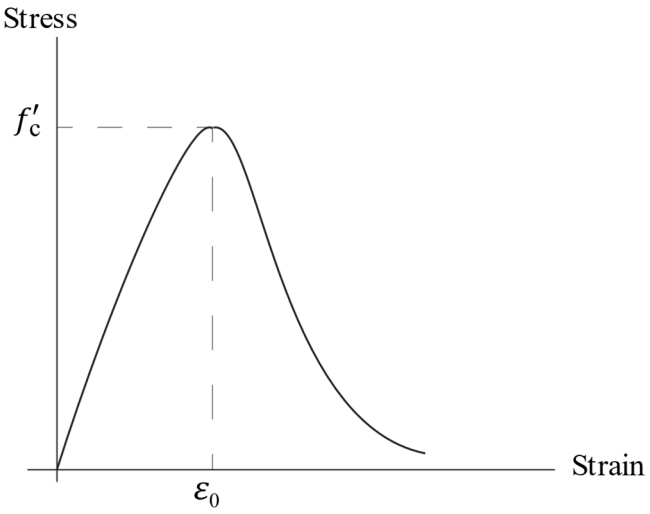

Figure 3.2: Stress-strain relationship for concrete

3.2.3 Stress-strain relationship – Steel Rebar

In this study, the stress-strain relationship for steel reinforcement is assumed to be elastic-perfectly plastic that is a model broadly used in the literature, this model enables us to show behaviour in the elastic range and the plastic range within the same model. The steel reinforcement stress (σ_s) is calculated using Equation (3.7).

$$\sigma_s = \begin{cases} E_s\varepsilon_s, & \varepsilon_s < \varepsilon_y \\ f_y, & \varepsilon_s \geq \varepsilon_y \end{cases} \tag{3.7}$$

Where E_s is the steel modulus of elasticity, ε_s is the steel reinforcement strain, ε_y is the steel yield strain, and f_y is the steel yield strength. The stress-strain relationship for steel reinforcement is shown in Figure 3.3.

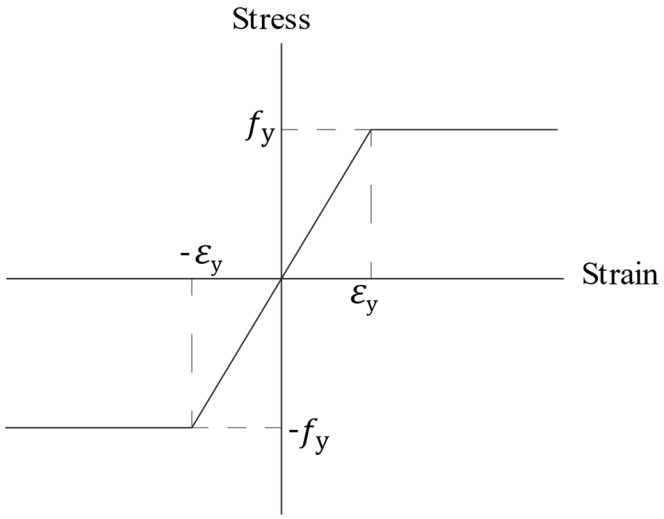

Figure 3.3: Stress-strain relationship for reinforcement steel

3.3 Behavioural Model for Non-slender Walls

The outcome of the behavioural model is an interaction diagram. The interaction diagram represents the structure's capacity (strength) against a combined action of axial load and bending moment. The strength of a cross section of the structural element is calculated based on three mechanics principles: equilibrium, strain compatibility, and constitutive relationships of the materials. Failure of the cross section can occur by yielding of tensile reinforcement, tensile cracking of masonry or concrete, crushing of extreme compression fibre at the ultimate compressive strain or any combination of the three criteria. If slenderness effects are taken into account, a fourth failure mechanism at the element level is introduced (buckling or geometrical failure) – however, second-order effects are not part of the scope of this study. The standard ultimate compressive strain in masonry (CSA S304-14) is taken as ε_{mu}=0.003 whereas the concrete crushing strain (CSA A23.3-19) is taken as ε_{cu}=0.0035.

A P-M interaction diagram for the wall section is built by adjusting the locations of the neutral axis of the section, while simultaneously setting the strain at the extreme compression fibre to be equal to the crushing strain. For each case, the stresses in the materials are calculated using the strain distribution and the relevant material constitutive relationships. The strain distribution is assumed to be linear, as the thickness of the wall-section is usually significantly smaller than the wall height (i.e., Bernoulli theory applies). Internal forces can be calculated from the material stresses, summed over the area of the different components of the section. The resulting internal forces and moments are then plotted as shown in Figure 3.4.

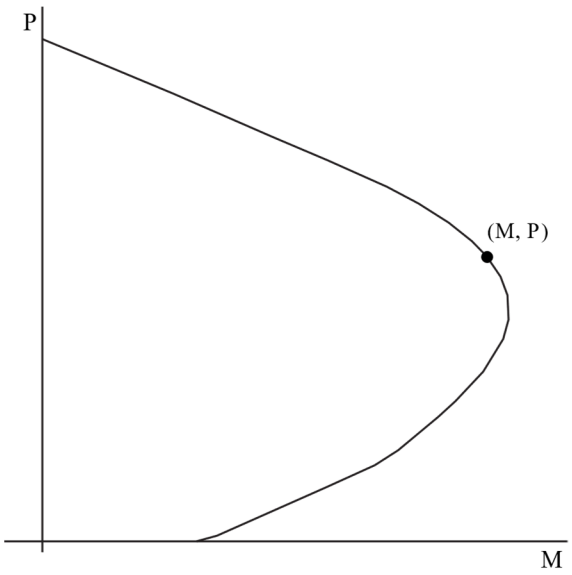

Figure 3.4: P-M interaction diagram.

3.3.1 The nominal and factored resistances

The limit-state design (LSD) (explained in chapter 2) states that the design of a structural member is satisfactory if the factored load effects are smaller than or equal to the factored design resistance (Equation 3.8):

$$\phi R_n \geq \gamma S_n \tag{3.8}$$

Where ϕ is the material strength reduction factor that accounts for variability of material properties and dimensions of structural elements, R_n is the nominal resistance or the true resistance of a structural element, and γ is the so-called load factor, used to account for the variability of loading

and the probability of having loads from different sources simultaneously. The parameter γ depends on the type of load. Finally, the load effect S_n corresponds to a specific nominal load or a load combination acting on the member.

Analyzing the terms on the left-hand side in Equation 3.8, it follows that two different strengths of a structural element can be considered. The nominal resistance (R_n) and the factored or design resistance (ϕR_n).

Applying the same logic to a wall, it turns out that the behavioural model can be used to obtain both the nominal interaction diagram and the factored interaction diagram. The nominal interaction diagram represents the true strength of the section; therefore, it is built by setting the material resistance factor ϕ=1.00 and the actual or curvilinear stress strain relationship of the materials should be used. Conversely, the factored or design interaction diagram is determined by setting the strength reduction factors to values to be less than 1. The Canadian masonry standard S304 and the Canadian concrete standard A23.3 state material strength reduction factors of $\phi_m = 0.60$, $\phi_c = 0.65$, $\phi_s = 0.85$ for masonry, concrete and steel structures respectively. The standards also direct designers to use rectangular stress blocks in lieu of the actual stress-strain relationships for the materials. Figure 3.5 shows the nominal and factored interaction diagrams.

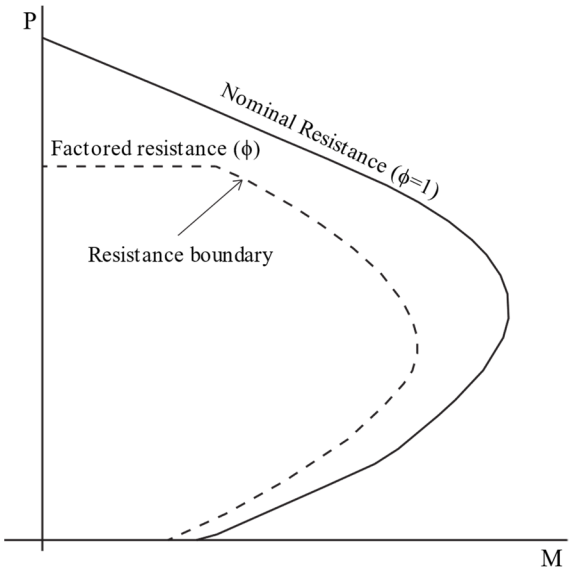

Figure 3.5: P-M interaction diagram.

In the next sections, the behavioural model for masonry and concrete walls is shown. The behavioural models of singly and doubly reinforced walls constructed out of concrete and masonry are derived and used to illustrate the differences between these two materials.

3.3.1.1 Behavioural Model – Singly Reinforced (SR) Masonry Walls

Figure 3.6 illustrates the procedure to obtain an interaction diagram described in section 3.3 for a singly reinforced (SR) masonry wall.

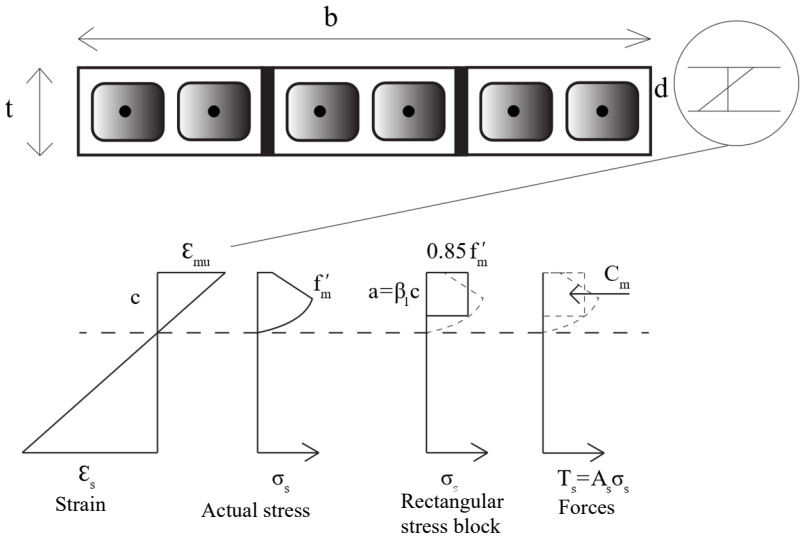

Figure 3.6: Strain profile, stress profile, and resultant forces for SR masonry walls.

The design axial force (P_{fr}) and design bending moment (M_{fr}) for the P-M factored interaction diagram are determined by the following equations:

$$P_{fr} = C_m - T_s \tag{3.9}$$

$$M_{fr} = C_m(\frac{t}{2} - \frac{a}{2}) \tag{3.10}$$

Where C_m and T_s are the masonry compression force and reinforcement steel force, respectively. These are calculated with the material strength reduction factor taken as ϕ_m=0.60 and ϕ_s=0.85, as indicated in Canadian standard S304. Equations (3.11) and (3.12) show C_m and T_s. The nominal resistance moment (M_r) and axial load (P_r) are obtained by taking the strength reduction factors equal to 1.00 and the curvilinear stress-strain relationships.

$$C_m = \phi_m 0.85 f'_m \beta_1 c b \tag{3.11}$$

$$T_s = \phi_s A_s f_y \tag{3.12}$$

3.3.1.2 Behavioural Model – Doubly Reinforced (DR) Masonry Walls

Figure 3.7 shows the strain and stress profiles, rectangular stress block, and forces for doubly reinforced (DR) masonry walls.

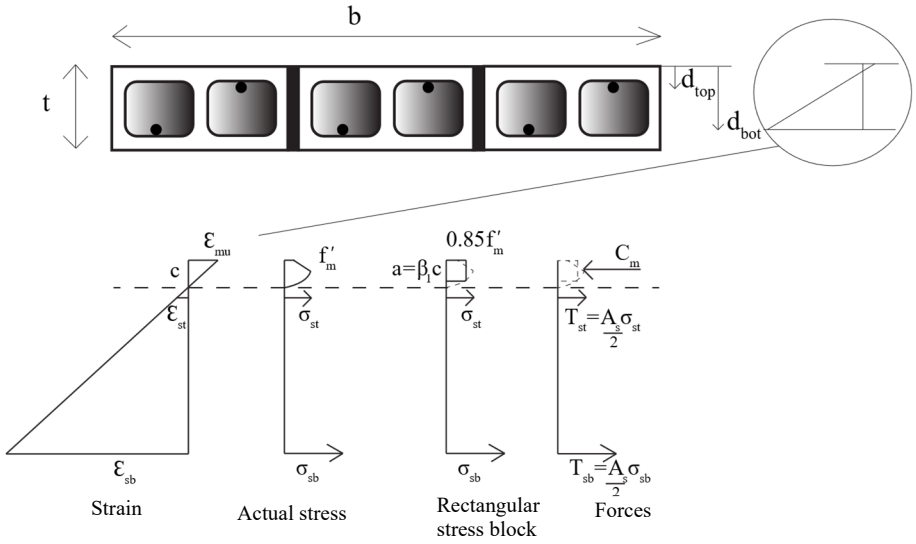

Figure 3.7: Strain profile, stress profile, and resultant forces for DR masonry walls.

For doubly reinforced masonry wall, following the same procedure described in section 3.3, P_{fr} and M_{fr} can be determined. For this case, the tension force in the steel at the top (T_{st}) of the wall section is considered:

$$P_{fr} = C_m - T_{sb} - T_{st} \tag{3.13}$$

$$M_{fr} = C_m\left(\frac{t}{2} - \frac{a}{2}\right) + T_{sb}\left(d_{bot} - \frac{t}{2}\right) - T_{st}\left(\frac{t}{2} - d_{top}\right) \tag{3.14}$$

Where C_m is the compression force in the masonry, d_{bot} and d_{top} are the effective depths of the bottom and top reinforcement steels, T_{sb} and T_{st} are the tension force in the steel located at the bottom and at the top of the wall cross section, respectively. Equations (3.15) and (3.16) show T_{sb} and T_{st}.

$$T_{sb} = \phi_s \frac{A_s}{2}\sigma_{sb} \tag{3.15}$$

$$T_{st} = \phi_s \frac{A_s}{2} \sigma_{st} \tag{3.16}$$

σ_{sb} and σ_{st} are the stresses at the bottom and top reinforcement steel.

The Canadian masonry design standard CSA S304-14 (Clause 10.2.7) allows compression to develop in steel reinforcement only if it is adequately tied. In this study, compression in steel reinforcement is ignored, as tying reinforcement is not the normal practice in masonry wall construction. This fact is one of the major differences in building P-M interaction diagrams between masonry and concrete, as the bars in reinforced concrete walls usually will be laterally restrained by horizontal bars.

Specifically, the Canadian concrete design standard CSA A23.3-19 Clause 14.1.8.7 states that distributed vertical reinforcement required as compression reinforcement shall be tied and detailed in accordance with the requirements for column reinforcement specified in Clause 7, except that ties may be omitted if the area of vertical steel is less than $0.005A_g$, and the size is 20M or smaller, both requirements are met in this study (see section 4.8 in the next chapter). In addition, Clause 10.10.4 of the Canadian concrete design standard CSA A23.3-19 provides an equation for walls that are both tied and not tied along the full length. Both equations allow for compression in the steel reinforcement.

3.3.1.3 Behavioural Model – Singly Reinforced (SR) Concrete Walls

Figure 3.8 illustrates the procedure described in section 3.3 for a singly reinforced (SR) concrete wall.

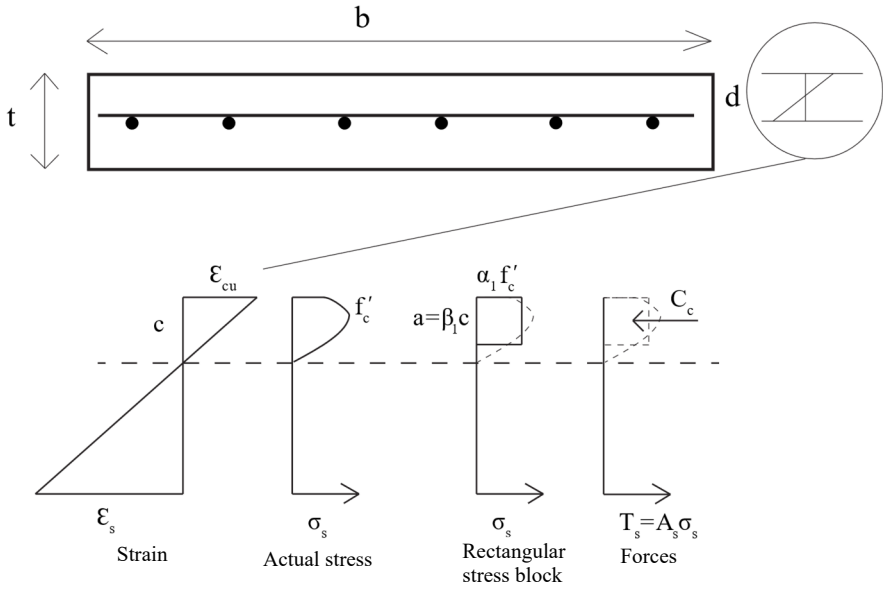

Figure 3.8: Strain profile, stress profile, and resultant forces for SR concrete walls.

Where α_1 and β_1 are the stress block parameters. For this case, the design axial force (P_{fr}) and design bending moment (M_{fr}) for the P-M factored interaction diagram are determined by the following equations:

$$P_{fr} = C_c - T_s \tag{3.17}$$

$$M_{fr} = C_c(\frac{t}{2} - \frac{a}{2}) \tag{3.18}$$

Where C_c is the concrete compression force, T_s is the tension force in the steel. These are calculated with the material reduction factor taken as ϕ_c=0.65 and ϕ_s=0.85, as indicated in Canadian standard A23.3. Equations (3.19) and (3.20) show C_C and T_s. The nominal resistance moment (M_r) and axial load (P_r) are obtained by taking the strength reduction factors equal to 1.00 and the curvilinear stress-strain relationships.

$$C_C = \phi_C \alpha_1 f'_C \beta_1 cb \tag{3.19}$$

$$T_s = \phi_s A_s f_y \tag{3.20}$$

3.3.1.4 Behavioural Model – Doubly Reinforced (DR) Concrete Walls

Figure 3.9 shows the strain and stress profiles, rectangular stress block, and forces for doubly reinforced (DR) concrete walls.

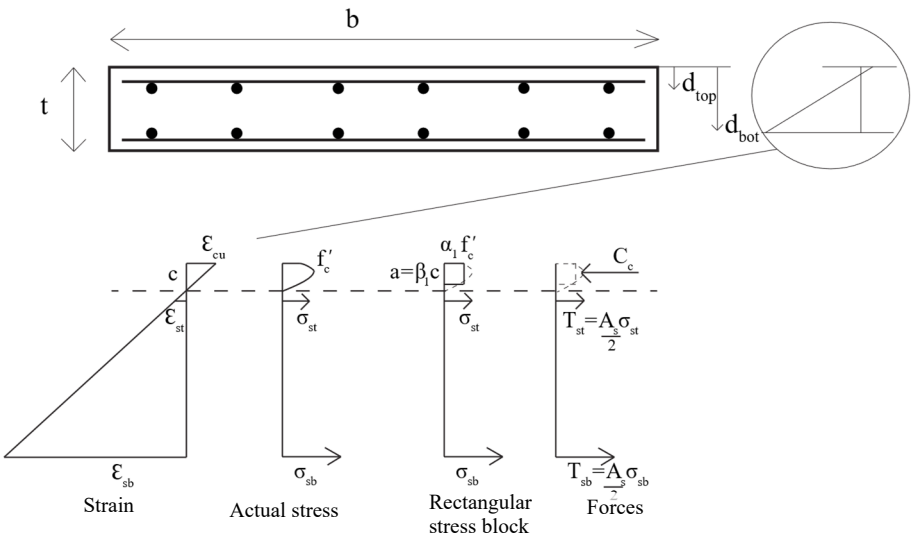

Figure 3.9: Strain profile, stress profile, and resultant forces for DR concrete walls.

For DR concrete wall, following the same procedure described in section 3.3, P_{fr} and M_{fr} can be determined. For this case the tension force in the steel at the top (T_{st}) of the wall section is considered:

$$P_{fr} = C_c - T_{sb} - T_{st} \tag{3.21}$$

$$M_{fr} = C_c\left(\frac{t}{2} - \frac{a}{2}\right) + T_{sb}\left(d_{bot} - \frac{t}{2}\right) - T_{st}\left(\frac{t}{2} - d_{top}\right) \tag{3.22}$$

Where C_c is the concrete compression force, d_{bot} and d_{top} are the effective depths of the bottom and top reinforcement steels, T_{sb} and T_{st} are the tension force in the steel located at the bottom and at the top of the wall cross section, respectively. Equations (3.23) and (3.24) show T_{sb} and T_{st}.

$$T_{sb} = \phi_s \frac{A_s}{2}\sigma_{sb} \tag{3.23}$$

$$T_{st} = \phi_s \frac{A_s}{2}\sigma_{st} \tag{3.24}$$

σ_{sb} and σ_{st} are the stresses at the bottom and top reinforcement steel.

The behavioural models were encoded in computer language and used to plot the P-M interaction diagrams of the walls. The computer codes of the behavioural models were developed based on the one developed by Moosavi (2017) for singly reinforced masonry walls. The computer code is provided in Appendix A to this thesis.

3.3.1.5 Parameters for masonry and concrete walls - Summary

Table 3.1 summarizes the values of concrete and masonry crushing strain, ε_{mu} and ε_{cu}, stress block parameters, α_1 and β_1, material resistance factors for masonry and concrete, ϕ_m and ϕ_c, and the reinforcement steel, ϕ_s, stress-strain relationships, used to derive the interaction diagrams.

Table 3.1: Parameters for the nominal interaction diagram, and for the factored interaction diagram computation according to Canadian Standards Association (CSA).

P-M	Factor	Masonry	Concrete
Factored interaction diagram	ε_u	0.003	0.0035
	ϕ_m and ϕ_c	0.60	0.65
	ϕ_s	0.85	0.85
	α_1	0.85	0.85-0.0015f_c'
	β_1	0.80	0.97-0.0025f_c'
Nominal interaction diagram	Stress-strain relationship	Priestley and Elder curve	Thorenfeldt curve
	Stress-strain steel	Elastic-perfectly plastic	Elastic-perfectly plastic

3.3.2 Loads side of the reliability equation – Optimal design

Masonry and concrete walls must resist a factored axial load (P_f) plus a factored moment (M_f), in addition to the out-of-plane factored shear force (V_f), which is assumed not to govern in this study. Combinations of axial load and moment that fall inside the design resistance boundary of the interaction diagram represent "safe" design scenarios and points that are outside represent "unsafe" designs. An optimal design, this is, the most economical while still safe, is to choose the wall properties and materials in such a way that the factored axial load (P_f) and factored moment (M_f) fall exactly at the boundary of the PM factored interaction diagram (Figure 3.10).

Most reliability analyses assume an optimal design approach. Therefore, to define the loads (S) in the limit state function ($g = R - S$), the factored load (γS) can be taken to be equal to the factored resistance of the wall (ϕR_n).

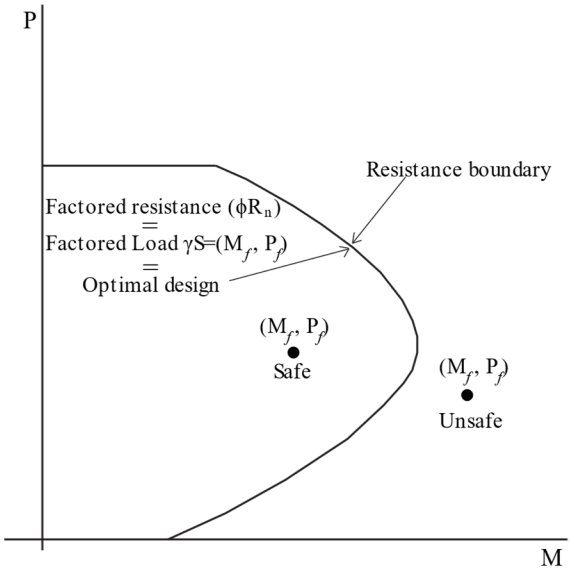

Figure 3.10: Optimal design on the P-M interaction Diagram.

3.4 Sensitivity Analysis

Using the behavioural model for masonry and concrete walls described above, the sensitivity of the P-M interaction diagram to different parameters, such as reinforcement ratio, compressive strength, and wall thickness, is presented in this section. The computer code developed in the previous section and presented in Appendix A was used to plot interaction diagrams for different walls and for different reinforcement ratios, material compressive strength, and wall thickness.

3.4.1 Reinforcement Ratio Variation

Figure 3.11 shows the effect of varying reinforcement ratios on the interaction diagram for singly and doubly reinforced masonry and concrete walls over the range of evaluated reinforced ratios. The thickness and compressive strength of both types of walls were kept constant to have and objective comparison.

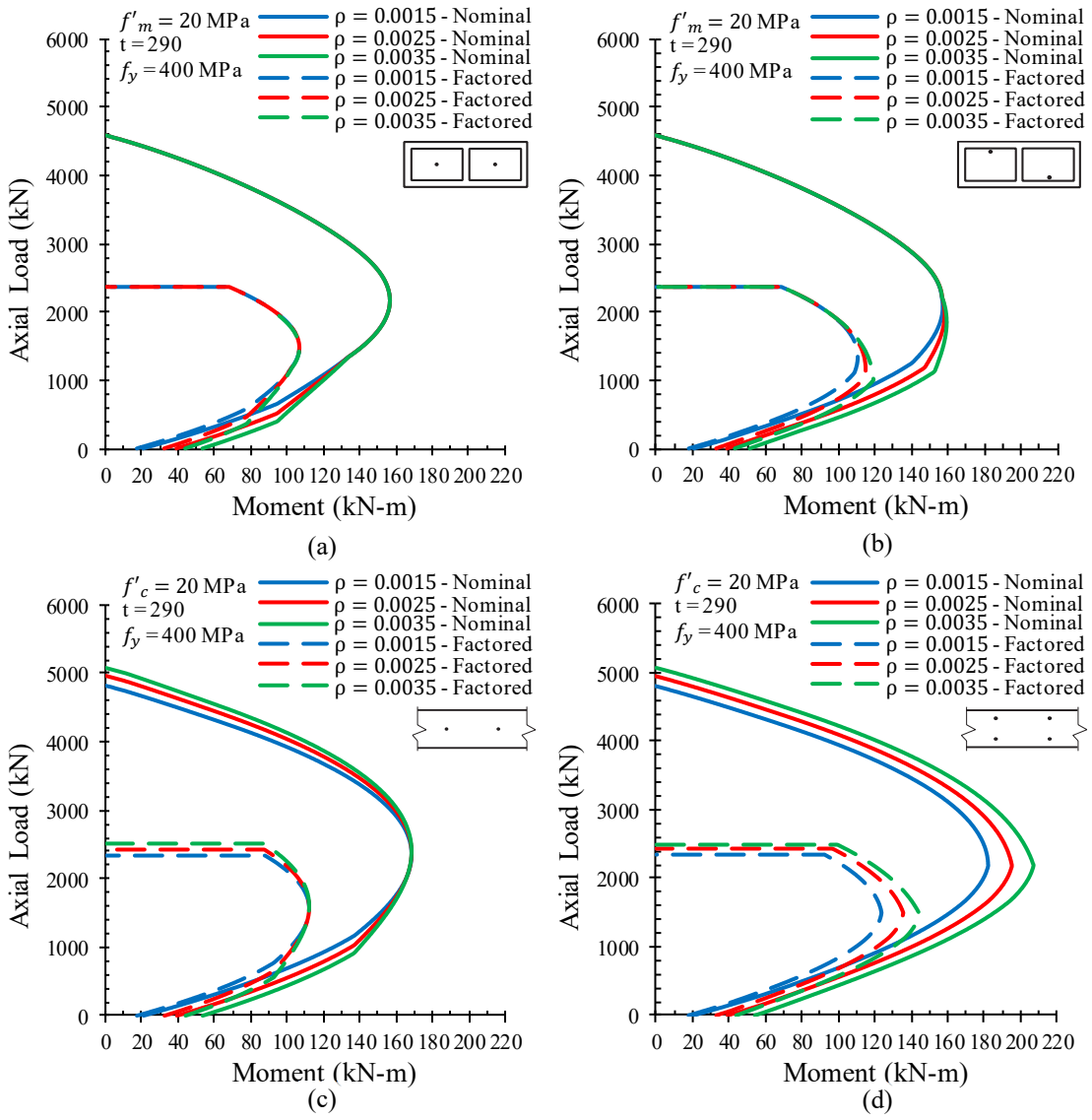

Figure 3.11: Effect of the change in the reinforcement ratio: (a) Singly reinforced masonry wall; (b) Doubly reinforced masonry wall; (c) Singly reinforced-concrete wall; (d) Doubly reinforced-concrete wall.

Figures 3.11a and 3.11b show the interaction diagrams for the singly and doubly reinforced masonry walls, while Figures 3.11c and 3.11d are for reinforced-concrete walls.

The change in the reinforcement ratio only had an effect in the tension zone of the interaction diagram of masonry walls. The lines of the interaction diagrams for masonry are bundled together within the region of high axial compression force, only separating in the tension region where the moments are large. This is true for all reinforcement ratios analyzed. The reason for this is the fact that in masonry constructions tying reinforcement is not the normal practice, so compression in

reinforcing bars is ignored (CSA S304-14). In contrast, for concrete walls (Figures 3.11c and 3.11d), the compression in steel reinforcement is not ignored (CSA A23.3-19). This results in sensitivity to the capacity throughout the entire curves, as the steel reinforcement is always active, either in tension or compression. Overall, the P-M diagrams of singly reinforced concrete walls show less sensitivity to changes in reinforcement ratio, compared to those obtained for doubly reinforced concrete walls.

For both materials, masonry and concrete, a double layer of reinforcement increases the capacity of the wall to take moments compared to placing the reinforcing bars in the center of the wall. The increment in capacity is more noticeable for concrete walls compared to masonry walls, because in concrete walls both layers of reinforcement are activated, unlike masonry walls where the only reinforcement layer that is activated is the one in tension.

3.4.2 Compressive Strength Variation

Compressive strength is a very important parameter, commonly used to measure the quality of concrete and masonry. The interaction diagrams were plotted for masonry and concrete walls, using different compressive strengths while keeping the reinforcement ratio and thickness of the walls constant.

As shown in Figure 3.12, the strengths of the walls in the compression-controlled zone (where moments are low) are directly proportional to the material compressive strengths of the wall material. Similarly, the maximum combination of bending moment and axial force a wall can withstand increased with material compressive strength. However, the compressive strength had no effect on the maximum strength of the wall in pure bending.

As can be seen, for both materials, masonry and concrete walls, the maximum factored axial load are similar, having a little increment for reinforced-concrete walls because of the compressive resistance of the reinforcing bars. However, the difference between masonry and concrete walls in these points are more noticeable for the maximum nominal axial load, this is because these curves (nominal resistances) are constructed using the actual or curvilinear stress strain relationship of the materials ,which are different, the presence of compressive resistance of the reinforcing bars, and the ultimate compressive strain. The standard ultimate compressive strain in masonry (CSA S304-

14) is taken as ε_{mu}=0.003 whereas the concrete crushing strain (CSA A23.3-19) is taken as ε_{cu}=0.0035.

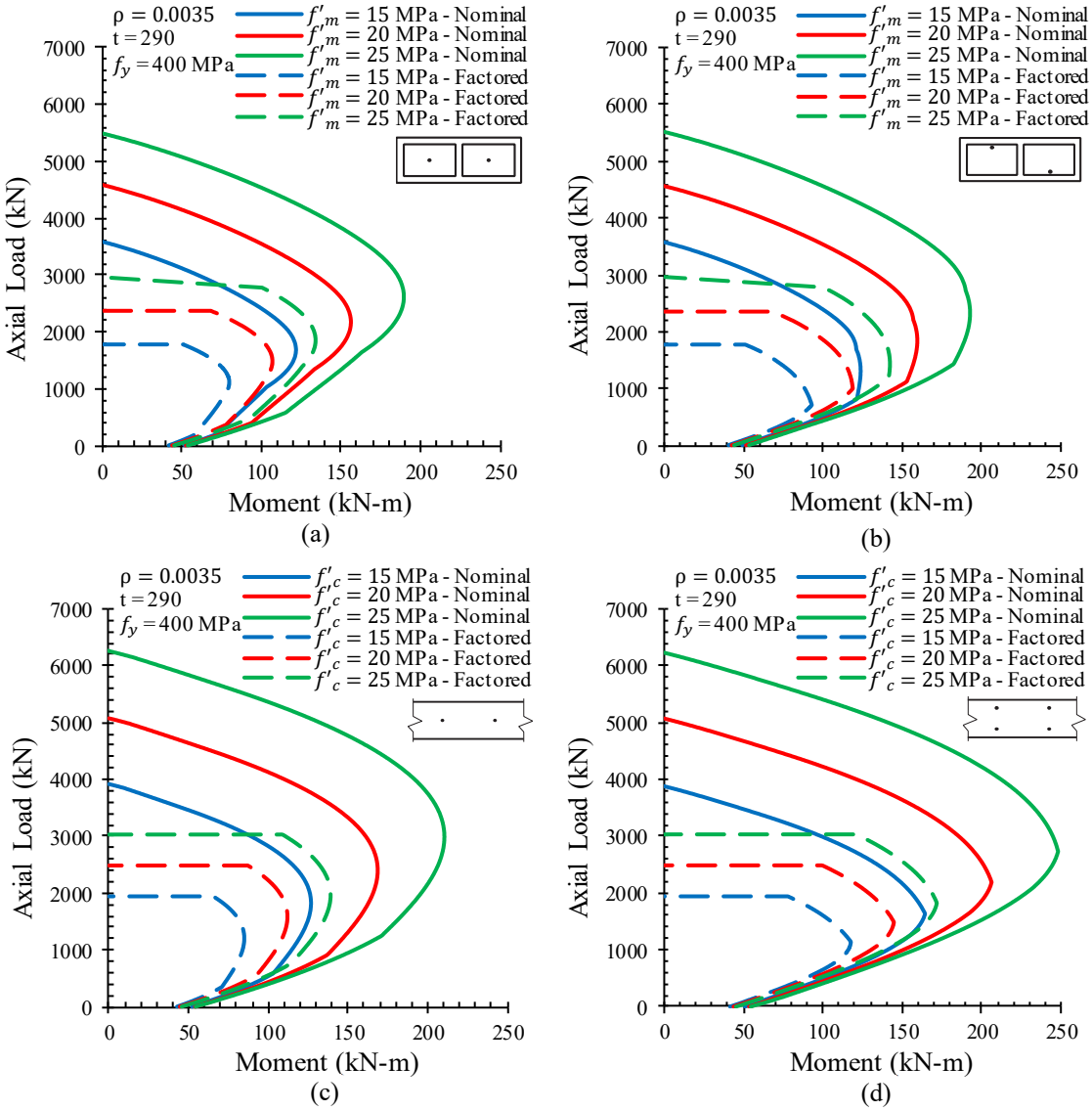

Figure 3.12: Effect of the change in the compressive strength: (a) Singly reinforced masonry wall; (b) Doubly reinforced masonry wall; (c) Singly reinforced-concrete wall; (d) Doubly reinforced-concrete wall.

3.4.3 Thickness Variation

As shown in Figure 3.13, the thickness variation is very important to the strength of the wall. It has an effect on the whole interaction diagram as demonstrated by the way the lines corresponding to wall thickness are separated from each other.

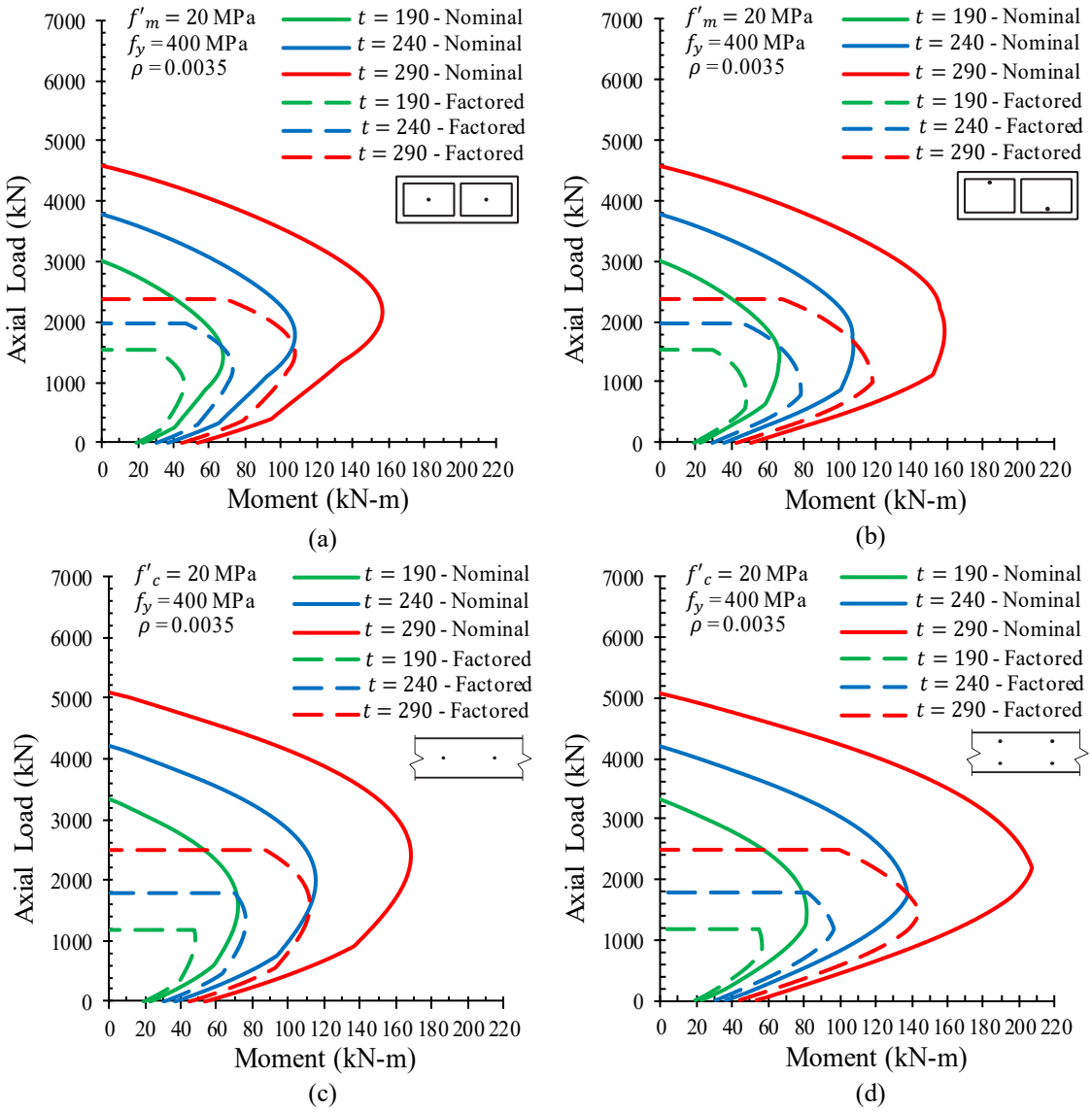

Figure 3.13: Effect of the change in the thickness: (a) Singly reinforced masonry wall; (b) Doubly reinforced masonry wall; (c) Singly reinforced-concrete wall; (d) Doubly reinforced-concrete wall.

The capacity of the wall, as indicated by the P-M interaction diagram, is highly influenced by the changes in its thickness. When the thickness of the wall increases, the geometric area of the cross-section also increases, resulting in an increase in the masonry and compressive forces available to resist moments and axial loads. Moreover, an increase in thickness leads to a greater moment arm, which in turn enhances the moment resistance of the cross-section.

3.4.4 Summary of the sensitivity analysis

The effect of different parameters on P-M interaction diagrams of reinforced masonry and reinforced-concrete walls have been investigated and the results is used in the parametric reliability analysis in the next chapter. Table 3.2 shows a summary of the observations from the sensitivity analysis conducted.

Table 3.2: Summary of the sensitivity analysis.

Parameter	Case	Region where sensitivity is observed	
		Compression-Controlled	Tension-Controlled
Reinforcement Ratio (ρ)	Singly and Doubly reinforced masonry wall	NO**	YES**
	Singly reinforced-concrete wall*	YES	YES
	Doubly reinforced-concrete wall	YES	YES
Compressive Strength (f'_m, f'_c)	All the walls	YES	NO
Thickness Variation (t)	All the walls	YES	YES

*The point of the maximum moment remains unchanged

**YES: changing the parameter have effect in the specified zone, NO: changing the parameter do not have effect in the specified zone.

4 STRUCTURAL RELIABILITY ANALYSIS OF MASONRY AND CONCRETE WALLS, RESULTS AND DISCUSSION

4.1 Introduction

This chapter presents the methodology to evaluate the reliability levels of masonry and concrete walls and the findings. Firstly, the definition of the limit state function for gravity loads is introduced, the statistical information for loading and the resistance parameters are discussed, and the properties of the analyzed walls are shown. Secondly, parametric analyses conducted on masonry and concrete walls are presented. Lastly, comparisons of the reliability levels of singly and doubly reinforced masonry and concrete walls are discussed.

4.2 The Structural Reliability Approach

As explained in Chapter 2, to perform a reliability analysis, the resistance (R) and the load (S) components of the limit state function ($g = R - S$) must be determined. To determine the resistance and load components, the nominal and factored P-M interaction diagrams of the structural element are required, as discussed in Chapter 3. This needs to be done for both masonry and concrete walls.

The nominal interaction diagram is determined from the behavioural model (section 3.3) by setting the strength reduction factor of the material, ϕ, equal to 1.00 (CSA S304-14; CSA A23.3-19). The factored interaction diagram of the material is determined by setting the strength reduction factors to values that are smaller than 1. For instance, $\phi_m = 0.60$, $\phi_c = 0.65$, and $\phi_s = 0.85$ for masonry, concrete and steel materials respectively (CSA S304-14; CSA A23.3-19). Figure 4.1a shows a typical nominal and factored interaction diagram. The factored interaction diagram represents the standard-compliant, allowable resistance of the structure, while the nominal resistance is the actual resistance of the structure. In the reliability analysis procedure, the resistance component (R) is obtained from the nominal interaction diagram, and the load component (S) is obtained using the factored interaction diagram by applying the concept of optimal design (section 3.3.2).

Optimal design is defined as the most economical, yet still safe scenario, where the designer chooses the properties of the structural element and materials in such a way that the factored axial

load (P_f) and factored moment (M_f) fall exactly at the boundary of the interaction diagram as shown in Figure 4.1b.

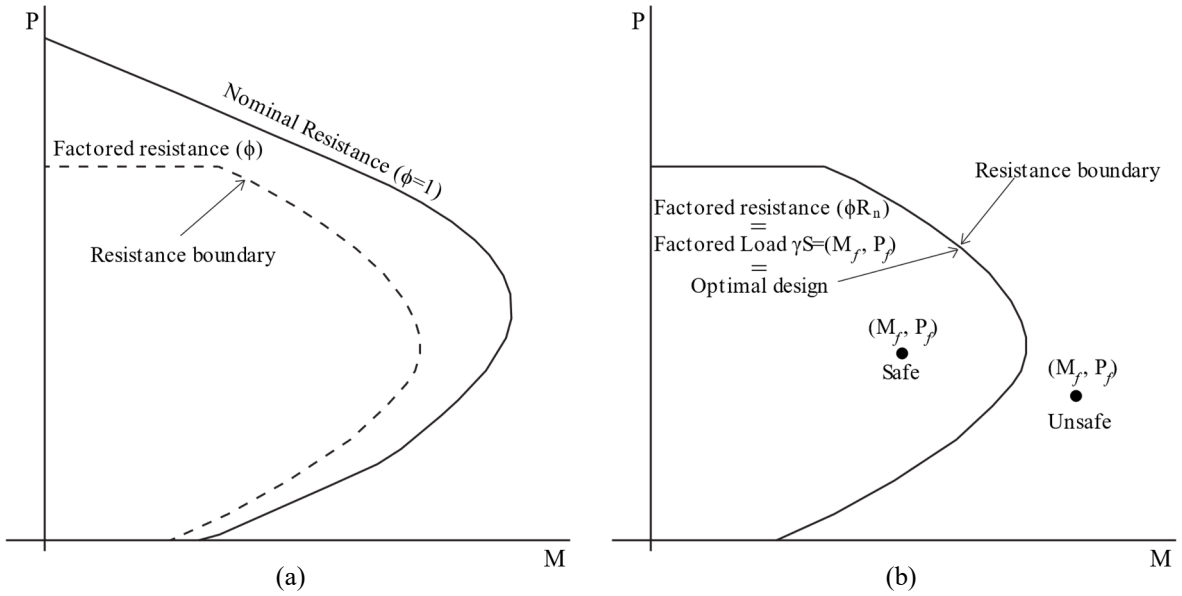

Figure 4.1: (a) Nominal and factored P-M interaction diagrams; (b) Optimal design on the P-M interaction diagram.

4.3 Limit state function for Eccentrically Applied Gravity Loads

To determine how the *R* and *S* components are related, a limit state function is necessary. Tychy and Vorlicek (1962) pointed out that the safety levels depend on how the limit state function is defined. For instance, for a given load combination effect (P_f and M_f), expressed by a point *S* on the P-M interaction diagram (Figure 2.6 reproduced below as Figure 4.2 for clarity), three possible distances can be drawn to the interaction curve, these can be seen as the reserve of strength that a structural element possesses, and three possible of safety measures can be indicated.

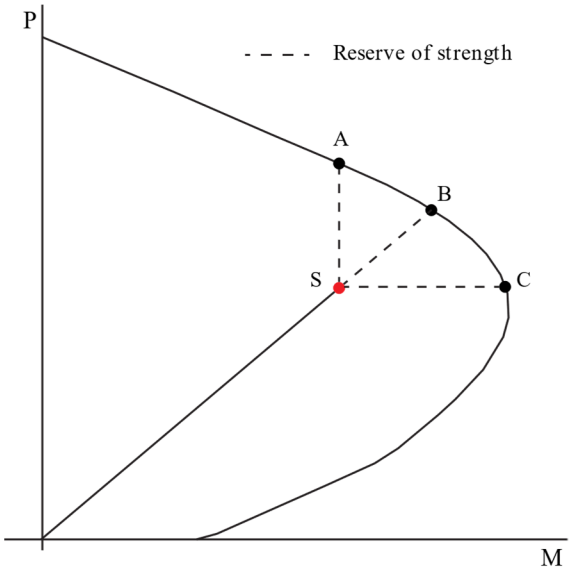

Figure 4.2: Three possible Limit-State Functions on the P-M interaction diagram.

The limit-state represented by line SA is known as "fixed moment." For this function, the axial load is assumed to be the only load parameter that is permitted to vary according to a suitable probability distribution while the moment remains constant. Line SB, representing a "fixed eccentricity," illustrates the case in which both variables, the axial load and the bending moment, are assumed to increase in the same proportion. This is the case for a short column subjected to an eccentric axial load, in which the eccentricity is kept constant, but the load is allowed to vary. Finally, Line SC, called the "fixed axial load" function, represents a situation in which the moment is allowed to vary but the axial load remains constant.

The fixed eccentricity approach is widely used to solve reliability problems for non-slender walls and columns under concentric and eccentric axial load. In this study, the fixed-eccentricity limit state was used, similarly as Moosavi (2017). The element experiences a constant moment along its height (h), that is proportional to the axial load (P) multiply by the eccentricity (e) (Figure 4.3).

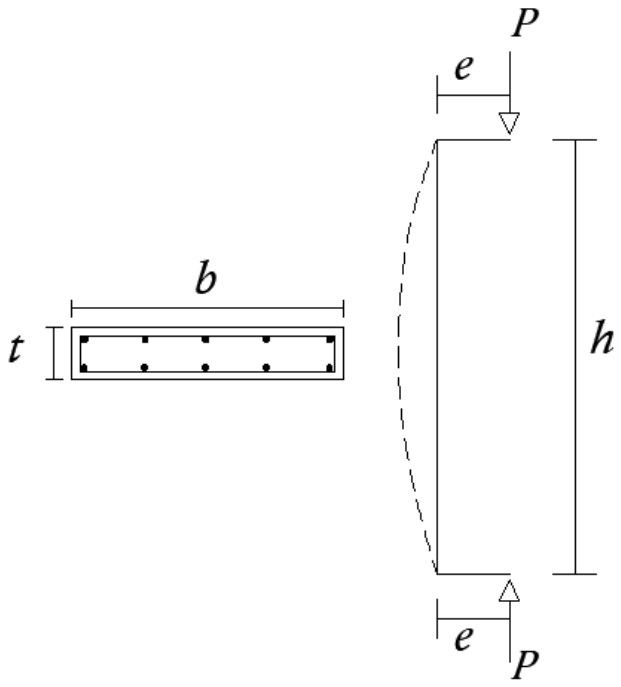

Figure 4.3: Wall under axial load and equal eccentricities.

As discussed in the previous section, the response of a non-slender structural element subjected to eccentric gravity load can be represented by an interaction diagram (Figure 4.4). *R(X)* is the probability distribution curve for resistance that is derived from the nominal resistance, and *S(X)* is the probability distribution curve for loads that is derived from the nominal loads. The curve labelled *nominal loads* represents the arbitrary unfactored loads acting on the structure that is obtained from the factored resistance curve and using the concept of optimal design previously described. *X* represents the vector containing all random variables such as those related to geometrical, material, load and workmanship parameters.

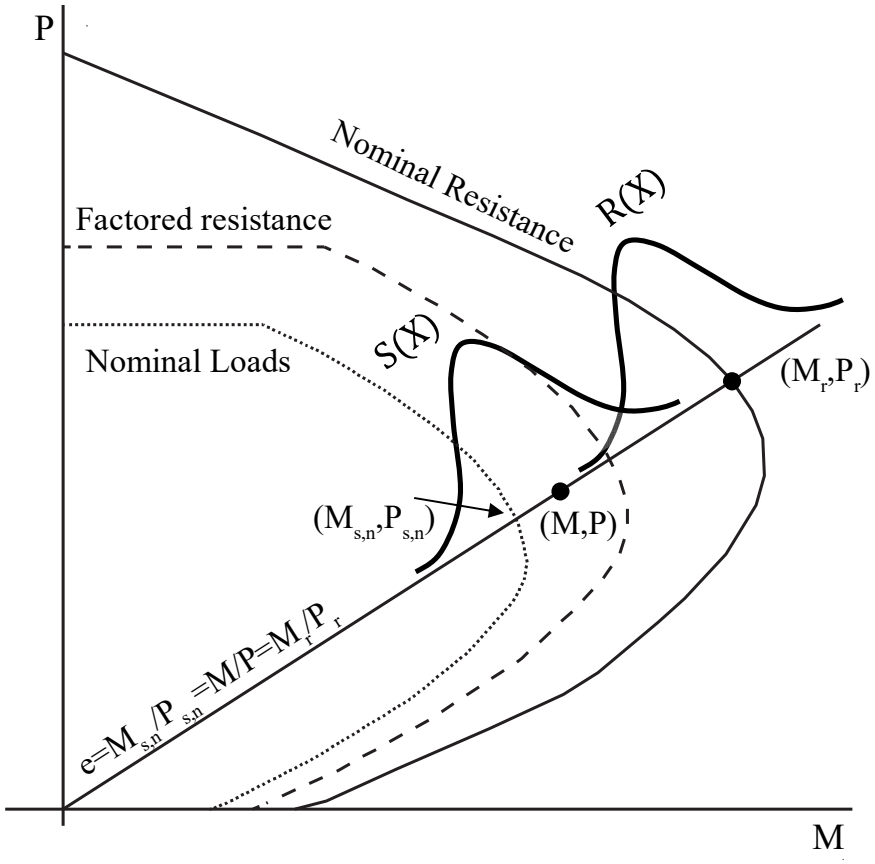

Figure 4.4: P-M interaction diagram with nominal and factored resistance, and nominal load curves.

(M_r, P_r) is a point on the probability distribution curve for resistance, (M, P) is a point on the probability distribution curve for loads, and ($M_{s,n}$, $P_{s,n}$) is a point on the nominal load curve. The eccentricity of the load is denoted e and is defined as the ratio of the resulting moment to the applied axial load. As mentioned in the previous section, the nominal resistance diagram is constructed using the principles of mechanics of materials, equilibrium, strain compatibility, and constitutive relationships, taking into consideration the geometric and material properties of the structural element, and using strength reduction factors $\phi = 1$. Conversely, the factored or design interaction diagram is determined by setting the strength reduction factors to values less than 1. The Canadian masonry standard S304 and the Canadian concrete standard A23.3 state material resistance factors of $\phi_m = 0.60$, $\phi_c = 0.65$, $\phi_s = 0.85$ for masonry, concrete and steel structures respectively, and the design standards allow for the use of a rectangular stress block.

Mathematically, the limit state function ($g(\boldsymbol{X})$) is expressed by Equation (4.1):

$$g(\boldsymbol{X}) = R(\boldsymbol{X}) - S(\boldsymbol{X}) \tag{4.1}$$

The resistance component (R) of the limit state function has the variables (M_r and P_r), representing the contributions by the moment resistance and axial load resistance. Similarly, the Load component (S) has the variables (M and P), representing the contributions of applied moment and axial force respectively. In practice, M and P exist as combined dead loads and live loads, denoted as M_D and M_L (dead and live moments), and P_D and P_L (dead and live axial loads).

For a constant eccentricity (Figure 4.4), the limit state function ($g(\boldsymbol{X})$) for reliability analysis can be re-cast as shown below:

$$g(X) = \sqrt{{M_r}^2 + {P_r}^2} - \sqrt{(M_D + M_L)^2 + (P_D + P_L)^2} \tag{4.2}$$

The resistance variables M_r and P_r are expressed in terms of the random variables related to the geometric and mechanical properties of the material such as material compressive strength, reinforcement yield stress, element (wall) thickness and width, and reinforcement bar location measured from compression face of the element. For the special case of masonry walls, a workmanship factor as one of the resistance random variables because workmanship affects the strength of masonry assemblies. Its value depends on the judgement and experience of the responsible engineer conducting the reliability analysis. The effect of the workmanship factor on the reliability of structural masonry is very significant. Based on limited experimental data and judgment, three sets of bias coefficients (ratio between mean value to nominal value) and coefficient of variations (COV) were proposed by Turkstra (1989) for the workmanship factor: 1.0 and 0.1 for well inspected, 0.8 and 0.15 for regularly inspected, and 0.7 and 0.2 for uninspected masonry. Moosavi and Korany (2014) based on the Turkstra study proposed a bias coefficient of 0.85 and a COV of 0.15 for regularly inspected masonry and these values were adopted in this study.

For a reliability analysis, the statistical means, variance (or standard deviations) of the random variables are used as inputs in the limit state equation to represent the resistance and the load components of the equation. The mean (μ) is also referred to as the first statistical moment of the

variables while the variance (or standard deviation σ) is referred to as the second statistical moments. In this study, the first and second statistical moments of the resistance random variables were adopted from previous studies (Moosavi, 2017).

To determine the first and second statistical moments for the load combination random variables (P_D, P_L, M_D, M_L), the nominal loads and the bias coefficients are required as input. The nominal loads are the unfactored load combinations. The bias coefficients are the ratio between the mean values to nominal loads. Therefore, having the nominal loads and the bias coefficients, the mean values of the load random variables can be determined. The bias coefficients and COV for loads have been adopted from Bartlett et al. (2003).

Usually, in the calibration of design standards, two generic procedures are used (Ellingwood et al. 1980, Israel et al. 1987). The first procedure considers that the total factored load effects are known. Then, the structural element is designed to resist the factored load effects. The second approach assumes that the actual structural element to be designed is given, and the total design load effect is assumed to be equal to the factored design resistance of that structural element (optimal design approach). The components of the design load effects associated with nominal dead load and nominal live load are obtained by using the total design load effect (which is known) and the ratios of nominal dead load to live load (which in this study are considered equal to one to represent the same level of dead and live load). This second procedure has been shown to be effective for various design cases (Hong, 1999) and was adopted in this study to determine the nominal loads.

Considering the load factors as per NBCC (2015) for dead load plus live load, the second procedure can be expressed as:

$$P_{fr} = 1.25\, P_{D,n} + 1.50\, P_{L,n} \tag{4.3}$$

$$M_{fr} = 1.25\, M_{D,n} + 1.50\, M_{L,n} \tag{4.4}$$

Where P_{fr}, M_{fr} and $P_{D,n}$, $P_{L,n}$, $M_{D,n}$, $M_{L,n}$ are the factored resistance and the nominal loads, respectively. To calculate the nominal loads it is necessary to assume the live-to-dead load ratios (α_P and α_M) for axial load and moment:

$$\alpha_P = \frac{P_{L,n}}{P_{D,n}} \tag{4.5}$$

$$\alpha_M = \frac{M_{L,n}}{M_{D,n}} \tag{4.6}$$

Substituting these values in Equations (4.3) and (4.4), it follows that,

$$P_{D,n} = \frac{P_{fr}}{1.25 + 1.50\alpha_P} \tag{4.7}$$

$$P_{L,n} = \frac{\alpha_P P_{fr}}{1.25 + 1.50\alpha_P} \tag{4.8}$$

$$M_{D,n} = \frac{\alpha_M M_{fr}}{1.25 + 1.50\alpha_M} \tag{4.9}$$

$$M_{L,n} = \frac{\alpha_M M_{fr}}{1.25 + 1.50\alpha_M} \tag{4.10}$$

An analysis of a variety of loadbearing masonry buildings performing by Moosavi and Korany (2014) revealed that the vast majority of live-to-dead load ratios are greater than 0.5 and less than 2.0. If only loads on floor and roof are considered for light wood flooring, the live load is higher than dead load. This translates into a live-to-dead load ratio higher than one. However, the self weight of the wall affects this ratio considerably. In this research, a value of live-to-dead ratio equal to 1.00 is adopted as an average value. It is important to note that axial load and the moment are not statistically independent because the bending moment is equal to the axial load multiplied by an eccentricity. Therefore, linear correlations are assumed between P_D and M_D and between P_L and M_L. Equations (4.7) to (4.10) are used to determine the nominal loads, which are then used to calculate their statistical means for reliability analysis.

4.4 Analysis procedure

In this study, the first order reliability method (FORM) (Madsen et al., 1986; Nowak, 2000) was used to assess the safety levels of non-slender masonry and concrete walls under combined axial load and out-of-plane bending. This method considers not only the means and coefficients of variation of the random variables but also the distribution type for each random variable.

A script was written in Mathematica programming language (Appendix A). The algorithm for the FORM procedure proposed by Rackwitz – Fiessler was followed in this research (section 2.2.4) to develop the script. To validate the computer code, reliability indices of a doubly reinforced-concrete wall obtained with the computer code are compared with those obtained with the computer program Rt, Rt is a reliability software developed by researcher at University of British Columbia in Vancouver – Canada (Mahsuli and Haukaas, 2013). Table 4.1 show the reliability indices obtained using Rt software and those obtained using the computer code developed in this study (see Appendix A).

Table 4.1: Reliability index comparison.

Eccentricity	Reliability index Rt software	Reliability index Computer Code developed	Variation (%)
0.1tn	3.8903	3.8901	0.005%
0.5tn	3.5915	3.5915	0.000%
1.0tn	3.1696	3.1696	0.000%
2.0tn	2.9642	2.96422	0.000%

4.5 Analysis of non-slender walls - Summary

The procedure for the reliability analysis of non-slender walls that was followed in this research is summarized below. Steps 1-3 relate to the loads, step 4 relates to the resistance, and step 5 evaluates the limit state function.

1. Define the wall's cross-sectional geometry.
2. Build the nominal and the factored interaction diagram and prescribe load eccentricity.
3. From the factored interaction diagram, calculate the design axial force (P_{fr}) and design bending moment (M_{fr}), which automatically determines the maximum factored loads (P_f, M_f) that the section can resist. To simplify the symbols, let $P_{fr} = P_f, and\ \ M_{fr} = M_f$ represent the factored axial load and moments respectively.

4. From the nominal interaction diagram, calculate the moment and axial load resistance (M_r, P_r) and express them in terms of material and geometric random variables (f'_m, f'_c,f_y, $t, d, and\ \rho_w$-the workmanship factor).
5. Finally, by solving the limit state function Equation (4.2), calculate the reliability index (β).

4.6 Statistical Information for Loading

In this study, the statistical information for the load has been adopted from Bartlett et al. (2003). There are loads (such as dead load) that do not depend on the frequency of occurrence; in other words, the time dependence of the loads is not considered. Conversely, there are other loads (such as live load) that is time-dependent. From the statistical point of view, there are two categories of live load: sustained live load (point-in time load) and transient load. Sustained live load is the typical weight of people and their possessions, furniture, movable partitions, and other portable fixtures and equipment (Nowak, 2000). The term "sustained" is used to indicate that the load can be expected to exist as a usual situation (nothing extraordinary). Transient live load is the load that might exist during an unusual event such as an emergency, when everybody gathers in one room, or when all the furniture is stored in one room (Nowak, 2000). The maximum live load is used for design purposes, it considers the expected combinations of sustained live load and transient loads that may occur during the buildings' design lifetime (around 50 years). Additionally, to convert the load into load effect (internal forces and moments) a new random variable that is called transformation to load effect is required. This variable considers modelling and analysis factors.

Table 4.2 shows the statistical characteristics for the maximum load (based on 50-year return period), the point-in-time load, and the load effect modelling factors.

Table 4.2: Statistical Information for loads (Bartlett et al., 2003).

Load	Bias	C.O.V.	Distribution
Dead load	1.050	0.100	Normal
Live load			
50-year maximum load	0.900	0.170	Gumbel
Point-in time load	0.273	0.674	Weibull
Transformation to load effect	1.000	0.206	Normal
Snow load			
50-year maximum depth	1.100	0.200	Gumbel
Point-in time depth	0.196	0.882	Weibull
Density	1.000	0.170	Normal
Transformation to load effect	0.600	0.420	Log-Normal
Wind load			
50-year maximum velocity	1.039	0.081	Gumbel
Point-in time velocity	0.156	0.716	Weibull
Transformation to load effect	0.680	0.220	Normal

4.7 Statistical Information for Resistance Parameters

The resistance part in the reliability problem is obtained from the behavioural model where mechanical and geometrical properties are involved. The model used in this study considers a nonlinear stress-strain relationship for masonry and concrete compressive strength. The constitutive law for masonry is constructed using a similar model proposed by Priestley and Elder (1983), but in this study, the maximum stress occurs at a strain equal to 0.002. For the case of concrete, the curve used is the one proposed by Thorenfeldt et al. (1987). The stress-strain relationship for reinforcement is assumed to be elastic-perfectly plastic.

To solve the reliability problem not only the statistical information for loading is necessary but also the statistical information for the mechanical and geometrical parameters involved in the behavioural model. The statistical information for the random variables used to calculate the resistance cross section is summarized in Table 4.3.

Table 4.3: Statistical Information for loads.

Parameter	Mean	COV	Distribution	Reference
Grouted masonry compressive strength (f'_m)	$1.60f_{mn}$	0.236	Gumbel	Moosavi & Korani, 2014
Concrete compressive strength (f'_c)	$1.30f_{cn}$	0.18	Normal	Bartlett 2007, 1999; Mirza et al. 1979
Wall thickness (t)	$1.00t_n$	0.010	Normal	Moosavi & Korani, 2014
Reinforcement location (d) (mm)	$1.00d_n$	$\frac{4}{d_n}$	Normal	Ellingwood 1980
Reinforcement yield strength (f_y)	$1.14f_{yn}$	0.07	Normal	Bournonville 2004
Workmanship factor (ρ_w)	0.85	0.15	Normal	Moosavi & Korani, 2014
Rate of loading* ($\rho_{r(D+L)}$)	0.88			Bartlett 2007, Mirza et al. 1979

*Considered as reduction factor on f'_m and f'_c.

4.7.1 Masonry compressive strength

After collecting 860 tests for grouted masonry prisms, Moosavi and Korany (2014) proposed the statistical characteristics for the masonry compressive strength. It was found that the Gumbel distribution is the most appropriate for grouted masonry. The statistical parameters for masonry compressive strength were determined using the concept of the professional factor. The professional factor is defined as the ratio of the measured axial load resistance from prims testing (test capacity) to the resistance predicted using the prescribed f'_m (predicted capacity). The professional factor computed from test results includes variation in the test procedures and specimen variability in addition to the theoretical model error. The variability in the professional factor was adjusted as follows:

$$V_P = \sqrt{{V_{model}}^2 - {V_{test}}^2 - {V_{spec}}^2} \tag{4.11}$$

Where V_P is the coefficient of variation (COV) of the professional factor, V_{model} is the COV of the theoretical model, V_{test} is the COV of the measured capacity due to inaccuracies in the test measurements and/or the definition of failure, and V_{spec} represents the COV related to the variability in test specimens. The COV of the professional factor was calculated as 0.236.

4.7.2 Concrete compressive strength

The statistical values for the compressive strength of concrete were proposed by Bartlett (2007). Based on concrete compressive strength characterizations presented elsewhere (Mirza et al., 1979; Bartlett and MacGregor, 1996), material strength properties were represented by the following equation:

$$M = f_{c,i-p}/f'_c = F_1 F_2 F_{i-p} \rho_r \quad (4.12)$$

Where $f_{c,i-p}$ is the in-place compressive strength of the concrete, and f'_c is the 28 days specified concrete strength. The ratio $f_{c,i-p}/f'_c$was modelled using parameters F_1, F_2, F_{i-p}, and ρ_r as described in this section. The parameter F_1 represents the ratio of the average 28-day control cylinder strength to the specified 28-day strength, which was assumed to have a mean value of 1.27 and a coefficient of variation of 0.122 (Bartlett and MacGregor 1996). The parameter F_2, the ratio of the mean in-place strength at 28 days to the mean 28-day cylinder strength, for cast-in-place concrete, is taken as $F_2 = 1.03$ with a coefficient of variation of 0.113, and it is adopted from Bartlett and MacGregor (1996). The parameter F_{i-p} accounts for the variation of the in-place strength in structures. It has a mean value of 1.0 and a coefficient of variation of 0.130 for a cast-in-place structure composed of many members (Bartlett and MacGregor 1999). The parameter ρ_r accounts for rate-of-loading effects and in this study is taken as a deterministic variable, with a detailed discussion in section 4.7.6.

The strength of concrete in a structure may differ from its specified design strength and may not be uniform throughout the structure (Mirza et al, 1979). The major sources of variation in concrete strength are the variations in mixing, transporting, placing, and curing methods, the variation in testing procedure, and variations due to concrete being in a structure rather than in control specimens.

The quality control of the concreting operation has an important role in the variability of concrete strength. The coefficient of variation of field-cast laboratory-cured specimens is, in many cases, between 15% and 20%, which suggests that 20% is a reasonable maximum value for average controls. However, the standard deviation and the coefficient of variation are not constant for different strength levels. In consequence, the average coefficient of variation can be taken as

roughly constant at 10%, 15%, and 20% for strength levels below 4000 psi (27.6 MPa) for excellent, average, and poor control, respectively (Mirza et al. 1979). Based on these results, MacGregor (1996) suggested that the coefficient of variation for concrete in a structure should be taken as 0.18.

4.7.3 Wall thickness

The statistical information for wall thickness was taken based on the research presented by Moosavi and Korany (2014). A normal probability distribution was proposed, with a bias coefficient of 1.00 and COV of 0.010.

4.7.4 Reinforcement location

The statistical values for the reinforcement location were taken based on a study presented by Ellingwood et al. (1985). A normal distribution with a mean of d_n and COV of 4 mm/d_n was suggested by Ellingwood.

4.7.5 Yield strength

Bournonville et al. (2004) evaluated the variability of mechanical properties and weight of steel reinforcing bars produced in the United States and Canada. Based on this study a normal distribution was assumed for the yield strength, with a bias coefficient of 1.14, and COV of 0.07.

4.7.6 Rate of loading

The rate of loading (ρ_r) has a significant influence on the strength of concrete. According to Mirza et al. (1979):

$$\rho_r = 0.89(1 + 0.88 \log_{10}(R)) \tag{4.13}$$

Where R is the loading rate in psi/s. The loading time to failure was assumed to be 1 hour for live loads, 10 min for wind loads, and 1 day for snow loads. The resulting values of ρ_r are 0.88, 0.96, and 0.79 for the dead plus live, dead plus wind, and dead plus snow load combinations, respectively. These values were adopted by Bartlett (2007) and the study conducted by Moosavi and Korany (2017). The variability in the rate of loading is negligible compared to the large coefficient of variations for the other parameters and therefore ignored in this analysis.

4.7.7 Workmanship factor

The effect of the workmanship factor on the reliability of structural masonry is very significant. The strength of masonry is highly sensitive to construction practices, mason qualifications, and inspection. Some of the problems that are included in the workmanship factor are the thickness and furrowing of mortar joints, grouting procedures, wall verticality, geometrical compliance with design values, and the quality control of construction materials. Based on limited experimental data and judgment, three sets of bias coefficients and COV were proposed by Turkstra (1989) for the workmanship factor: 1.0 and 0.1 for well inspected, 0.8 and 0.15 for regularly inspected, and 0.7 and 0.2 for uninspected masonry. Moosavi and Korany (2014), based on the Turkstra study proposed a bias coefficient of 0.85 and a COV of 0.15 for regularly inspected masonry and these values were used in this study.

4.8 Properties of Analyzed Walls

The thickness of the walls analyzed in this investigation was 290 mm, corresponding to a nominal 30 cm block. The masonry compressive strengths, f'_m, that were selected to observe their effect on the reliability analysis, were 5 MPa, 10 MPa, 15 MPa, 20 MPa, and 25 MPa. The minimum compressive strength for grouted masonry recognized by the Canadian masonry standard, without laboratory testing, is 5 MPa, and the maximum is 13 MPa – higher values than these were also considered to achieve a range that would overlap with the lower end of typical concrete compressive strengths. For concrete walls, the concrete compressive strengths, f'_c, were taken as 20 MPa, 25 MPa, and 30 MPa. The minimum concrete compressive strength given by the Canadian concrete standard CSA A23.3-19 is 20 MPa.

The minimum reinforcement ratio for masonry and concrete walls 0.0013 and 0.0015 (CSA S304-14, CSA A23.3-19), respectively. Upper ranges of reinforcement ratios (ρ_s) were taken as 0.0025 and 0.0035. From a practical point of view, $\rho_s = 0.0013$, $\rho_s = 0.0025$ and $\rho_s = 0.0035$ translate into 20M bars spaced at $s = 800$ mm, 20M bars spaced at $s = 400$ mm and 15M bars spaced at $s = 200$ mm, respectively. The properties of the analyzed walls are summarized in Table 4.4 and Table 4.5.

Table 4.4: Properties of masonry analyzed walls.

		Reinforcement Ratio ρ		
		0.0013 / 0.0015	0.0025	0.0035
Compressive strength f'_m (MPa)	5	→	→	→
	10	→	→	→
	15	→	→	→
	20*	→	→	→
	25*	→	→	→

*Considered to masonry and concrete comparison (see section 4.9.3).

Table 4.5: Properties of concrete analyzed walls.

		Reinforcement Ratio ρ		
		0.0013 / 0.0015	0.0025	0.0035
Compressive strength f'_c (MPa)	20*	→	→	→
	25*	→	→	→
	30	→	→	→

* Considered to masonry and concrete comparison (see section 4.9.3).

4.9 Results and Discussion

4.9.1 Parametric Analysis

i. Effect of Reinforcement Ratio Variation on reliability of non-slender walls

The reliability was calculated for different amounts of reinforcement in singly reinforced (SR) and doubly reinforced (DR) masonry and concrete walls (Figure 4.5).

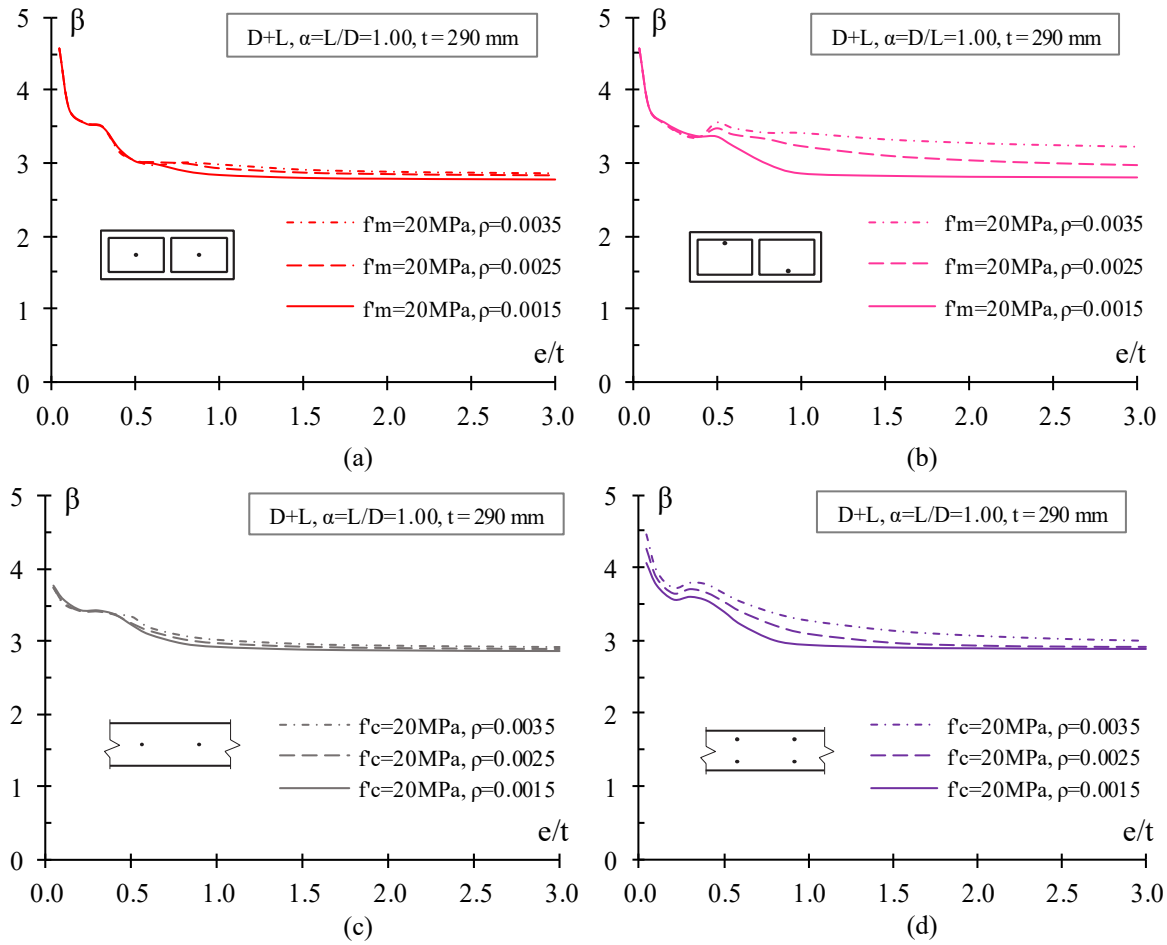

Figure 4.5: Effect of the change in the reinforcement ratio: (a) Singly reinforced (SR) masonry wall; (b) Doubly reinforced (DR) masonry wall; (c) Singly reinforced (SR) concrete wall; (d) Doubly reinforced (DR) concrete wall.

As can be seen in Figure 4.5b, the DR masonry walls show highest sensitivity/variability of reliability indices with the change of the reinforcement ratio, followed by DR concrete walls (Figure 4.5d), and then SR masonry walls (Figure 4.5a). SR concrete walls (Figure 4.5c) are not influenced by the change in the reinforced ratio. One of the major differences between masonry and concrete walls is their COV of their compressive strength (masonry COV=0.236 and concrete COV=0.18). The COV is a convenient dimensionless measure of uncertainty that conveys the concept of variability of the predictable (mean) value. This statement is used to explain the difference in sensitivity. Figure 4.6 shows the reliability values of DR masonry walls for these two COVs. These results show that COV of the compressive strength (f'_m) matters in terms of sensitivity even in the variation of reinforcement ratio. Lower COV increases the reliability indices, and also reduce the sensitivity of the curves. The resistance component (R) of the limit

state function, for both materials, takes into account statistical characteristics of f'_m and f'_c even when this is taken constant and reinforcement ratio varies. In addition, this variability is aggravated by the presence of the workmanship random variable in masonry wall construction.

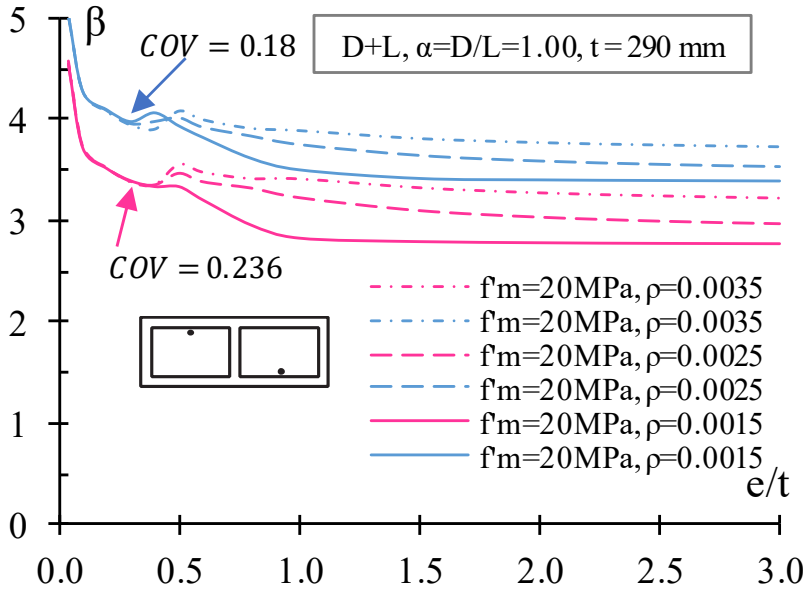

Figure 4.6: Effect of the change in the coefficient of variation (COV): Doubly reinforced (DR) masonry wall.

It is worth mentioning that the changes in the reinforcement ratio have higher influence in the tension region (region of large eccentricities) than in the compression region (region of low eccentricities), especially for masonry walls (Figures 4.5a and 4.5b). It is seen that the changes in the reinforcement ratio produce large variations in reliability index within the tension zone of the masonry graphs, but reliability within the compression zone remains unaffected by changes in reinforcement ratio. Similar observations were made when conducting sensitivity analysis. The tension zones of the interaction diagrams for masonry were found to be sensitive to changes in reinforcement ratio while the compression zones were not (Figure 4.7). This is attributed to the fact that in the compression zone the effect of the reinforcement ratio is negligible, since the behaviour is dominated by the masonry or concrete compressive strengths. In addition, compression in steel rebars is ignored in masonry walls because the bars cannot be laterally restrained within the cells of the masonry unit. For the compression zone and a given eccentricity, the resistance (derived from the nominal P-M interaction diagram) and the loads (derived from the

factored P-M interaction diagram) at different reinforcement ratios have the same values, the curves overlap each other (see Figure 4.7); therefore, the resistance (R) and the load (S) components are the same in the limit state equation (g(X)=R-S), so the reliability indices are equal as well (Figures 4.5a and 4.5b).

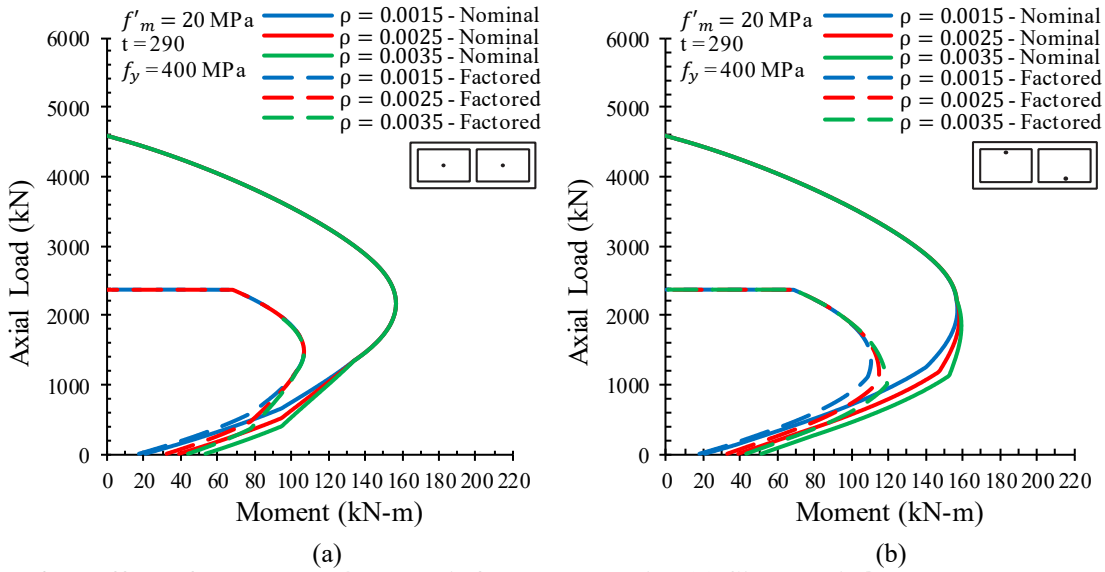

Figure 4.7: Effect of the change in the reinforcement ratio: (a) Singly reinforced masonry wall; (b) Doubly reinforced masonry wall.

For concrete walls (Figures 4.5c and 4.5d), particularly for doubly reinforced walls, it is seen that the compression-controlled region is sensitive to the change in the reinforcement ratio. The reason for this is that vertical reinforcement is laterally restrained by the horizontal reinforcement in the wall and is thus able to carry compression forces.

The higher the reinforcement ratio, the higher the reliability indices for all walls. This observation is consistent with results obtained by H.P. Hong and W.Zhou (1999) on their study on reliability evaluation of reinforced-concrete columns. Moreover, Gonzales et al. (2021) showed that increasing the steel area greatly improves the response in term of resistance of masonry walls, which results in safer structures.

ii. Effect of the compressive strength variation on the reliability of non-slender walls

Figure 4.8 shows the effect of varying the material compressive strength on the reliability levels for doubly reinforced (DR) and singly reinforced (SR) masonry and concrete walls. The compressive strength for masonry was varied from 5 to 25 MPa and its effect on reliability index at different eccentricities was determined. The procedure was repeated for reinforced-concrete walls with compressive strength value ranging from 20 to 30 MPa.

The reliability of DR masonry wall (Figure 4.8b) is the most sensitive to the changes in compressive strength, followed by DR concrete walls (Figure 4.8d), and SR masonry walls (Figure 4.8a). The reliability of SR concrete walls (Figure 4.8c) is not affected by change in the compressive strength of the concrete. The reason for this is the higher variability in strength data for masonry walls (COV =0.236) than concrete walls strength data (COV=0.18). This higher variability in masonry is due to the fact that its strength is highly dependent on construction practices, mason qualifications, and inspection. In addition, this variability is aggravated by the presence of the workmanship random variable in masonry wall construction.

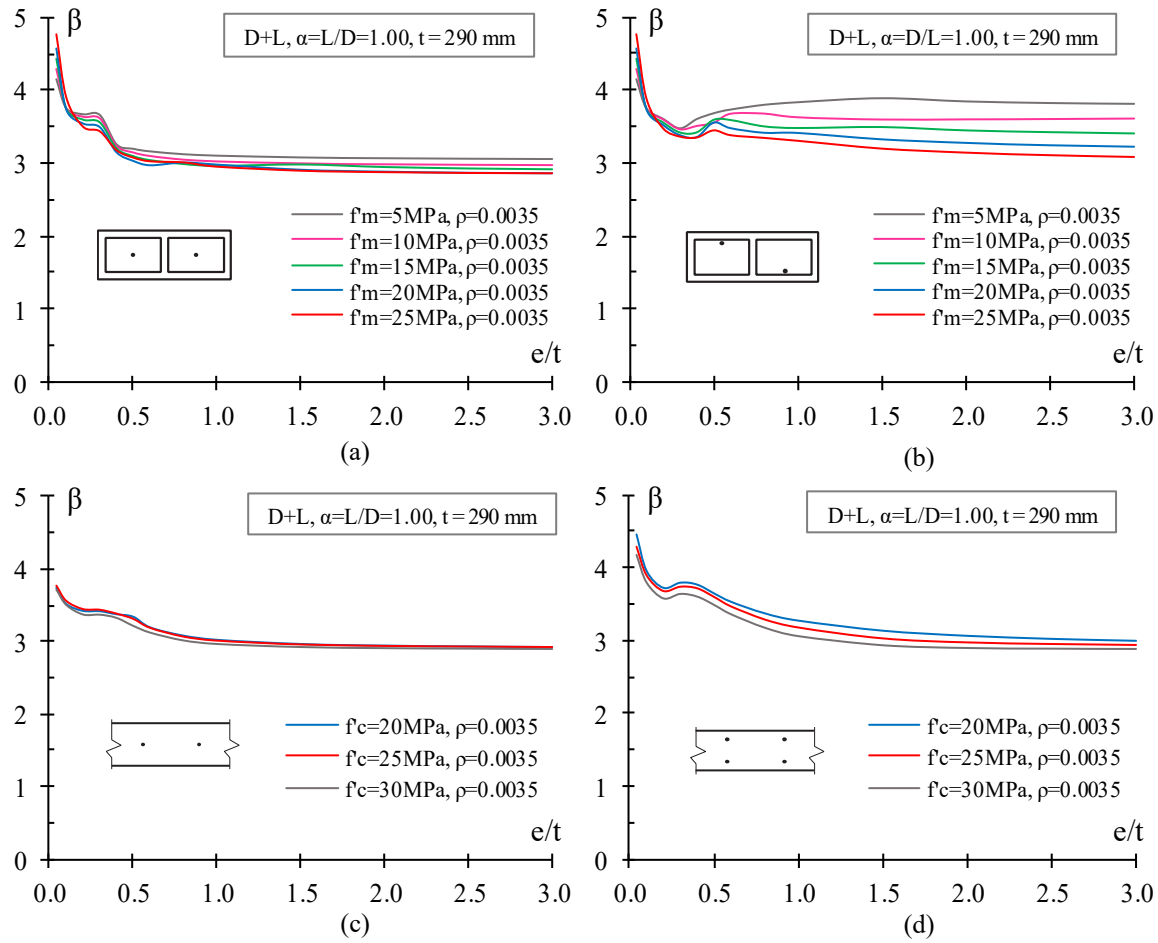

Figure 4.8: Effect of the change in the compressive strength on reliability index: (a) SR masonry wall; (b) DR masonry wall; (c) SR concrete wall; (d) DR concrete wall.

At low eccentricities (e/t<0.15), the reliability of masonry walls increases with compressive strength of the wall (Figures 4.8a and 4.8b). The behaviour is reversed at higher eccentricities, where the lower compressive strength walls have higher reliability index. It is important to point out that in the initial region (e/t<0.15) the curves almost overlap with each other. This means that the effect of the compressive strength is negligible; therefore, it is seen that as the compressive strength increases, the reliability values decrease.

Generally, the reliability of concrete walls decreased with an increase in the compressive strength, regardless of the eccentricity level. The drops in reliability were more evident in doubly reinforced-concrete walls than in singly reinforced-concrete walls (Figures 4.8c and 4.8d).

In order to confirm the relationships between the compressive strength of walls and reliability, a Monte Carlo simulation was performed to determine means and standard deviations of the

resistance (R) and load (S) variables in the limit state function. Then, their COV is determined using the definition of the Cornell reliability index (β_C):

$$\beta_C = \frac{\mu_R - \mu_S}{\sqrt{{\sigma_R}^2 + {\sigma_S}^2}} = \frac{1}{COV} \tag{4.14}$$

The results of this analysis are summarized in Tables 4.6-4.9.

Table 4.6: Results of Monte Carlo simulation – SR concrete wall - $e/t = 1.5$.

Parameter	$f'_c = 20\ MPa$		$f'_c = 25\ MPa$		$f'_c = 30\ MPa$	
	μ	σ	μ	σ	μ	σ
Resistance (R)	$9.47734 * 10^7$	$1.71071 * 10^7$	$9.84102 * 10^7$	$1.77454 * 10^7$	$1.00384 * 10^8$	$1.81142 * 10^7$
Load (S)	$4.36055 * 10^7$	$6.51383 * 10^6$	$4.56640 * 10^7$	$6.82220 * 10^6$	$4.70821 * 10^7$	$7.02548 * 10^6$
$\mu_R - \mu_S$	$5.11679 * 10^7$		$5.27462 * 10^7$		$5.33019 * 10^7$	
$\sqrt{{\sigma_R}^2 + {\sigma_S}^2}$	$1.83053 * 10^7$		$1.90116 * 10^7$		$1.94289 * 10^7$	
COV	0.35775		0.36044		0.36451	

Table 4.7: Results of Monte Carlo simulation – DR concrete wall - $e/t = 1.5$.

Parameter	$f'_c = 20\ MPa$		$f'_c = 25\ MPa$		$f'_c = 30\ MPa$	
	μ	σ	μ	σ	μ	σ
Resistance (R)	$9.21756 * 10^7$	$1.54074 * 10^7$	$9.76778 * 10^7$	$1.72948 * 10^7$	$1.00399 * 10^8$	$1.80811 * 10^7$
Load (S)	$4.27651 * 10^7$	$6.38539 * 10^6$	$4.48349 * 10^7$	$6.68718 * 10^6$	$4.66674 * 10^7$	$6.96462 * 10^6$
$\mu_R - \mu_S$	$4.94105 * 10^7$		$5.28429 * 10^7$		$5.37316 * 10^7$	
$\sqrt{{\sigma_R}^2 + {\sigma_S}^2}$	$1.66782 * 10^7$		$1.85426 * 10^7$		$1.93761 * 10^7$	
COV	0.33754		0.35090		0.36061	

Table 4.8: Results of Monte Carlo simulation – SR masonry wall - $e/t = 1.5$.

Parameter	$f'_m = 5\ MPa$		$f'_m = 15\ MPa$		$f'_m = 25\ MPa$	
	μ	σ	μ	σ	μ	σ
Resistance (R)	$4.68503 * 10^7$	$1.18306 * 10^7$	$9.99860 * 10^7$	$2.504863 * 10^7$	$1.06405 * 10^8$	$2.55690 * 10^7$
Load (S)	$1.69974 * 10^7$	$2.16861 * 10^6$	$3.97002 * 10^7$	$5.53349 * 10^6$	$4.53328 * 10^7$	$6.75579 * 10^6$
$\mu_R - \mu_S$	$2.98529 * 10^7$		$6.02858 * 10^7$		$6.02858 * 10^7$	
$\sqrt{{\sigma_R}^2 + {\sigma_S}^2}$	$1.20278 * 10^7$		$2.56525 * 10^7$		$2.64464 * 10^7$	
COV	0.40290		0.42552		0.43304	

Table 4.9: Results of Monte Carlo simulation – DR masonry wall - $e/t = 1.5$.

Parameter	$f'_m = 5\ MPa$		$f'_m = 15\ MPa$		$f'_m = 25\ MPa$	
	μ	σ	μ	σ	μ	σ
Resistance (R)	$7.41716 * 10^7$	$1.54469 * 10^7$	$8.97213 * 10^7$	$1.83557 * 10^7$	$9.79725 * 10^7$	$2.04992 * 10^7$
Load (S)	$3.04857 * 10^7$	$4.55426 * 10^6$	$3.97504 * 10^7$	$5.93374 * 10^6$	$4.36779 * 10^7$	$6.52326 * 10^6$
$\mu_R - \mu_S$	$4.36859 * 10^7$		$4.99709 * 10^7$		$5.42946 * 10^7$	
$\sqrt{{\sigma_R}^2 + {\sigma_S}^2}$	$1.61043 * 10^7$		$1.92910 * 10^7$		$2.15121 * 10^7$	
COV	0.36864		0.38604		0.39621	

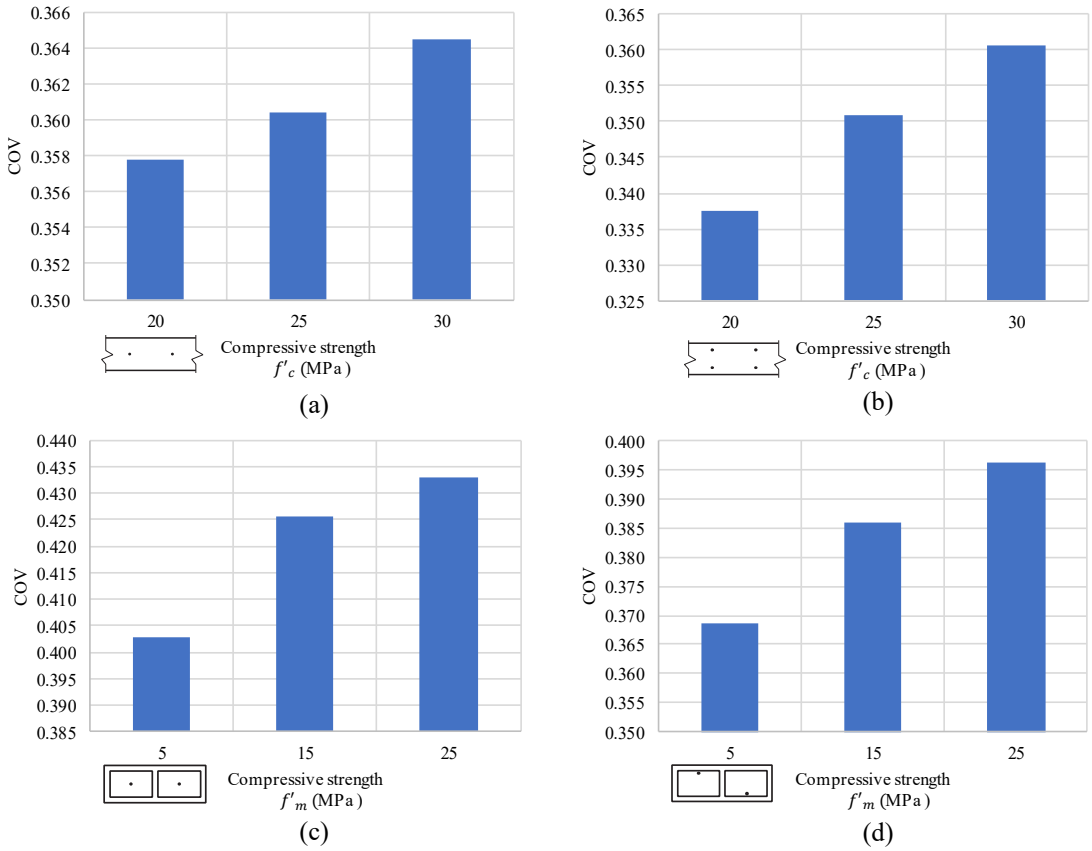

Figure 4.9: Effect of the change in the coefficient of variation (COV) with an increment of the compressive strength: (a) Singly reinforced-concrete wall; (b) Doubly reinforced-concrete wall; (c) Singly reinforced masonry wall; (d) Doubly reinforced masonry wall.

As can be seen in Tables 4.6-4.9 and Figure 4.9, higher compressive strengths have the highest coefficient of variation, -i.e., more variability and consequently, the least reliability value. These results are related with engineering practice since higher compressive strength is more difficult to achieve and it is subjected to more variability. This observation is consistent with results obtained by Guzman (2022) on their study on reliability assessment for loadbearing reinforced-concrete masonry walls subjected to gravity and lateral loads.

4.9.2 Comparison between Singly and Doubly Reinforced Walls

i. Singly and Doubly reinforced masonry walls.

The reliability of singly and doubly reinforced masonry walls were compared to determine the effect of reinforcement placement on the reliability indices.

❖ *Effect of reinforcement ratio on reliability*

Figures 4.10 shows the effect of varying reinforcement ratio on the reliability index of singly reinforced (SR) and doubly reinforced (DR) masonry walls. The reinforcement ratios were varied from 0.0013 to 0.0035, while keeping the masonry compressive strength constant at 25MPa and the wall thickness at 290mm.

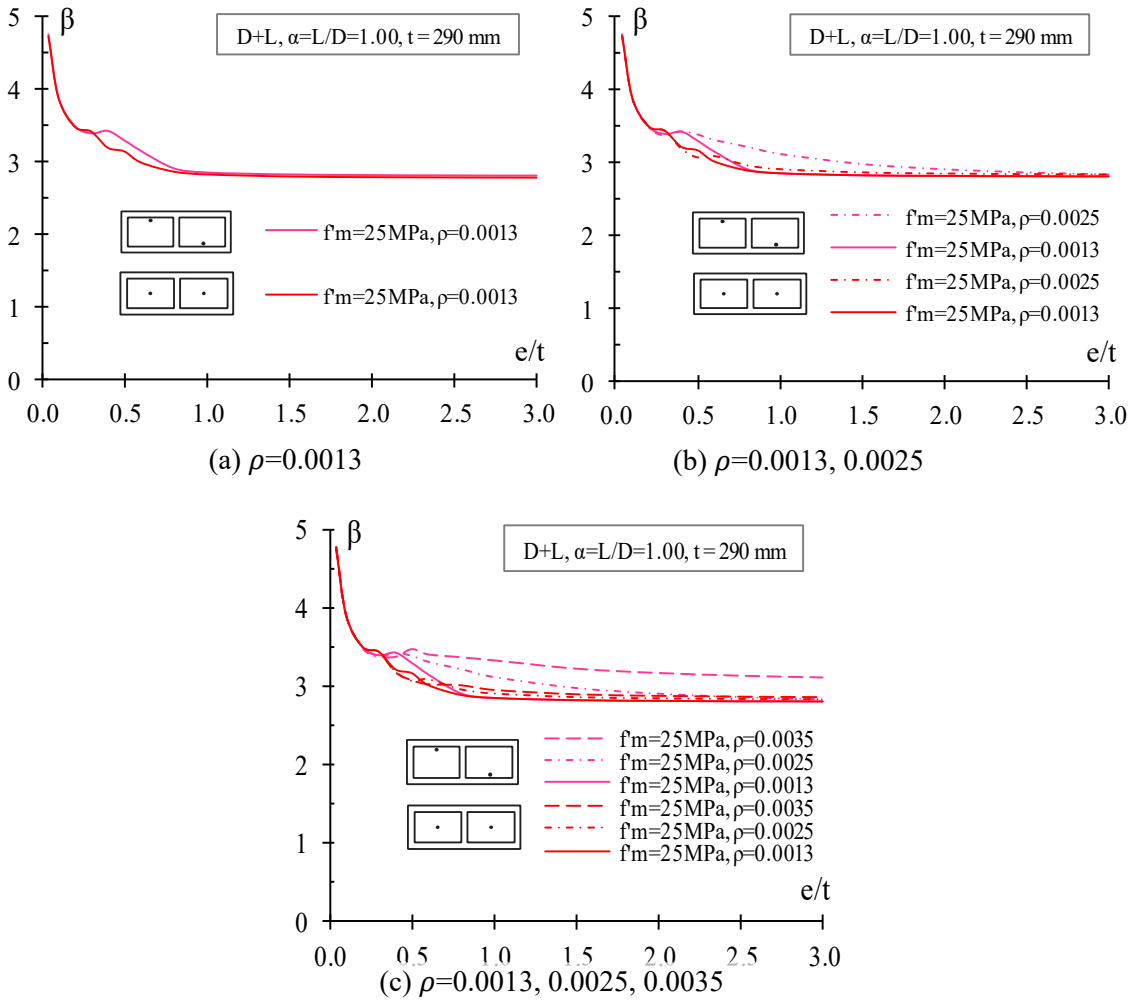

Figure 4.10: Comparison between SR masonry and DR masonry walls for the same $f'_m = 25\ MPa$ and for different reinforcement ratios.

❖ *Effect of compressive strength on reliability*

The effect of compressive strength on reliability of singly and doubly reinforced masonry walls was assessed by varying the compressive strength of masonry from 5 to 25 MPa, while keeping the reinforcement ratio constant at 0.0035 (Figure 4.11).

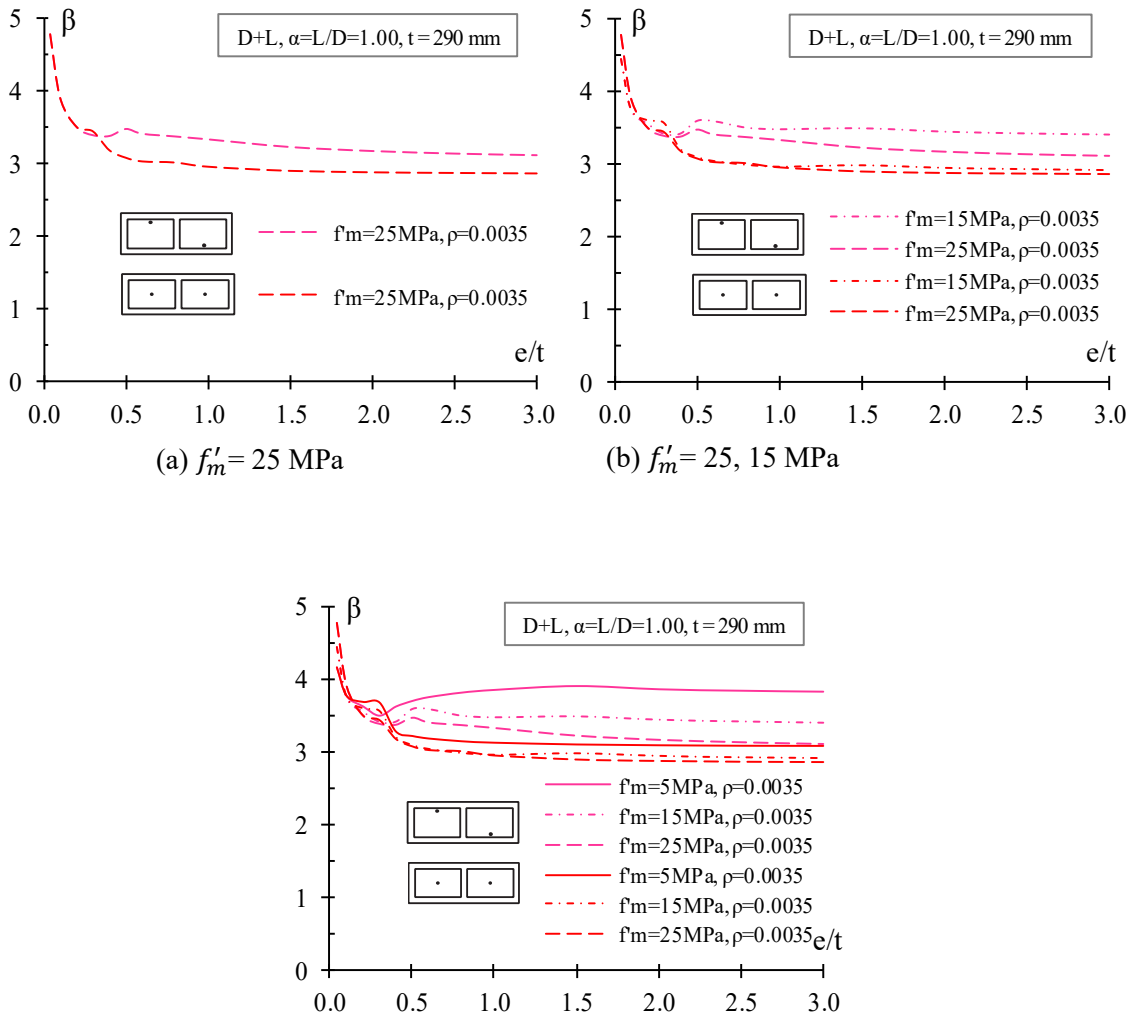

(a) f'_m= 25 MPa (b) f'_m= 25, 15 MPa

(c) f'_m= 25, 15, 5 MPa

Figure 4.11: Comparison between SR masonry and DR masonry walls for the same $\rho = 0.0035$ and for different compressive strength.

As shown in Figure 4.10 and Figure 4.11 DR masonry walls generally had higher reliability values than SR masonry walls. At lower eccentricities ($e/t<0.4$), the whole cross section of the wall is in compression, so the reinforcing bars are not activated This explains why SR and DR have equal reliability levels in this range, as only the masonry is participating in the resistance. For higher eccentricities, the double layer of reinforcement in the DR masonry walls increases the capacity of the wall (leading to a safer structure, with higher reliability values) compared to placing a single layer of reinforcing bars in the center of the wall. This increment in the capacity is due to higher moment arms in DR walls. The finding is consistent with results obtained by Gonzalez et al. (2021). The reliability index increased with the reinforcement ratio (Figure 4.10) but dropped with increase in compressive strength (Figure 4.11), mirroring the findings previously discussed in section 4.9.1.

The differences in reliability of singly and doubly reinforced masonry walls become more noticeable for higher reinforcement ratios (Figure 4.10) and for lower compressive strengths (Figure 4.11). This is because the high sensitivity of DR to the change of the reinforcement ratio and compressive strength (Parametric Analysis section 4.9.1).

ii. Singly and Doubly reinforced-concrete walls

The reliability index of singly and doubly reinforced-concrete walls were compared. Figure 4.12 shows the variation of the reliability of these walls with respect to their reinforcement ratio, while Figure 4.13 shows the reliability variation with respect to the compressive strength of concrete.

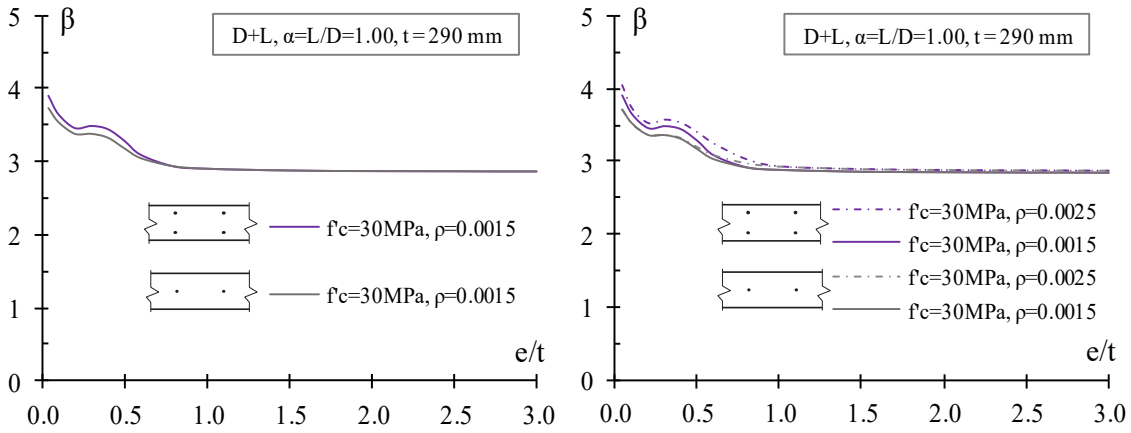

(a) ρ=0.0015

(b) ρ=0.0015, 0.0025

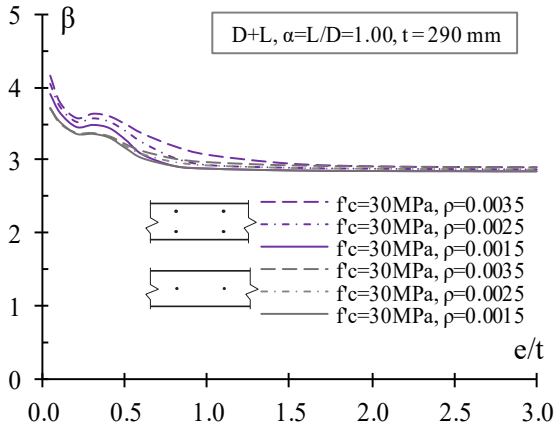

(c) ρ=0.0015, 0.0025, 0.0035

Figure 4.12: Comparison between SR concrete and DR concrete walls for the same $f'_m = 30\ MPa$ and for different reinforcement ratios.

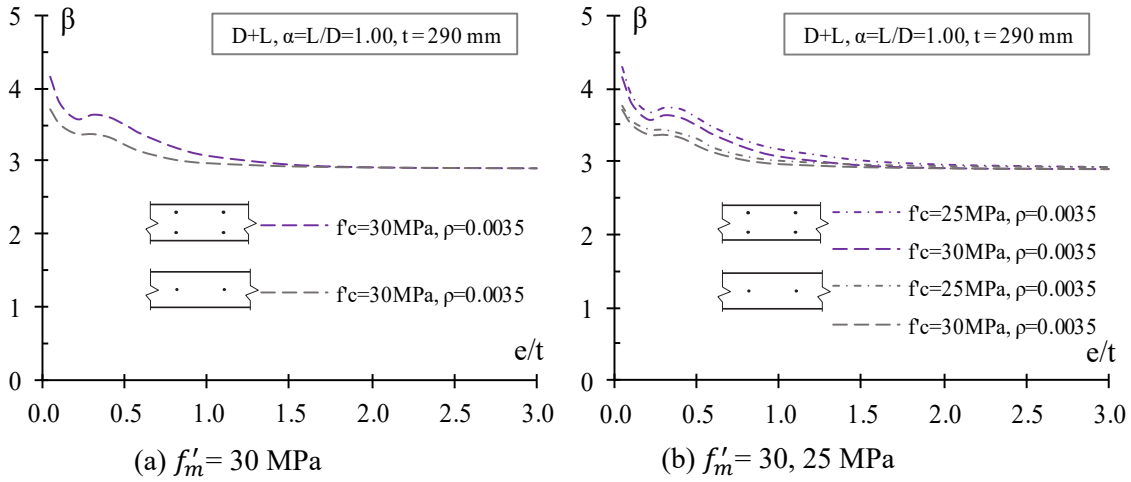

(a) f'_m= 30 MPa (b) f'_m= 30, 25 MPa

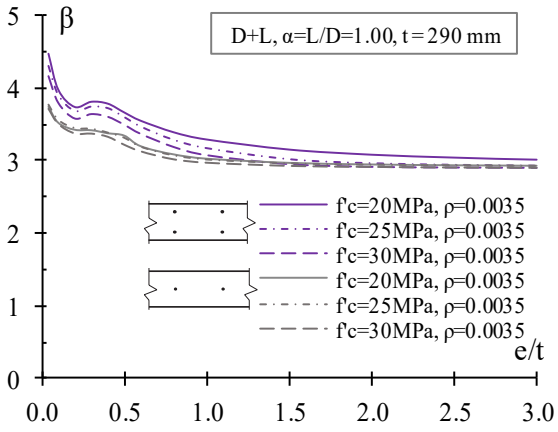

(c) f'_m= 30, 25, 20 MPa

Figure 4.13: Comparison between SR concrete and DR concrete walls for the same $\rho = 0.0035$ and for different compressive strength.

The findings in this section largely mirrored those obtained for masonry walls. Doubly reinforced-concrete walls had higher reliability than singly reinforced-concrete walls. As found by Gonzalez et.al (2021), a double layer of reinforcement increases the capacity of the wall. Unlike masonry walls, the reliabilities of concrete walls differed across all eccentricities (including lower e/t <0.5). This is because for concrete walls reinforcements are tied together and are always activated. Therefore, the steel bars are allowed to take compressive forces even for lower eccentricities (Figure 4.12 and 4.13).

The reliability of singly and doubly reinforced-concrete walls increased with the reinforcement ratio but dropped with an increase in concrete compressive strength.

The differences in reliability of singly and doubly reinforced-concrete walls become more noticeable for higher reinforcement ratios (Figure 4.12) and for lower compressive strengths (Figure 4.13). This is because the highest sensitivity of DR concrete walls to the change of the reinforcement ratio and compressive strength (Parametric Analysis section 4.9.1).

Also, DR walls of either material were more sensitive to the change of the compressive strength and reinforcement ratio than SR walls because in DR walls the moment capacity considered the moment arms of both reinforcement layers. Therefore, additional random variables such as the effective depth of the compressive reinforcing bars (d') and yield stress (f_y) of the compressive steel are involved, adding more variability to the limit state function (Figure 4.14).

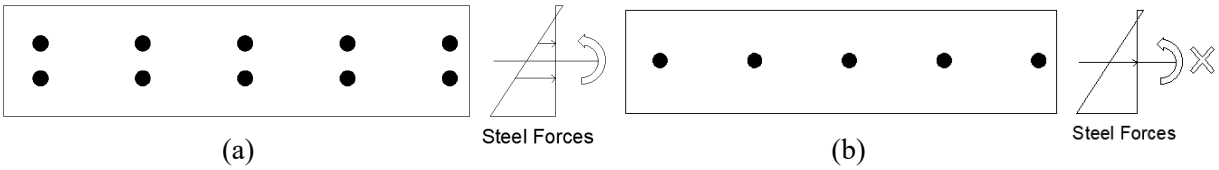

Figure 4.14: Contribution to the moment capacity: (a) Doubly reinforced wall; (b) Singly reinforced wall.

Walls with higher compressive strength and lower reinforcement ratio had similar reliabilities irrespective of whether they were doubly or singly reinforced. However, for walls made of lower compressive strength materials and having higher reinforcement ratios, the reliability index for singly reinforced wall was lower than for doubly reinforced wall. These observations are consistent with the higher sensitivity of DR masonry and concrete walls to the change of the reinforcement ratio and compressive strength (Parametric Analysis section 4.9.1).

4.9.3 Comparison between Masonry and Concrete Walls

As shown in Table 4.4 and 4.5, masonry and concrete walls will be compared using the same compressive strength (20 MPa, 25 MPa) and the same reinforcement ratio (ρ=0.0015, 0.0025, 0.0035).

Figures 4.15, 4.16, 4.17 and 4.18 show the step by step process of this comparison. For this process, a compressive strength of 25 MPa and a reinforcement ratio of 0.0015 were taken. Figure 4.15

shows the reliability values for singly reinforced (SR) masonry walls. In Figure 4.16, reliability values for SR concrete walls are added to Figure 4.15. In Figure 4.17, reliability values for doubly reinforced (DR) masonry walls are added to Figure 4.16. In Figure 4.18, reliability values for DR concrete walls are added to Figure 4.17.

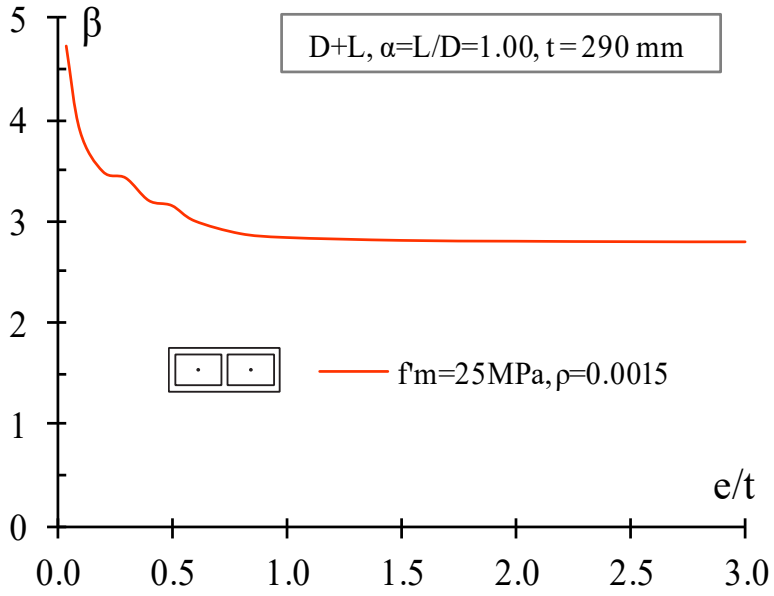

Figure 4.15: Reliability levels comparison for the same $f'_m = f'_c = 25\ MPa$ and $\rho = 0.0015$: Singly reinforced (SR) masonry wall.

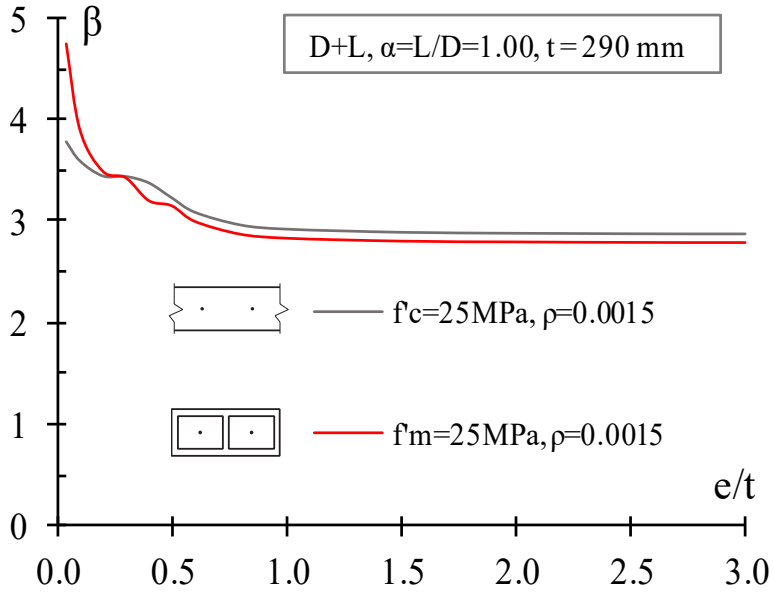

Figure 4.16: Reliability levels comparison for the same $f'_m = f'_c = 25\ MPa$ and $\rho = 0.0015$: SR masonry and concrete walls.

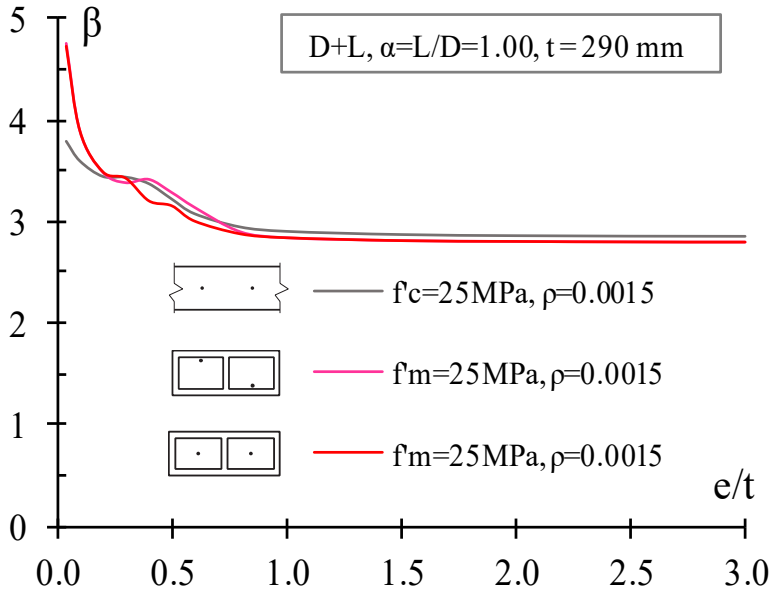

Figure 4.17: Reliability levels comparison for the same $f'_m = f'_c = 25\ MPa$ and $\rho = 0.0015$: SR masonry, concrete walls and Doubly reinforced (DR) masonry wall.

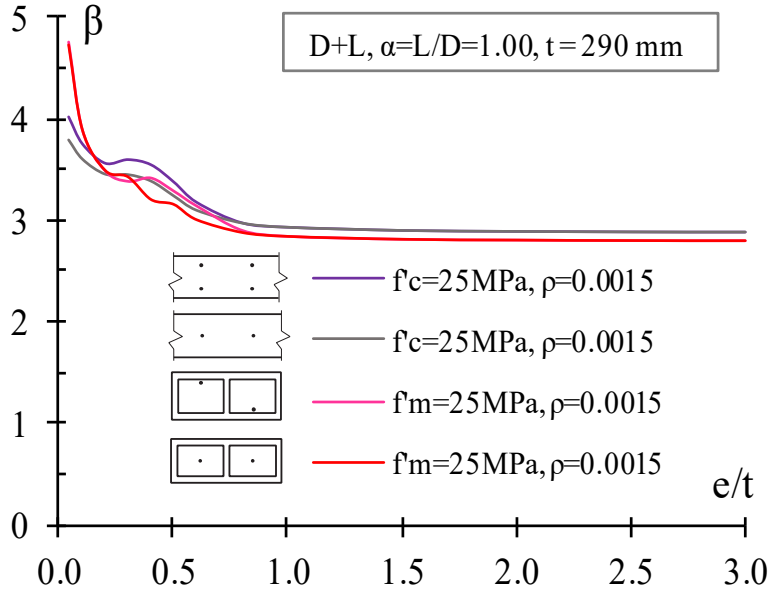

Figure 4.18: Reliability levels comparison for the same $f'_m = f'_c = 25\ MPa$ and $\rho = 0.0015$: SR and DR masonry and concrete walls.

Figure 4.18 shows the comparison between masonry and concrete walls for the same $f'_m = f'_c = 25\ MPa$ and $\rho = 0.0015$. It is seen that for this level of compressive strength and reinforcement ratio, reliability values for masonry and concrete wall are very similar. However, having in mind

the different sensitivity of the analyzed cases to the variation of the parameters in comparison (i.e., compressive strength and reinforcement ratio), it is necessary to see these differences in reliability values for different reinforcement ratios. Therefore, following the same procedure a more general comparison varying the reinforcement ratio is provided in Figures 4.19, 4.20, and 4.21.

Figures 4.19, 4.20 and 4.21 show a comparison in terms of reliability levels between masonry and concrete walls, the graphs correspond to a compressive strength of 25 MPa and reinforcement ratio varying from 0.0015 to 0.0035.

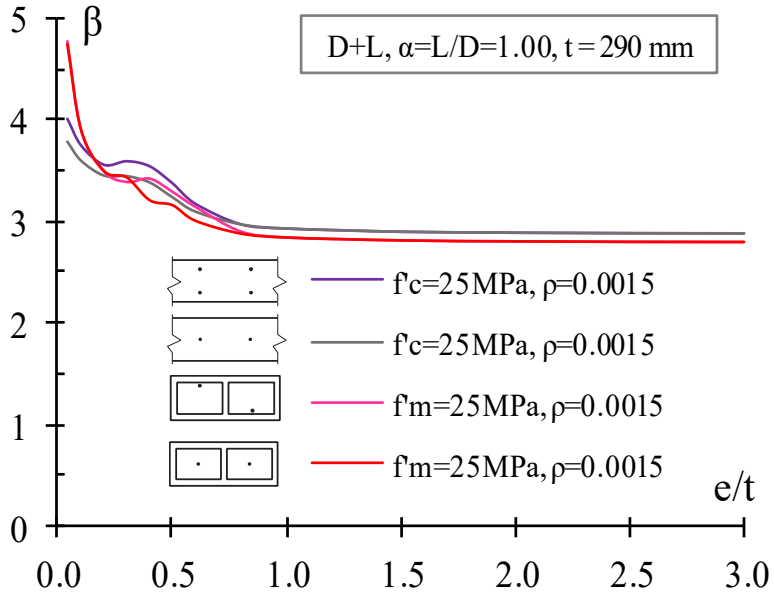

Figure 4.19: Reliability levels comparison between masonry and concrete walls, $f'_m = f'_c = 25\ MPa$ and $\rho = 0.0015$.

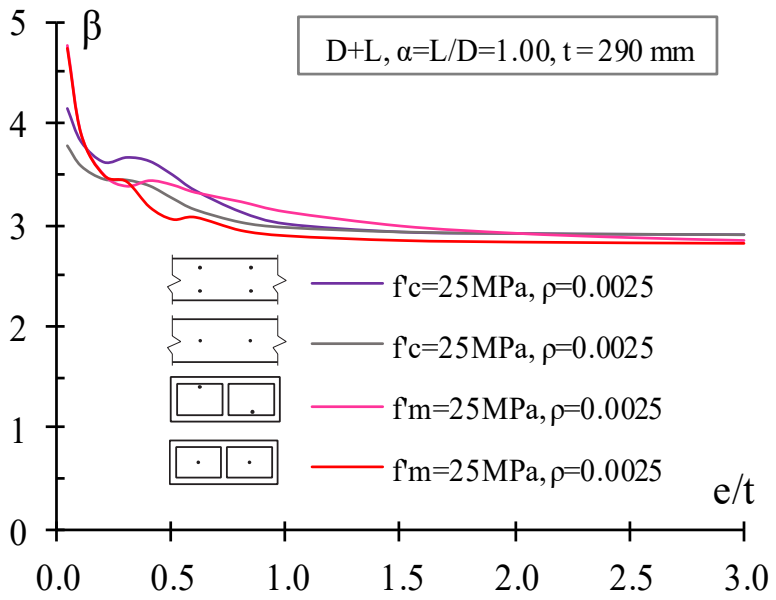

Figure 4.20: Reliability levels comparison between masonry and concrete walls, $f'_m = f'_c =$ 25 MPa and $\rho = 0.0025$.

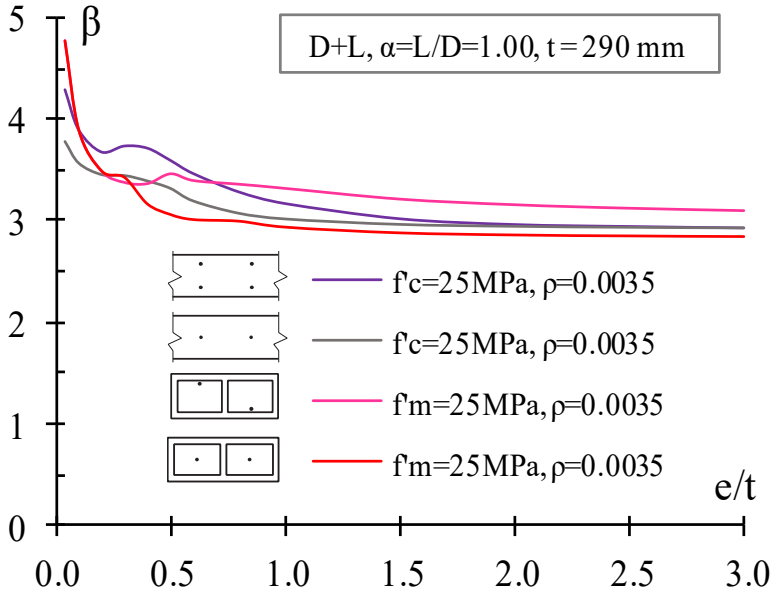

Figure 4.21: Reliability levels comparison between masonry and concrete walls, $f'_m = f'_c =$ 25 MPa and $\rho = 0.0035$.

As can be shown in Figures 4.19-4.21, when comparing reliability indices between masonry and concrete walls, it is seen that the reliability indices are similar (average reliability index of 3.5).

However, masonry walls exhibit higher sensitivity in reliability indices with a change in the reinforcement ratio compared to walls made of concrete. It has been shown that the resistance component (R) of the limit state function takes into account the variability (COV) of the compressive strength, even when it remains constant and reinforcement ratio varies (parametric analysis 4.9.1). Decreasing this variability increases the reliability level and reduces sensitivity. The compressive strength for masonry possesses higher COV than the compressive strength of concrete, which means higher sensitivity. Another important factor is the workmanship random variable in masonry wall construction, which adds uncertainty to the problem. The curve that shows highest sensitivity to the reinforcement ratio is DR masonry wall, followed by DR concrete wall, SR masonry wall, and SR concrete wall.

The reliability of doubly reinforced walls is more sensitive to the load eccentricity than singly reinforced walls. Consequently, the differences between the curves are higher when the reinforcement ratio is higher, and the reliability curves are very close each other for the lowest reinforcement ratio. This is consistent with results obtained in the comparison between singly and doubly reinforced walls and the observed sensitivity of the curves.

For the other compressive strength comparison (20 MPa), the behaviour of the curves is similar to that described above for 25 MPa (see section 4.9.2). The data is shown in Appendix B.

Walls with minimum strength and reinforcement ratios

The standards requirements give minimum acceptable safety levels. Canadian concrete standard (CSA A23.3-2019) require concrete walls to have a minimum strength of 20MPa, and a minimum reinforcement ratio of 0.0015. The Canadian masonry standard (CSA S304-14) limit grouted masonry strength to not less than 5MPa, without laboratory testing, and reinforcement ratios of 0.0013. Figure 4.22 shows a comparison of the reliabilities of masonry and concrete walls designed to the minimum standard requirements ($f'_m = 5\ MPa, \rho_s = 0.0013;\ f'_c = 20\ MPa, \rho_s = 0.0015$).

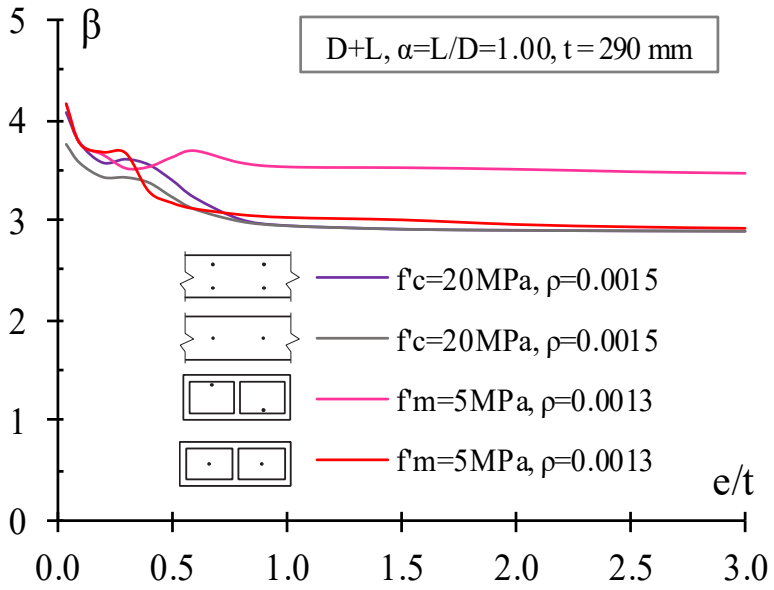

Figure 4.22: Comparison between masonry and concrete walls, minimum standard requirements.

For smaller eccentricities (e<0.40), the reliability values between masonry and concrete walls are very similar. For larger eccentricities than this value DR masonry walls have higher reliability values than the other curves, which still have the same reliability levels. This observation is expected since the parametric analyses show that for lower compressive strengths correspond higher reliability values (5 MPa for masonry, 20 MPa for concrete).

The difference in reliability levels for concrete and masonry are in part due to variations in material resistance factors ϕ_m=0.60 and $\phi_c = 0.65$ used in factored resistance interaction diagram. Similarly, parameters such as α_1 and β_1 are different for masonry and concrete. Additionally, for the nominal interaction diagram, the material behavioural models are different, as well as the ultimate compressive strain. In the method to solve the limit state function, the statistical parameters such as the bias factor, coefficient of variations and probability distribution function of the material compressive strength are different.

5 CONCLUSIONS AND RECOMMENDATIONS

Comparison of the reliability of masonry and concrete walls

For the same compressive strength (in the range of 20-25 MPa), both concrete and masonry walls had similar reliability values for different reinforcement ratios (average reliability value of 3.5). However, masonry walls exhibit higher sensitivity in reliability indices with a change in the reinforcement ratio compared to walls made of concrete. It has been shown that the resistance component (R) of the limit state function takes into account the variability (COV) of the compressive strength, even when it remains constant and reinforcement ratio varies (parametric analysis 4.9.1). Decreasing this variability increases the reliability level and reduces sensitivity. The compressive strength for masonry possesses higher COV than the compressive strength of concrete, which means higher sensitivity. Another important factor is the workmanship random variable in masonry wall construction, which adds uncertainty to the problem.

Therefore, enhanced supervision control is required for masonry construction and this will reduce the variability in masonry walls. Reducing variability through enhanced supervision control of masonry would lead to increase in safety and, consequently, an increase in the strength reduction factor. This, in turn, results in a higher design capacity of structural masonry.

The reliability of singly reinforced walls of either material was not significantly sensitive to the changes in the compressive strength and reinforcement ratio. In contrast, doubly reinforced walls exhibited sensitivity to these parameters. In DR walls the moment capacity considered the moment arms of both reinforcement layers; therefore, additional random variables such as effective depth of the reinforcement bars and their yield stress play a role, adding more variability to the limit state function.

Due to the sensitivity of the curves to changes in reinforcement ratio and compressive strength, it is expected that, for compressive strengths lower than 20-25 MPa (rare for concrete elements but possible with poor supervision) the differences between masonry and concrete reliability curves will be greater. Conversely, for compressive strengths higher than the studied range (20-25 MPa), which is more likely to occur in concrete walls and less likely in masonry walls, the differences

between reliability curves will be smaller. Both cases are exacerbated by higher reinforcement ratios.

Effect of Reinforcement ratio variation on reliability of concrete and masonry walls

- Changes in the reinforcement ratio have greater influence on reliability of walls when the eccentricity is high (i.e., the moment is high, since $e = M/P$). This is because the role of the steel reinforcement is dominant when the moment is high while the value of the compressive strength is dominant for low eccentricity (i.e., behaviour dominated by axial load).
- The following relationships can be observed: the higher the reinforcement ratio, the higher the reliability indices. Increasing the steel area greatly improves the response in term of resistance of walls, which translates into safer structures.

Effect of Compressive strength variation on reliability of concrete and masonry walls

- When the compressive strength increases, the reliability indices decrease for both masonry and concrete walls. This is consistent with results obtained in a Monte Carlo analysis carried out on singly and doubly reinforced masonry and concrete walls. It was observed that walls with higher compressive strength possess higher coefficient of variation, -i.e., more variability and consequently, smaller reliability values.

Overall conclusion for both previous analyses (reinforcement ratio variation, compressive strength variation)

- Doubly reinforced masonry (DR) walls are the most sensitive to the variation of these parameters, followed by DR concrete walls, and singly Reinforced (SR) masonry wall.
- The reliability of SR concrete walls seemed not to be affected by the change in these parameters.
- Masonry walls possess higher sensitivity than concrete walls. The reason for this is the higher variability in strength data for masonry walls (COV =0.236) than concrete walls strength data (COV=0.18). This higher variability in masonry is due to the fact that its strength is highly dependent on construction practices, mason qualifications, and

inspection. In addition, this variability is aggravated by the presence of the workmanship random variable in masonry wall construction.

Effect of Single vs Double reinforcement on reliability

- It was observed that the reliability indices of DR walls, for both masonry and concrete, were generally higher than reliability indices of SR walls. The differences are more noticeable for walls with higher reinforcement ratios and lower compressive strengths. A double layer of reinforcement increases the capacity of the wall (leading to a safer structure, with higher reliability values) compared to placing the reinforcing bars singly at the center of the wall This increment in the capacity is due to higher moment arms in DR walls.
- Reliability indices of DR walls, for both materials masonry and concrete, are more sensitive to changes in design parameters than the reliability of SR walls. In DR walls the moment capacity considered the moment arms of both reinforcement layers; therefore, additional random variables such as effective depths, yield stress of the compressive steel are involved, adding more variability to the limit state function.
- Walls, for both materials masonry and concrete, made of higher compressive strength and lower reinforcement ratio had similar reliabilities irrespective of whether they were doubly or singly reinforced, although slightly higher for DR walls. However, for walls made of lower compressive strength materials and having higher reinforcement ratios, the reliability index for singly reinforced wall was much lower than for doubly reinforced wall. This is a consequence of the higher sensitivity of DR walls than SR walls to the change in reinforcement ratio and compressive strength.

5.1 Recommendations for future work

Based on the outcomes of this study, the following recommendations can be made:

- This study only considered gravity loads: dead load plus live load. Future studies should evaluate reliability indices considering different load conditions such as dead load plus snow load, dead load plus wind load. These have different factored load in their combination and different statistical information.

- This study focused on gravity loads where the moment is linearly correlated with the axial load. Future studies can be carried out for the cases where the axial load is not linearly correlated with the moment (lateral loads, second order effect due to slenderness) This can imply a selection of a new limit state function whose fundamentals are according to the behaviour of the analyzed wall case. Because of the selection of new limit state function, different reliability levels can be expected.
- In this study a particular behavioural model for masonry (Priestley and Elder modified model) and concrete (Thorenfeldt model) were chosen to construct the nominal and factored interaction diagrams. Future studies can select different models for masonry (Romano model, Naraine and Sinha model) and concrete walls (Hognestad concrete curve, kent and Park model, Popovics curve). Different behavioural models might lead to different reliability values.

REFERENCES

Bartlett, F.M. (2007). "Canadian Standards Association standard A23.3-04 resistance factor for concrete in compression." *Canadian Journal of Civil Engineering*, 34(9), 1029-1037.

Bartlett, F., Hong, H., and Zhou, W. (2003). "Load factor calibration for the proposed 2005 edition of the National Building Standard of Canada: Statistics of loads and load effects." *Canadian Journal of Civil Engineering*, 30(2), 429-439.

Bartlett, F.M., and MacGregor, J. G. (1996). "Statistical Analysis of the Compressive Strength of Concrete in Structures." *ACI Material Journal*, 93(2), 158–168.

Canadian Standard Association. (2014). *S304-14 Design of Masonry Structures*. Mississauga, Canada.

Canadian Standard Association. (1994). *S304-94 Masonry design for buildings (limit states design)*. Ontario, Canada.

Canadian Standard Association. (2019). *A23.3-19 Design of Concrete Structures*. Canadian Standards Association.

Canadian Standard Association. (1984). *A23.3-84 Design of Concrete Structures for buildings*. Canadian Standards Association.

Ellingwood, B.M. (1977). "Statistical Analysis of RC Beam-Column Interaction." *Journal of the Structural Division*, 103(7), 1377–1388.

Grant, L. H., Mirza, S. A., and MacGregor, J. G. (1978). "Monte Carlo study of strength of concrete columns." *ACI Structural Journal*, 75(8), 348–358.

Gonzalez, R., Alonso, A., Cruz, C., and Tomlinson, D. (2021). "Numerical Study of the Response of Reinforced Slender Masonry Walls with various Reinforcement Arrangements." *14th Canadian Masonry Symposium*, Montreal, Canada.

Guzman, O. (2022). "Reliability assessment for Loadbearing Reinforced-concrete Masonry Walls Subjected to Gravity and Lateral Loads". Ph.D. Candidacy Exam, University of Alberta.

Hong, H. P., and Zhou, W. (1999). “Reliability evaluation of RC columns.” *Journal of Structural Engineering*, 125(7), 784–790.

Israel, M., Ellingwood, B., and Corotis, R. (1987). “Reliability-Based Standard Formulations for Reinforced-concrete Buildings.” *Journal of the Structural Division*, ASCE, 113(10), 2235–2252.

Laird, D.A., Drysdale, R.G., Stubbs, D.W., and Sturgeon, G.R. (2005). “The New CSA S304.1-04 Design of Masonry Structures.” *Proceedings of the 10th Canadian Masonry Symposium*. 10.

Lind, N.C. (1971). “Consistent partial safety factors.” *Journal of the Structural Division*, ASCE, 97(6), 1651–1669.

Madsen, H. O., krenk, S., and Lind, N.C. (1986). *Methods of Structural Safety*. Dover, New York, US.

Mahsuli, M., and Haukaas, T. (2013). Computer program for multimodel reliability and optimization analysis. *Journal of Computing in Civil Engineering*, 27(1), 87–98.

Melchers, R. E., Beck, A.T. (2018). *Structural Reliability Analysis and Prediction*. Jhon Wiley and Sons, New York, US.

Metwally, Z., Zeng, B., and Li, Y. (2022). “Probabilistic behavior and Variance-Based Sensitivity Analysis of Reinforced-concrete Masonry Walls Considering Slenderness Effect.” *Journal of Risk and Uncertainty in Engineering Systems*, ASCE, 8(4), 04022051.

Mirza, S.A., Hatzinikolas, M., and MacGregor, J.G. (1979). “Statistical Description of Strength of Concrete.” *Journal of the Structural Division*, 106(6), 1021–1037.

Moosavi, H., and Korany, Y. (2014). “Assessment of the structural reliability of loadbearing concrete masonry designed to the Canadian Standard S304.1.” *Canadian Journal of Civil Engineering*, 41(12), 1046-1053.

Moosavi, S.A.H. (2017). “Structural Reliability of Non-Slender Loadbearing Concrete Masonry Members under Concentric and Eccentric Loads.” Ph.D. dissertation, University of Alberta.

Nowak, A.S. (2000). *Reliability of Structures*. McGraw-Hill, Boston, US.

Ruiz, S.E. (1993). “Reliability Associated with Safety Factors of ACI 318-89 and the Mexico City Concrete Design Regulations.” *ACI Structural Journal*, 90(3), 262–268.

Ruiz, S.E., and Aguilar, J.C. (1994). "Reliability of Short and Slender Reinforced-Concrete Columns." *Journal of Structural Engineering*, ASCE, 120(6), 1850–1865.

Stewart, M.G., and Lawrence, S. (2002). "Structural Reliability of Masonry Walls in Flexure." *Masonry international*, 15(2), 48–52.

Stewart, M.G., and Lawrence, S. (2007). "Model Error, Structural Reliability and Partial Safety Factors for Structural Masonry in Compression." *Masonry international*, 20(3), 107–116.

Stewart, M.G., and Masia, M.J. (2019). "Reliability-Based Assessment of Safety Factors for Masonry Walls in Vertical Bending." *13th North American*, Salt Lake City, UT, US.

Turkstra, C., and Daly, M.J. (1978). "Two moment structural safety analysis." *Canadian Journal of Civil Engineering*, 5(3), 414-426.

Turkstra, C., and Ojinaga, J. (1980). "Towards a Canadian Limit States Masonry Design Code." *Proceedings of the Second Canadian Masonry Symposium*, 133-141.

Turkstra, C., Ojinaga, J., and Shyu, C. (1983). "Development of a Limit States Masonry Code." *Proceedings of the 3rd Canadian Masonry Symposium*. 2.1-2.13.

Tichy, M, and Vorlicek, M. (1962). "Safety of eccentrically loaded reinforced-concrete columns." *Journal of the Structural Division*, 88(5), 1–10.

Zhai, X., and Stewart, M.G. (2008). "Structural Reliability Analysis of Reinforced Grouted Concrete Block Masonry Walls in Compression Designed to Chinese Standard GB 50003." *Research Report No. 268.08.08*.

APPENDICES

APPENDIX A

COMPUTER SCRIPTS

COMPUTER CODE FOR DOUBLY REINFORCED-CONCRETE WALL

```
Do[
(*Nominal Values*)
es=2*10^5;
{fcn,fyn,dbn,dtn,tn,ρ}={25,400,240,50,290,0.0035};
(* Stress-strain relationship – Steel rebar*)
σsTop[ϵt_,fy_]:=If[ϵt<-(fy/es),-fy,If[ϵt<fy/es,es*ϵt,fy]];
σsBot[ϵb_,fy_]:=If[ϵb<-(fy/es),-fy,If[ϵb<fy/es,es*ϵb,fy]];
(* Stress-strain relationship – Concrete*)
γc = 2400;
fc0=fcn*0.87;
ec = If[20<=fc0<= 40, 4500*Sqrt[fc0],
(3300*Sqrt[fc0]+6900)*(γc/2300)^1.5];
n = 0.8+fc0/17.2;
ϵ0 =- (fc0/ec)*(n/(n-1));
k1=1;
k2=Max[0.67+fc0/62,1];
σc[ϵc_,fc_]:=If[ϵc>0,0,If[ϵc>=-ϵ0,s=-fc*(n*(ϵc/ϵ0))/((n-
1)+(ϵc/ϵ0)^(n*k1)),s=-fc*(n*(ϵc/ϵ0))/((n-1)+(ϵc/ϵ0)^(n*k2))]];
(*FACTORED INTERACTION DIAGRAM*)
A23[fc_,fy_,dBot_,dTop_,t_,e_]:=Module[{φc,φs,ae,ag,ast,ϵy,β1,prmax,cb
,a,cm,sTop,tr,prb,mrb,eb,pr,mr,list,cO,c,a1,listp,pA23,pmA23,mA23,thru
st,sub,guessP,ϵu,order,guessP2,b,λ,α1},
list={};
```

```
φc=0.65;φs=0.85;ϵu=0.0035;

b=1000;

λ=1;

ρ;

ae=b*t;

ag=b*t;

ast=ρ*ag;

α1 = 0.85-0.0015*fc;

β1=0.97-0.0025*fc;

fr = 0.6*λ*Sqrt[fc];

ρb = (α1*φc*fc*β1)/(φs*fy)*(ϵu/(ϵu+ϵy));

(*Axial Load*)

pro = (φc*α1*fc*(ag-ast)+φs*fy*ast)/1000;

prmax=If[(0.15+0.002*t)*pro <= 0.75*pro,(0.15+0.002*t)*pro,0.75*pro];

Print["Prmax: ",prmax];

(*Balanced Case*)

cb=ϵu/(fy/es+ϵu) dBot;

a=β1* cb;

cm=φc*α1*fc*b*a;

sTop=φs*ρ/2*ag*σsTop[ϵu (dTop-a/β1)/(a/β1),fy];

tr=φs*ρ/2*ag*fy;

prb=cm-sTop-tr;

mrb=cm(t/2-a/2)+tr(dBot-t/2)-sTop*(t/2-dTop);
```

```
eb=mrb/prb;

(*Pure bending*)

a=a1/.Solve[{φc*α1*fc*b*a1-φs*σsTop[(dTop-a1/β1)/(a1/β1)
ϵu,fy]*ρ/2*ag==φs*σsBot[(dBot-a1/β1)/(a1/β1) ϵu,fy]*ρ/2*ag,
a1>0},a1][[1]] ;

If[ϵu (dBot-a/β1)/(a/β1)>fy/es,yield="Steel Yields in pure
bending",Print["Steel does not yield in pure bending"]];

cm=φc*α1*fc*b*a;

sTop=φs*ρ/2*ag*σsTop[ϵu (dTop-a/β1)/(a/β1),fy];

tr=φs*σsBot[ϵu (dBot-a/β1)/(a/β1),fy]*ρ/2*ag;

mr=cm*(t/2-a/2)+tr*(dBot-t/2)-sTop*(t/2-dTop);

AppendTo[list,{mr/10^6,0}];

cO=a/β1;

(*Other points*)

c=cO+1;

While[c<t,{a=β1*c, cm=φc*α1*fc*b*a,sTop=φs*ρ/2*ag*σsTop[ϵu*(dTop-
a/β1)/(a/β1),fy],tr=φs*σsBot[ϵu*(dBot-a/β1)/(a/β1),fy]*ρ/2*ag,pr=cm-
sTop-tr,mr=cm*(t/2-a/2)+tr*(dBot-t/2)-sTop*(t/2-dTop),

AppendTo[list,{mr/10^6,Min[pr/1000,prmax+c/10000]}],c=c+1} ];

(*Last Point*)

c=t;

a=β1 *c;

cm=φc*α1*fc*b*a;

sTop=φs*ρ/2*ag*σsTop[ϵu*(dTop-a/β1)/(a/β1),fy];
```

```
tr=φs*σsBot[ϵu (dBot-a/β1)/(a/β1),fy]*ρ/2*ag;
pr=cm-sTop-tr;
mr=cm*(t/2-a/2)+tr*(dBot-t/2)-sTop*(t/2-dTop);
AppendTo[list,{mr/10^6,Min[pr/1000,prmax+c/10000]}];
AppendTo[list,{0,prmax+(c+1)/10000}];
listp=Table[{list[[i,2]],list[[i,1]]},{i,Length[list-5]}];
pmA23=Interpolation[listp,InterpolationOrder->1];
guessP=10^-3;
order=10^IntegerPart[Log[10,list[[-1,2]]]];
Do[{While[
And[guessP<list[[-
1,2]],pmA23[guessP]/guessP>e/1000],guessP=guessP+order],
guessP=guessP-order,
order=order/10},{10}];
sub=FindRoot[pmA23[guessP2]/guessP2==e/1000,{guessP2,guessP}];
mA23=pmA23[guessP2/.sub];
pA23=guessP2/.sub;
{list,{{mrb/10^6,prb/10^3}},{{mA23,pA23}}};
Print["mA23=",mA23];
Print["pA23=",pA23];
{mA23, pA23}
];
{mn,pn}=A23[fcn,fyn,dbn,dtn,tn,en];
```

```
mn;

pn;

(*NOMINAL INTERACTION DIAGRAM*)

realPM[fc_,fy_,dBot_,dTop_,t_,e_]:=

Module[{interaction,interaction2, list,b,listn,
sub,ae,ag,cO,cO1,cO2,єui,cm,tr,mr,c,yield,pr,listp,listnp,mReal,pReal,
cReal,thrust,maxp,finalInteraction,finalInteraction2,finalList,guessP,
cStep,order,z,cb,mrb,prb,ec,n,є0,k1,k2,sTop},

interaction={};

list={};

listn={};

b=1000;

ae=b*t;

ag=b*t;

maxp=0;

interaction=

Table[list={};

(*Pure bending*)

cO1=0.01;

order=10;

Do[{While[-b*NIntegrate[σc[-(єui/cO1)*x,fc],{x,0,cO1}]-σsTop[(dTop-
cO1)/cO1*єui,fy]*ρ/2*ag<σsBot[(dBot-
cO1)/cO1*єui,fy]*ρ/2*ag,{cO1=cO1+order}],cO1=cO1-
order,order=order/10},{3}];
```

```
sub=FindRoot[-b*Integrate[σc[-(εui/cO2)*x,fc],{x,0,cO2}]-σsTop[(dTop-
cO2)/cO2*εui,fy]*ρ/2*ag==σsBot[(dBot-
cO2)/cO2*εui,fy]*ρ/2*ag,{cO2,cO1}];

cO=cO2/.sub;

sTop=σsTop[εui (dTop-cO)/cO,fy]*ρ/2*ag;

tr=σsBot[(dBot-cO)/cO*εui,fy]*ρ/2*ag;

If[εui*(dBot-cO)/cO>fy/es,{mr=-b*NIntegrate[(t/2-cO+x)*σc[-
(εui/cO1)*x,fc],{x,0,cO}]-sTop*(t/2-dTop)+tr*(dBot-t/2)},{mr=-
b*NIntegrate[(t/2-cO+x)*σc[-(εui/cO1)*x,fc],{x,0,cO}]-sTop*(t/2-
dTop)+tr*(dBot-t/2)}];

Print["mr=",mr];

AppendTo[list,{mr/10^6,0}];

AppendTo[listn,{cO,0}];

(*BALANCED POINT*)

cb=εui/(εui+fy/es) dBot;

cm=b*NIntegrate[σc[-(εui/cb)*x,fc],{x,Max[0,cb-t],cb}];

sTop=σsTop[εui (dTop-cb)/cb,fy]*ρ/2*ag;

tr=σsBot[(dBot-cb)/cb*εui,fy]*ρ/2*ag;

mrb=-b*NIntegrate[(t/2-cb+x)*σc[-(εui/cb)*x,fc],{x,Max[0,cb-t],cb}]-
sTop*(t/2-dTop)+tr*(dBot-t/2);

prb=-(cm+tr+sTop);

Print["mrb=",mrb];

Print["prb=",prb];

Print["cb=",cb];
```

```
(*Other Points*)

If[cO<0, Print["Error c is negative"]];

cStep=1;

c=cO+cStep;

While[Or[mr>10000,Length[list]<10],{cm=b*NIntegrate[σc[-
((ϵui*x)/c),fc],{x,Max[0,c-t],c}],

sTop=σsTop[ϵui (dTop-c)/c,fy]*ρ/2*ag,

tr=σsBot[(dBot-c)/c*ϵui,fy]*ρ/2*ag,

mr=-b*NIntegrate[(t/2-c+x)*σc[-(ϵui/c)*x,fc],{x,Max[0,c-t],c}]+-
sTop*(t/2-dTop)+tr*(dBot-t/2),

pr=-(cm+tr+sTop),

AppendTo[list,{mr/10^6,pr/1000}],

AppendTo[listn,{c,pr/1000}],

cStep=Min[1/Abs[list[[-1,1]]-list[[-2,1]]],20/Abs[list[[-1,2]]-list[[-
2,2]]]]*cStep,

c=c+cStep}];

listp=Table[{list[[i,2]],list[[i,1]]},{i,Length[list]}];

listnp=Table[{listn[[i,2]],listn[[i,1]]},{i,Length[listn]}];

interaction2=Interpolation[listnp,InterpolationOrder->1];

AppendTo[listp,{listp[[-1,1]]+10^-3,0}];

maxp=Max[maxp,listp[[-1,1]]];

Interpolation[listp,InterpolationOrder-
>1],{ϵui,0.0035,0.0035,0.0002}];
```

```
finalInteraction=interaction[[1]];

finalInteraction2=interaction2;

guessP=10^-3;

order=10^IntegerPart[Log[10,maxp]];

Off[InterpolatingFunction::dmval];

Do[{While[And[guessP<maxp,finalInteraction[guessP]/guessP>e/1000],gues
sP=guessP+order],

guessP=guessP-order,

order=order/10},{3}];

sub=FindRoot[finalInteraction[guessP2]/guessP2==e/1000,{guessP2,guessP
}];

mReal=finalInteraction[guessP2/.sub];

pReal=guessP2/.sub;

cReal=finalInteraction2[guessP2/.sub];

{list,{{mrb/10^6,prb/10^3}},{{mReal,pReal}}};

Print["mReal=",mReal];

Print["pReal=",pReal];

Print["cReal=",cReal];

{mReal,pReal,cReal}

];

{mReal,pReal,c}=realPM[fcn*0.87,fyn,dbn,dtn,tn,en];

mReal;

pReal;
```

```
c;
(*Random Variables*)
RANDOMVAR[fco_,fyo_,dBoto_,dTopo_,to_,ρo_,c_]:=Module[{wo,bo,ϵui,ag,ϵb
,ϵt,σsrBot,σsrTop,γc,fc0,ec ,n,ϵ0,k1,k2,σcr,s,cm,sTop,tr,mrb,prb},
fc;
fy;
dTop;
dBot;
t;
ϵui=0.0035;
bo=1000;
ag=bo*to;
tied="False";
ϵt=((dTopo-c)/c)*ϵui;
ϵb=((dBoto-c)/c)*ϵui;
(*Steel rebar - Constitutive Law*)
σsrTop[ϵt_,fyr_]:=If[ϵt<-(fyr/es),-fy,If[ϵt<fyr/es,fy/0.002*ϵt,fy]];
σsrBot[ϵb_,fyr_]:=If[ϵb<-(fyr/es),-fy,If[ϵb<fyr/es,fy/0.002*ϵb,fy]];
(*Thorenfeld curve*)
γc = 2400; (* normal density *)
fc0=fco*0.87;
ec = If[20<=fc0<= 40, 4500*Sqrt[fc0],
(3300*Sqrt[fc0]+6900)*(γc/2300)^1.5];
```

```
n = 0.8+fc0/17.2;

ϵ0 =- (fc0/ec)*(n/(n-1));

k1=1;

k2=Max[0.67+fc0/62,1];

σcr[ϵc_,fcr_]:=If[ϵc>0,0,If[ϵc>=-ϵ0,s=-fcr*(n*(ϵc/ϵ0))/((n-
1)+(ϵc/ϵ0)^(n*k1)),s=-fcr*(n*(ϵc/ϵ0))/((n-1)+(ϵc/ϵ0)^(n*k2))]];

cm=bo*Integrate[σcr[-(ϵui/c)*x,0.87*fc],{x,Max[0,c-to],c}];

sTop=σsrTop[ϵt,fyo]*ρo/2*ag;

tr=σsrBot[ϵb,fyo]*ρo/2*ag;

Print["cm=",cm//FullSimplify//Expand];

Print["cm=",sTop//FullSimplify//Expand];

Print["tr=",tr//FullSimplify//Expand];

mrb=-bo*Integrate[(t/2-c+x)*σcr[-(ϵui/c)*x,0.87*fc],{x,Max[0,c-
to],c}]-sTop*(t/2-dTopo)+tr*(dBoto-t/2);

prb=-(cm+tr+sTop);

Print["pr = ", prb/1//FullSimplify//Expand];

Print["mr = ", mrb/1//FullSimplify//Expand];

{mrb//FullSimplify//Expand,prb//FullSimplify//Expand}

];

{mr,pr}=RANDOMVAR[fcn,fyn,dbn,dtn,tn,ρ,c];

mr;

pr;
```

```
(*FORM – Rackwitz-Fiessler procedure*)

fc;

μfc=1.30*fcn;

σfc=0.18*μfc;

fy;

μfy=fyn*1.14;

σfy=0.07*μfy;

t;

μt=1.00*tn;

σt=0.010*μt;

Pr=pr;

Mr=mr;

α =1.0;

β=1.0;

mdn=(mn*10^6 )/(1.50*α+1.25);

mln=(α*mn*10^6)/(1.50*α+1.25);

pdn=(pn*10^3)/(1.50*β+1.25);

pln=(β*pn*10^3)/(1.50*β+1.25);

Pd;

μPd=1.05*pdn;

vpd=0.100;

σPd=vpd*μPd;

Md;
```

```
μMd=1.05*mdn;

vmd=0.100;

σMd=vmd*μMd;

Pl;

μPl=0.90*pln;(*Gumbel Distribution*)

vpl=0.170;

σPl=vpl*μPl;

Ml;

μMl=0.90*mln;(*Gumbel Distribution*)

vml=0.170;

σMl=vml*μMl;

el;

μel=1.000;

σel=0.206;

po={{1,0,0,0,0,0,0,0},

{0,1,0,0,0,0,0,0},

{0,0,1,0,0,0,0,0},

{0,0,0,1,1,0,0,0},

{0,0,0,1,1,0,0,0},

{0,0,0,0,0,1,1,0},

{0,0,0,0,0,1,1,0},

{0,0,0,0,0,0,0,1}};
```

```
(*Limit State Function*)
M=Sqrt[Mr^2+Pr^2]-Sqrt[(Md+el*Ml)^2+(Pd+el*Pl)^2];
Equ=M/.{fc->μfc,fy->μfy,t->μt(*,el μel*),Pd->μPd,Md->μMd,Pl->μPl,Ml->
μMl};
sol=NSolve[Equ==0,el,PositiveReals];
el^*=el/.sol[[1]];
(*Equivalent normal Parameters*)
(*fc is normal*)
σfce=σfc;
μfce=μfc;
(*fy is Normal*)
σfye=σfy;
μfye=μfy;
(*Pl*)
betha=Sqrt[(6*σPl^2)/Pi^2];(*1/a*)
alpha=μPl-0.5772*betha;(*u*)
fq=PDF[ExtremeValueDistribution[alpha,betha],μPl];
Fq=CDF[ExtremeValueDistribution[alpha,betha],μPl];
IN1=InverseCDF[NormalDistribution[0,1],Fq];
σPle=(1/fq)*PDF[NormalDistribution[0,1],IN1];
μPle=μPl-σPle*IN1;
(*Ml*)
betha=Sqrt[(6*σMl^2)/Pi^2];(*1/a*)
```

```
alpha=μMl-0.5772*betha;(*u*)

fq=PDF[ExtremeValueDistribution[alpha,betha],μMl];

Fq=CDF[ExtremeValueDistribution[alpha,betha],μMl];

IN1=InverseCDF[NormalDistribution[0,1],Fq];

σMle=(1/fq)*PDF[NormalDistribution[0,1],IN1];

μMle=μMl-σMle*IN1;

(*Reduced Variates*)

zs1=(μfc-μfce)/σfce;

zs2=(μfy-μfye)/σfye;

zs6=(μPl-μPle)/σPle;

zs7=(μMl-μMle)/σMle;

zs8=(el^*-μel)/σel;

zs={zs1,zs2,0,0,0,zs6,zs7,zs8};

(*Determine {G} vector*)

G1=-D[M,fc]*σfce/.{fc-> μfc,fy-> μfy,t-> μt,Pd-> μPd,Md->μMd,Pl->
μPl,Ml->μMl,el-> el^*};

G2=-D[M,fy]*σfye/.{fc-> μfc,fy-> μfy,t-> μt,Pd-> μPd,Md->μMd,Pl->
μPl,Ml->μMl,el-> el^*};

G3=-D[M,t]*σt/.{fc-> μfc,fy-> μfy,t-> μt,Pd-> μPd,Md->μMd,Pl-> μPl,Ml-
>μMl,el-> el^*};

(*G4=-D[M,el]*σel/.{fc  μfc,fy  μfy,t  μt,Pd  μPd,Md μMd,Pl
μPl,Ml μMl,el  el^*};*)

G4=-D[M,Pd]*σPd/.{fc-> μfc,fy-> μfy,t-> μt,Pd-> μPd,Md->μMd,Pl->
μPl,Ml->μMl,el-> el^*};
```

```
G5=-D[M,Md]*σMd/.{fc-> μfc,fy-> μfy,t-> μt,Pd-> μPd,Md->μMd,Pl->
μPl,Ml->μMl,el-> el^*};

G6=-D[M,Pl]*σPle/.{fc-> μfc,fy-> μfy,t-> μt,Pd-> μPd,Md->μMd,Pl->
μPl,Ml->μMl,el-> el^*};

G7=-D[M,Ml]*σMle/.{fc-> μfc,fy-> μfy,t-> μt,Pd-> μPd,Md->μMd,Pl->
μPl,Ml->μMl,el-> el^*};

G8=-D[M,el]*σel/.{fc-> μfc,fy-> μfy,t-> μt,Pd-> μPd,Md->μMd,Pl->
μPl,Ml->μMl,el-> el^*};

G={G1,G2,G3,G4,G5,G6,G7,G8};

(*Reliability Index Value*)

β=G.zs/Sqrt[G.po.G];

(*α Values*)

α=po.G/Sqrt[G.po.G];

(*New Values of Z*)

zs=β*α;

(*Working with list*)

X={fc,fy,t,Pd,Md,Pl,Ml,el};

μ={μfce,μfye,μt,μPd,μMd,μPle,μMle,μel};

σ={σfce,σfye,σt,σPd,σMd,σPle,σMle,σel};

For[j=1,j<=12,j++,

xs=Table[i,{i,1,8}];

For[i=1,i<=8,i++,

xs[[i]]=μ[[i]]+zs[[i]]*σ[[i]];

Print["xs",xs[[i]]];
```

```
];
Equ=M/.{fc-> xs[[1]],fy-> xs[[2]],t-> xs[[3]](*,el  xs[[4]]*),Pd->
xs[[4]],Md-> xs[[5]],Pl-> xs[[6]],Ml-> xs[[7]]};
sol=NSolve[Equ==0,el,PositiveReals];
xs[[8]]=el/.sol[[1]];
Print["xs[[8]]",xs[[8]]];
(*Equivalent normal Parameters*)
(*fc is normal*)
σfce=σfc;
μfce=μfc;
(*fy is normal*)
σfye=σfy;
μfye=μfy;
(*Pl*)
betha=Sqrt[(6*σPl^2)/Pi^2];(*1/a*)
alpha=μPl-0.5772*betha;(*u*)
fq=PDF[ExtremeValueDistribution[alpha,betha],xs[[6]]];
Fq=CDF[ExtremeValueDistribution[alpha,betha],xs[[6]]];
IN1=InverseCDF[NormalDistribution[0,1],Fq];
σPle=(1/fq)*PDF[NormalDistribution[0,1],IN1];
μPle=xs[[6]]-σPle*IN1;
(*Ml*)
betha=Sqrt[(6*σMl^2)/Pi^2];(*1/a*)
```

```
alpha=μMl-0.5772*betha;(*u*)

fq=PDF[ExtremeValueDistribution[alpha,betha],xs[[7]]];

Fq=CDF[ExtremeValueDistribution[alpha,betha],xs[[7]]];

IN1=InverseCDF[NormalDistribution[0,1],Fq];

σMle=(1/fq)*PDF[NormalDistribution[0,1],IN1];

μMle=xs[[7]]-σMle*IN1;

μ[[1]]=μfce;

σ[[1]]=σfce;

μ[[2]]=μfye;

σ[[2]]=σfye;

μ[[6]]=μPle;

σ[[6]]=σPle;

μ[[7]]=μMle;

σ[[7]]=σMle;

(*Reduced Variates*)

For[i=1,i<=8,i++,

zs[[i]]=(xs[[i]]-μ[[i]])/σ[[i]];

];

For[i=1,i<=8,i++,

G[[i]]=-D[M,X[[i]]]*σ[[i]]/.{fc-> xs[[1]],fy-> xs[[2]],t-> xs[[3]],Pd-
> xs[[4]],Md-> xs[[5]],Pl-> xs[[6]],Ml-> xs[[7]],el-> xs[[8]]};

];

β=G.zs/Sqrt[G.po.G];
```

```
Print["Reliability index Value:",β];

α=po.G/Sqrt[G.po.G];

zs=β*α;];

PutAppend[β,"results.txt"];

Print["en=",en],{en,{11.6,29,58,87,116,145,174,232,290,435,580,725,870
}}]
```

APPENDIX B

Comparison between Masonry and Concrete walls 20 MPa

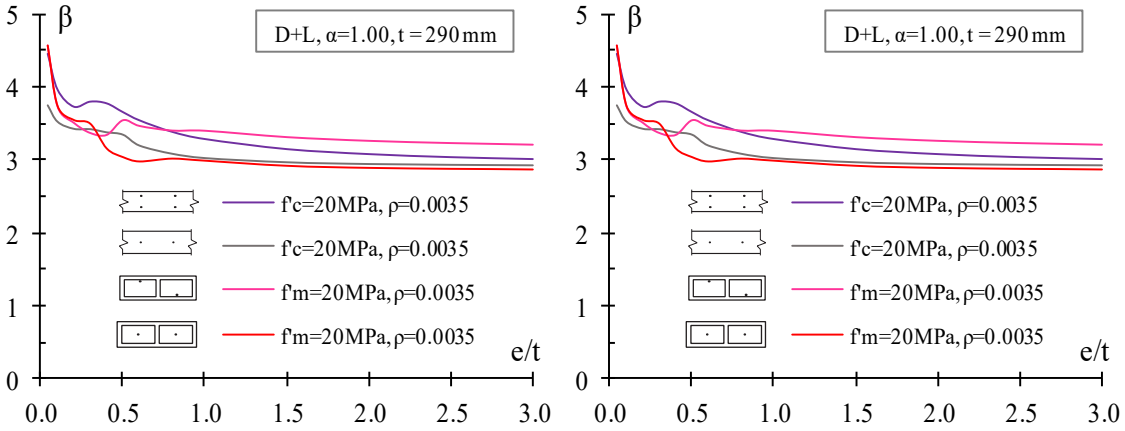

(a) $f'_m = f'_c$ = 20 MPa, ρ=0.0035

(b) $f'_m = f'_c$ = 20 MPa, ρ =0.0025

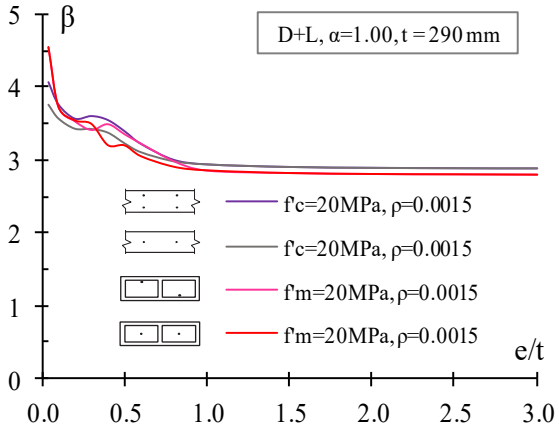

(c) $f'_m = f'_c$ = 20 MPa, ρ =0.0015

Figure A.1: Reliability levels comparison between masonry and concrete walls.